Targeting the cannabinoid and mu opioid receptors with heterodimerized and allosteric ligands

Ph.D. Thesis

Szabolcs Dvorácskó

Supervisor:

Dr. Csaba Tömböly

Universitiy of Szeged, Faculty of Medicine

Doctoral School of Theoretical Medicine

Laboratory of Chemical Biology, Institute of Biochemistry

Biological Research Center of the Hungarian Academy of Sciences

Szeged, Hungary

2019

TABLE OF CONTENTS

LIST OF PUBLICATIONS

List of thesis related publications:

I. Dvorácskó, Sz., Keresztes, A., Mollica, A., Stefanucci, A., Macedonio, G., Pieretti, S., Zádor, F., Walter, F., Deli, M., Kékesi, G., Bánki, L., Tuboly, G., Horváth, Gy., Tömböly, Cs. **Preparation of bivalent agonists for targeting the mu opioid and cannabinoid receptors** *Eur. J. Med. Chem.* in press (2019). **IF: 4,816**

II. Dvorácskó, Sz., Tömböly, Cs., Berkecz, R., Keresztes, A. **Investigation of the receptor binding and functional characteristics of hemopressin(1-7)**. *Neuropeptides* **58**, 15-22 (2016). **IF: 2,915**

III. Dvorácskó, Sz., Stefanucci, A., Novellino, E., Mollica, A. **Design of multi target ligands for chronic and neuropathic pain**. *Future Med. Chem.* **7**, 2469-83 (2015). **IF: 3,969**

Other publications:

1. Mollica, A., Mirzaie, S., Costante, R., Carradori, S., Macedonio, G., Stefanucci, A., Dvorácskó, Sz., Novellino, E. Exploring the biological consequences of conformational changes in aspartame models containing constrained analogues of phenylalanine. *J. Enzyme Inhib. Med. Chem.* **31**, 953-63 (2016). **IF: 3,638**

2. Monti, L., Stefanucci, A., Pieretti, S., Marzoli, F., Fidanza, L., Mollica, A., Mirzaie, S., Carradori, S., De Petrocellis, L., Schiano, M. A., Benyhe, S., Zádor, F., Szűcs, E., Ötvös, F., Erdei, A., Samavati, R., Dvorácskó, Sz., Tömböly, Cs., Novellino, E. Evaluation of the analgesic effect of 4-anilidopiperidine scaffold containing ureas and carbamates. *J. Enzyme Inhib. Med. Chem*. **31**, 1638-47 (2016). **IF: 3,638**

3. Stefanucci, A., Costante, R., Macedonio, G., Dvorácskó, Sz., Mollica, A. Cysteine-, methionine- and seleno-cysteine-proline chimeras: Synthesis and their use in peptidomimetics design. *Curr. Bioact. Comp.* **12**, 200-206 (2016). **IF: 0**

4. Szűcs, E., Dvorácskó, Sz., Tömböly, Cs., Büki, A., Kékesi, G., Horváth, Gy., Benyhe, S. Decreased CB receptor binding and cannabinoid signaling in three brain regions of a rat model of schizophrenia. *Neurosci. Lett*. **633**, 87-93 (2016). **IF: 2,159**

5. Mollica, A., Pelliccia, S., Famiglini, V., Stefanucci, A., Macedonio, G., Chiavaroli, A., Orlando, G., Brunetti, L., Ferrante, C., Pieretti, S., Novellino, E., Benyhe, S., Zádor, F., Erdei, A., Szűcs, E., Samavati, R., Dvorácskó, Sz., Tömböly, Cs., Ragno, R., Patsilinakos, A., Silvestri, R. Exploring the first Rimonabant analog-opioid peptide hybrid compound, as bivalent ligand for CB1 and opioid receptors. *J. Enzyme Inhib. Med. Chem*. **32**, 444–451 (2017). **IF: 3,638**

6. Nagy-Grócz, G., Zádor, F., Dvorácskó, Sz., Bohár, Zs., Benyhe, S., Tömböly, Cs., Párdutz, Á., Vécsei, L. Interactions between the Kynurenine and the Endocannabinoid System with Special Emphasis on Migraine. *Int. J. Mol. Sci.* **18**, e1617 (2017). **IF: 3,687**

7. Adamska-Bartłomiejczyk, A., Borics, A., Tömböly, Cs., Dvorácskó, Sz., Lisowski, M., Kluczyk, A., Wołczański, G., Piekielna-Ciesielska, J., Janecka, A. Synthesis, receptor binding studies, optical spectroscopic and in silico structural characterization of morphiceptin analogs with cis-4-amino-L-proline residues. *J. Pept. Sci.* **23**, 864-870 (2017). **IF: 1,969**

8. Leone, S., Recinella, L., Chiavaroli, A., Martinotti, S., Ferrante, C., Mollica, A., Macedonio, G., Stefanucci, A., Dvorácskó, Sz., Tömböly, Cs., De Petrocellis, L., Vacca, M., Brunetti, L., Orlando, G. Emotional disorders induced by Hemopressin and RVD-hemopressin(α) administration in rats. *Pharmacol. Rep.* **69**, 1247-1253 (2017). **IF: 2,787**

9. Ferrante, C., Recinella, L., Leone, S., Chiavaroli, A., Di Nisio, C., Martinotti, S., Mollica, A., Macedonio, G., Stefanucci, A., Dvorácskó, Sz., Tömböly, Cs., De Petrocellis, L., Vacca, M., Brunetti, L., Orlando, G. Anorexigenic effects induced by RVD-hemopressin(α) administration. *Pharmacol. Rep.* **69**, 1402-1407. (2017). **IF: 2,787**

10. Stefanucci, A., Novellino, E., Macedonio, G., Dimmito, M. P., Mirzaie, S., Cardoso, F. C., Lewis, R., Zádor, F., Erdei, A., Dvorácskó, Sz., Tömböly, Cs., Benyhe, S., Pieretti, S., Minosi, P., Mollica, A. Design, synthesis and biological profile of mixed opioid agonist/N-VGCC blocker peptides. *New J. Chem.* **42**, 5656-5659 (2018). **IF: 3,201**

11. Recinella, L., Chiavaroli, A., Ferrante, C., Mollica, A., Macedonio, G., Stefanucci, A., Dimmito, M. P., Dvorácskó, Sz., Tömböly, Cs., Brunetti, L., Orlando, G., Leone, S. Effects of central RVD-hemopressin(α) administration on anxiety, feeding behavior and hypothalamic neuromodulators in the rat. *Pharmacol. Rep.* **70**, 650-657 (2018). **IF: 2,787**

12. Stefanucci, A., Macedonio, G., Dvorácskó, Sz., Tömböly, Cs., Mollica, A. Novel Fubinaca/Rimonabant hybrids as endocannabinoid system modulators. *Amino Acids.* **50**, 1595-1605 (2018). **IF: 2,906**

13. Leone, S., Ferrante, C., Recinella, L., Chiavaroli, A., Mollica, A., Tömböly, Cs., Stefanucci, A., Dimmito, M. P., Dvorácskó, Sz., Verratti, V., De Petrocellis, L., Orlando, G., Brunetti, L. Effects of RVD-hemopressin (α) on feeding and body weight after standard or cafeteria diet in rats. *Neuropeptides*. **72**, 38-46 (2018). **IF: 2,915**

ABBREVIATIONS

ACN	acetonitrile
AM 251	*N*-(piperidin-1-yl)-5-(4-iodophenyl)-1-(2,4-dichlorophenyl)-4-methyl-1*H*-pyrazole-3-carboxamide
AM 630	6-iodo-2-methyl-1-[2-(4-morpholinyl)ethyl]-1*H*-indol-3-yl](4-methoxyphenyl)methanone
BBB	blood-brain barrier
Boc	*tert*-butyloxycarbonyl
BSA	bovine serum albumin
CB	cannabinoid
DAMGO	H-Tyr-D-Ala-Gly-*N*-MePhe-Gly-ol
DCM	dichloromethane
Δ^9-THC	(–)-*trans*-Δ^9-tetrahydrocannabinol
DIC	*N*,*N*'-diisopropylcarbodiimide
DIEA	diisopropylethylamine
DMF	dimethylformamide
DOR	delta opioid receptor
EDC	N-(3-Dimethylaminopropyl)-N′-ethylcarbodiimide hydrochloride
EGTA	ethylene glycol-bis(2-aminoethylether)-*N*-*N*-*N'*-*N'*-tetraacetic acid
E_{max}	efficacy, the maximal effect that an agonist can elicit in a given setting
EC_{50}	potency, half-maximal effective concentration
EtOAc	ethyl acetate
EtOH	ethanol
GDP	guanosine 5'-diphosphate
GPCR	G-protein-coupled receptor
GTPγS	guanosine 5'-*O*-(3-thiotriphosphate)
HOBt	benzotriazol-1-ol
HPLC	high-performance liquid chromatography
HS-665	3-(2-((cyclobutylmethyl)(phenethyl)amino)ethyl)phenol
i.t.	intrathecal

JWH-018 (or AM 678)	naphthalen-1-yl(1-pentyl-1*H*-indol-3-yl)methanone
k’	retention factor (HPLC)
K_d	equilibrium dissociation constant
K_i	inhibitory constant
KOR	kappa opioid receptor
MOR	mu opioid receptor
MsCl	methanesulfonyl chloride
NMM	4-methylmorpholine
NMR	nuclear magnetic resonance (spectroscopy)
R_f	retention factor (TLC)
r.t.	room temperature
RVD-hemopressin	H-Arg-Val-Asp-Pro-Val-Asn-Phe-Lys-Leu-Leu-Ser-His-OH
SEM	standard error of mean
TEA	triethylamine
TFA	trifluoroacetic acid
THF	tetrahydrofuran
TLC	thin layer chromatography
Tris	tris-(hydroxymethyl)-aminomethane
WIN-55,212-2	(*R*)-(+)-[2,3-dihydro-5-methyl-3-(4-morpholinylmethyl)pyrrolo[1,2,3-de]-1,4-benzoxazin-6-yl]-1-naphthalenylmethanone mesylate

ACKNOWLEDGEMENTS

I am sincerely grateful to my supervisor Dr. Csaba Tömböly for giving me the opportunity to perform this work in the Laboratory of Chemical Biology and for all of his kind support, suggestion and guidance throughout my studies.

I am deeply thankful to Dr. Attila Keresztes for his selfless supporting and supervising me and for teaching me *in vitro* techniques.

I would like to thank Dr. Adriano Mollica for allowing me to perform experiments in his laboratory and for the successful collaboration.

I am deeply thankful to the members of the Laboratory of Chemical Biology for their help and kindness.

I'm grateful to Dr. Ferenc Zádor and Dr. Sándor Benyhe for their help.

I greatly acknowledge our collaborators Dr. Gyöngyi Horváth and her colleagues for *in vivo* characterization of the novel ligands and Dr. Mária Deli and her group members for the *in vitro* blood-brain-barrier studies.

I would like to thank to Prof. Dr. Gábor Jancsó for the motivation and for useful pieces of advice.

I would like to thank the Institute of Biochemistry of the Biological Research Centre for giving me a 3-year fellowship to perform these studies.

I would like to thank Dr. Anita Tóth and Tibor Varga at the Hungarian Institute for Forensic Sciences for their help in synthetic cannabinoid research.

Finally, special thanks to my family and to my wife for their patience and for all their support.

1. Introduction

1.1. The cannabinoid system

The cannabinoid system is involved in various functions of the central nervous system as well as in the periphery. Therefore, molecules interfering with the endocannabinoid signaling may have application in the investigation or in the treatment of diverse pathological conditions including neuropathic pain, chronic inflammatory diseases, movement disorders (Parkinson's, Huntington's disease), multiple sclerosis, obesity, mood and anxiety disorders, drug addiction, psychosis, myocardial infarction.[1-4]

The endocannabinoid system (ECS) consists of two well characterized receptors (CB1 and CB2), their primary endogenous lipid agonists 2-arachidonoyl glycerol (2-AG), anandamide (AEA) and peptide endocannabinoid allosteric modulators (hemopressins, pepcans), and the enzymes responsible for the synthesis and degradation of endocannabinoids. Furthermore, the cannabinoid system also interacts with exogenous phyto- and synthetic cannabinoid compounds.[4-6]

1.1.1. Cannabinoid receptors

The biological effects of the endocannabinoids, the phyto- and synthetic cannabinoids and cannabimimetics are mediated by two types of cannabinoid receptors, the CB1 and CB2 receptors that belong to the family of $G_{i/o}$ protein coupled receptors (GPCRs).[7-9] The CB1 receptor is located at central and peripheral synapses and it is one of the most widespread presynaptic regulators of neurotransmitter release in the brain.[10,11] The CB1 receptors are responsible for elevating mood or precipitating emotions (e.g. anxiety and panic), they mediate the acute psychoactive effects of cannabinoids, but the activation of the CB1 receptors can also induce antinociception, hypothermia, and hypomobility.[12] In contrast, the CB2 receptors are expressed predominantly in immune and hematopoietic cells,[13,2] but they can also be found in the brain, especially in microglia[14], in myocardium and in endothelial cells.[15] The main function of the CB2 receptor is the control of cytokine release and immune cell migration. Additionally, CB2 activation reduces inflammation-induced pain, induces peripheral antinociception, and inhibition of tumor growth.[16]

1.1.2. Lipid type endocannabinoids

Lipid endocannabinoids are the most extensively characterized endogenous ligands of the cannabinoid receptors and their physiological effects are primarily mediated through the CB1 receptors.[17,18] The endogenous ligands of the CB receptors are hydrophobic lipid-derived compounds, among them the *N*-arachidonoylethanolamine (anandamide, AEA) and 2-arachidonoyl glycerol (2-AG) are the most studied. Anandamide is synthesized from membrane phospholipids by *N*-acyltransferase and phospholipase D, and rapidly metabolized by the fatty acid amide hydrolase (FAAH). 2-AG is produced from phosphatidylinositol mainly through two enzymatic steps by phospholipase C (PLC) and diacylglycerol lipase (DAGL), and hydrolyzed by the monoacylglycerol lipase (MAGL) enzyme.[1,19-23] Endocannabinoids are produced in activity-dependent manner and released from postsynaptic neurons "on demand". They act as retrograde signalling messengers.[20,24,25] Anandamide is a partial agonist for both CB receptors and it is found only in low concentrations (pmol/g) in the brain, while 2-AG acts as a full agonist at CB1 and CB2 receptors and it is present in higher concentration (nmol/g) in the brain.[25] Anandamide produces analgesia, controls motor activity, reduces emesis, stimulates appetite and induces hypothermia. 2-AG induces apoptosis and acts as a messenger molecule in the endocrine and immune systems.[23,26]

1.1.3. Hemopressins (Pepcans), the putative peptide endocannabinoids

Over the past decades, lipid-derived endocannabinoids were believed to be the only endogenous agonists of the cannabinoid receptors. However, as a result of the pioneering works of Heimann[27] and Rioli[28], hemopressin (PVNFKFLSH, Hp(1–9)) was identified as a putative inverse agonist peptide ligand of the CB1 receptor in rats. This peptide is a metabolic product of the hemoglobin α-chain and it was demonstrated to exert non-opioid antinociceptive effects, similar to those of the endo- , phyto- and synthetic cannabinoids.[27,29] Hemopressins have been demonstrated to possess *in vitro* and *in vivo* pharmacological potencies similar to those of the prototypic endogenous and synthetic cannabinoid ligands, but with less side-effects.[27,30-32] The Hp(1–9) peptide and its extended or truncated derivatives were demonstrated to be orally active and to exert antinociceptive effects that were apparently mediated by the CB1 receptors.[32] The physiological activity upon oral administration suggests that these peptides are at least partially resistant to proteolysis, and also that they may be able to cross the blood–brain barrier.

Soon after the discovery and pharmacological characterization of Hp(1–9), the *N*-terminally extended RVD-Hp(1-9) and VD-Hp(1-9)[31], and the *C*-terminally truncated Hp(1–6) and Hp(1–7) peptides were identified as further potent cannabinoid ligands.[30] RVD-Hp(1-9) and VD-Hp(1-9) were suggested being agonists of the CB1 receptor. *In vivo* data for the *C*-terminally truncated hemopressins demonstrated that Hp(1–9) was not essential for antinociceptive activity, because Hp(1–6) and Hp(1–7) exerted antihyperalgesic effects similar to the *N*-terminally extended peptides. Further *C*-terminal truncation, however, led to the loss of biological activity.[32] VD- and RVD-Hps exhibited hypotensive, hypothermic and hypoactive effects at antinociceptive doses, and inhibited bombesin-induced central activation of the adrenomedullary outflow in rats.[33,34] In addition, central administration of VD-Hpα resulted in tolerance to antinociception and stimulated food consumption in a CB1-dependent manner.[34,35] The signaling characteristics and regulation of receptor endocytosis by the *N*-terminally extended peptide fragments were found to be distinct, in part, from those of the classical cannabinoid agonists.[31]

Recently, it was described that the nonapeptide hemopressin might rather be a hot acidic extraction artifact and it is not present endogenously.[31,41] Instead, RVD-hemopressin (RVD-Hp(1-9), RVD-Hpα, Pepcan-12, RVDPVNFKLLSH), the most abundant peptide among the α1 hemoglobin derived hemopressin peptides can be a real endocannabinoid (Figure 1). Using a very sensitive immunoaffinity and specific LC-MS/MS method RVD-Hp(1-9) was identified both in rodent CNS (e.g. striatum, prefrontal cortex (noradrenergic neurons)) and in periphery (e.g. adrenals, liver).[5,40,41] It was found that this peptide could interact with the CB1 allosteric binding site(s). Also, RVD-Hpα has been recently described as the first endogenous negative allosteric modulator of CB1 receptors that acts at the same time as a potent CB2 receptor positive allosteric modulator.[40,41] These allosteric binding sites which topographically distinct from the orthosteric site have recently been characterized.[36,37] According to *in vivo* assays RVD-Hpα showed anxiolytic and antidepressant effects in different behavioral tests, and it induced anorexigenic effects.[38,39] Stimulation of CB1 receptors by hemopressins leads to the activation of a signaling pathway (allosteric binding site) distinct from that activated by lipid type endocannabinoids (orthosteric binding site). The undesirable psychoactive side effects that are characteristic of CB1 receptor orthosteric ligands can possibly reduced by targeting the allosteric site with hemopressins.[5,40,41]

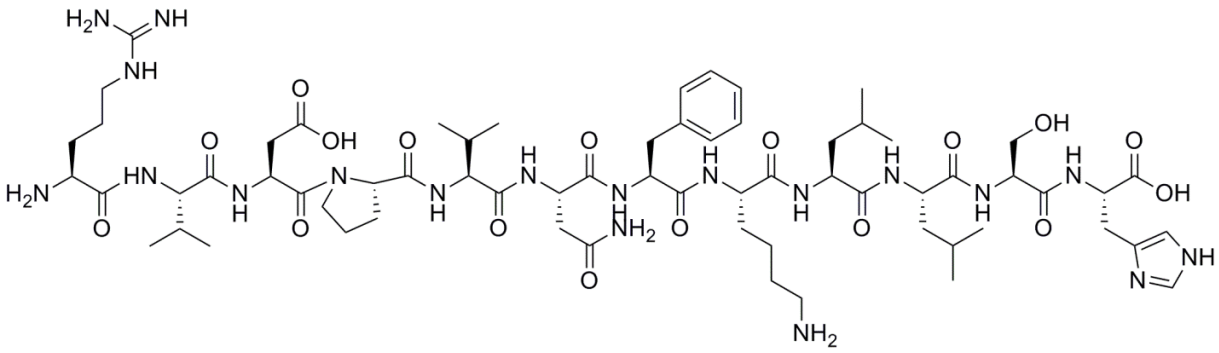

Figure 1. The structure of RVD-Hpα, an allosteric peptide endocannabinoid

1.1.4. Phyto- and synthetic cannabinoids

Marijuana with the primary psychoactive substituent Δ^9-tetrahydrocannabinol (Δ^9-THC) is one of the oldest and most widely used drugs in the world.[42] Δ^9-THC and other plant-derived cannabinoid agonists related research studies were soon expanded by experiments with chemically more stable synthetic cannabinoids.[43] Furthermore, the discovery and identification of endocannabinoids led to the development of important synthetic orthosteric cannabinoid agonists and allosteric modulators allowing to study the clinical potential of cannabinoids more effectively.[44,42] CP 55,940 [(–)-cis-3-[2-hydroxy-4-(1,1-dimethylheptyl)phenyl]-trans-4-(3- hydroxypropyl)cyclohexanol] is one of the well known 'non-classical' bicyclic synthetic cannabinoid agonist ligands.[45,43] It has high affinity for both CB1 and CB2 receptors (10-100 times more potent *in vivo* than Δ^9-THC) and shows high enantioselectivity. These properties made [^{3}H]CP-55,940 a useful radioligand for binding studies to characterize the cannabinoid receptors.[46,47] Aminoalkylindoles (AAIs) form another important class of synthetic cannabinoid ligands. WIN 55,212-2 [(*R*)-(+)-[2,3-dihydro-5-methyl-3-(4-morpholinylmethyl)pyrrolo[1,2,3-de]-1,4-benzoxazin-6-yl]-1-naphthalenylmethanone mesylate represents the prototypic cannabinoid agonist AAI, which led to further synthetic indole cannabinoids.[48] WIN 55,212-2 has higher affinity for cannabinoid receptors (K_i(CB2)= 0.28 nM, K_i(CB1)= 1.89 nM) than Δ^9-THC and in *in vitro* functional [^{35}S]GTPγS binding assays WIN 55,212-2 acts as a full agonist while Δ^9-THC acts as a partial agonist.[49,50]

JWH-018 (naphthalen-1-yl(1-pentyl-1*H*-indol-3-yl)methanone was identified as the most potent synthetic cannabinoid receptor agonist of the initial series of indole-derived cannabinoids. This alkylindole structurally relates to WIN 55,212-2 but lacking a methyl group at C-2 position and possessing an *N*-pentyl side chain that is similar to the C-3 pentyl

side chain of Δ^9-THC. JWH-018 exhibits typical *in vivo* cannabinoid pharmacology just like Δ^9-THC, i.e. good potency in the cannabimimetic effect predictor test (tetrad tests: hypothermia, analgesia, hypolocomotion, catalepsy) and has high affinity for both cannabinoid receptors (K_i(CB1)= 9 nM, K_i(CB2)= 2.94 nM).[51,52] Recently, it was detected among the most prevalent active agents in drugs of abuse such as Spice or K2 and other herbal blends (Figure 2.).

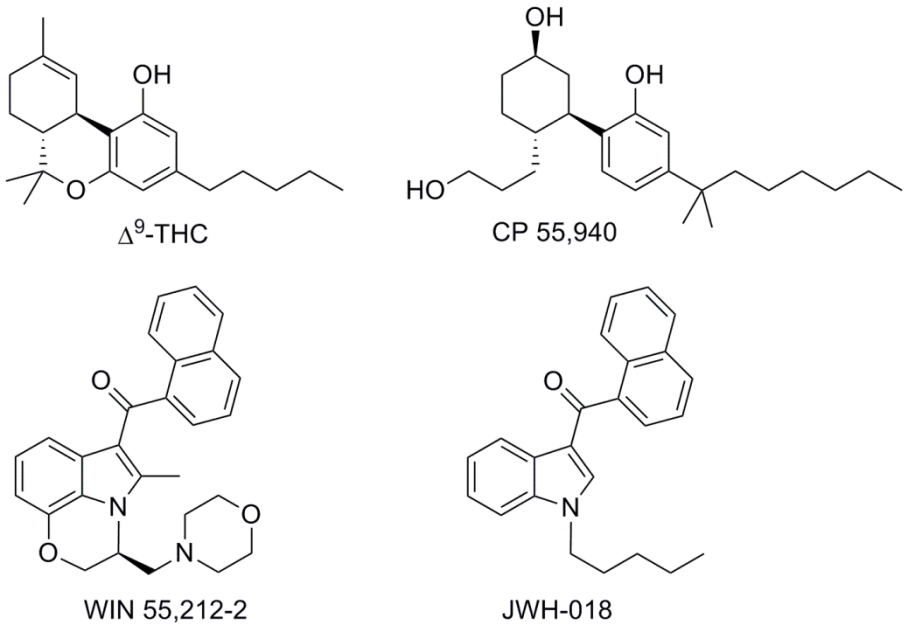

Figure 2. The structure of cannabinoid receptor agonists.

1.2. The opioid system

The endogenous opioid system is mostly known for its role in pain regulation,[53] however, it also modulates several other physiological functions such as mood, feeding behavior, learning and memory, locomotor activity. The endogenous opioid system is also involved in the regulation of the respiration, cardiovascular functions, gastrointestinal motility, immune functions, thermoregulation, hormone secretion, the development of tolerance and dependence, which form the basis of the unwanted side-effects of opioid administration.[54-57]

This system consists of three major “classical” classes of receptors, complemented by the non-classical nociceptin (NOR) receptor, endogenous opioid peptides which are derived from distinct preproproteins and plant opium alkaloids with their synthetic derivatives.

1.2.1. Opioid receptors

The opioid receptor family also belongs to the GPCR superfamily and they interact mostly with G_i/G_o type G proteins.[58] Three types of opioid receptors have been identified, MOR (μ, morphine), DOR (δ, *vas deferens*) and KOR (κ, ketocyclazocine) which are encoded by unique genes.[59,60] MOR, DOR, KOR are located in both spinal and supraspinal areas as well as at the periphery and are involved in the antinociceptive action of opioids. MOR is located in the central nervous system and it is also widely distributed in the peripheral nervous system (e.g. myenteric neurons in the gut). The abundance of MOR is the highest in the caudate putamen, that is followed by neocortex, thalamus, nucleus accumbens, hippocarnpus and amygdala in decreasing order. Moderate concentrations are found in the periaqueductal gray and raphe nuclei, dorsal horn of the spinal cord and low density is present in the hypothalamus, globus pallidus.[57,61,62] Tolerance and physical dependence, the major opioid side effects are associated mainly with the MOR under long term MOR agonist (morphine) administration during the treatment of severe acute and chronic pain.[63,64] These undesirable effects limit the use of MOR agonists and numerous strategies were developed for decreasing the MOR related side effects such as the co-administration of MOR agonist and other GPCR ligands.[65,66] The DORs are mostly expressed in the olfactory bulb, neocortex, caudate putarnen and nucleus accumbens. Thalamus, hypothalamus and brainstem have moderate receptor density.[62] The highest KOR densities were observed in the nucleus accumbens, claustrum, dorsal endopiriform, nucleus accumbens. KOR also found in the cerebral cortex, the substantia nigra and only low level found in cerebral cortex.[53,57] The DOR and KOR mediated analgesia is mainly spinal and supraspinal.[67]

1.2.2. Endogenous opioids

The peptidic endogenous opioids act as neurotransmitters, neuromodulators or neurohormones. The three main families of endogenous opioid peptides are endorphins[159], those interact with all three opioid receptors, Met- and Leu-enkephalins (Tyr-Gly-Gly-Phe-Met/Leu) for DOR[160], and dynorphins for KOR[163]. Additionally, endomorphin-1 (H-Tyr-Pro-Trp-Phe-NH_2) and endomorphin-2 (H-Tyr-Pro-Phe-Phe-NH_2) have been isolated from bovine and human brain[166] and found to interact with high affinity and selectivity with MOR.[57,165] The opioid peptides are synthesized from distinct precursor proproteins in post-translational steps. Endorphins are enzymatically cleaved from prepro-opiomelanocortin (POMC)[159],

enkephalins from preproenkephalin[160,161], while dynorphin A, dynorphin B and neoendorphin from preprodynorphin.[162,164] After their synthesis these endogenous opioid peptides are stored in vesicles.[68-73] These endogenous opioid peptides share the common *N*-terminal sequence of Tyr-Gly-Gly-Phe, that is termed the opioid motif, followed by diverse *C*-terminal sequences (5-31 residues). In contrast endomorphins contain the Tyr-Pro-Phe/Trp sequence as the message domain.[74] Endorphins are mostly produced in the central nervous system by hypothalamus and pituitary gland and released during severe pain to produce analgesia. β-endorphins have the highest affinity for the MOR. The DOR selective pentapeptide neurotransmitters, enkephalins found also in the brain and are involved in regulating nociception in the body. Dynorphins are produced in many brain region, such hypothalamus, hippocampus, midbrain, medulla, pons and the spinal cord and mediated KOR they act as modulators of pain response, control appetite and circadian rhythm. Endomorphins produced widely and abundantly in the brain, brainstem cortex, the amygdala, thalamus, hypothalamus, striatum and spinal cord (endomorphin-2). They play important role in pain management, stress responses, reward and cognitive functions and homeostasis.[67,75-77]

1.2.3. Phyto- and synthetic opioids

The MOR agonist alkaloid morphine is the major active ingredient of poppy seed opium (*Papaver somniferum*) and its derivates (semisynthetic agonists oxymorphone, oxycodone) are still widely used nowadays for the treatment of acute and chronic pain.[78] Furthermore, the synthetic agonist fentanyl with a ring system distinct from morphine is a more potent morphinomimetic compound (Figure 3).[79] For experimental purposes the biologically stable synthetic enkephalin analog DAMGO ([D-Ala^2, N-MePhe^4, Gly-ol]-enkephalin) with high MOR specificity is the most frequently used peptide agonist.[80] MOR agonists such as morphine are powerful analgesics but their major limitation is that in long lasting treatments they cause adverse side effects (e.g. respiratory depression, sedation, constipation, nausea, development of tolerance, physical dependence and addiction).[81,82]

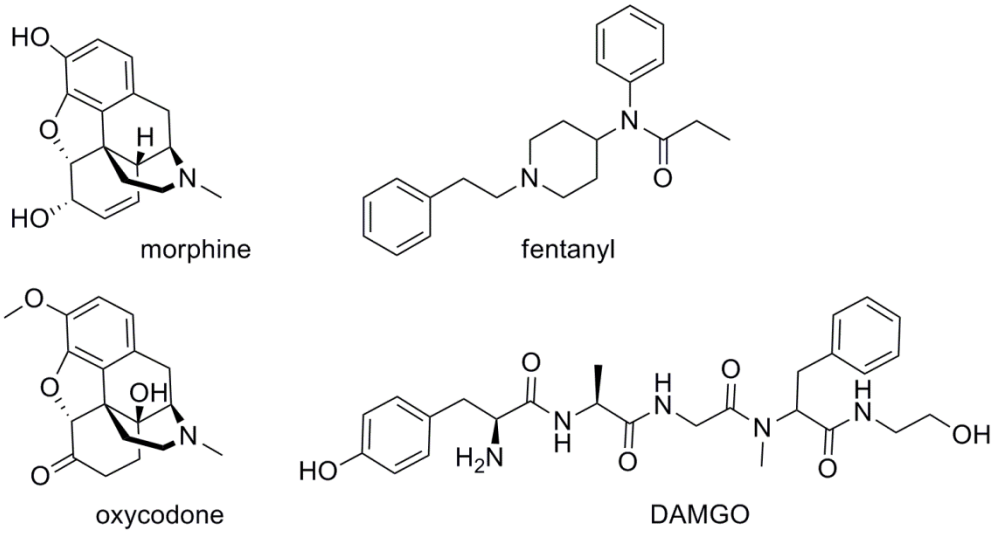

Figure 3. The structure of opioid receptor agonists.

1.3. G-protein-coupled receptors and measurement assays

Heterotrimeric G-protein-coupled receptors (GPCRs) mediate many important physiological processes (sensory transduction, cell–cell communication, neuronal transmission, hormonal signaling) and are considered as the largest therapeutic and druggable (>50% of receptors) targets of various diseases. GPCRs are seven transmembrane receptors containing an extracellular *N*-terminal region and an intracellular *C*-terminal region.[83] They are divided into six main classes according to the A-F system. Class A contains the rhodopsin-like receptors, that is the largest group of GPCRs involving also the opioid and cannabinoid receptors. Crystal structure has been determined for both classes of receptors.[84-87] The heterotrimeric G-proteins consist of G_α subunit that interacts with the dimer of the G_β and G_γ subunits ($\beta\gamma$ complex). According to the effector target of the G_α subunit there are four main families: $G_{\alpha s}$ (activates adenylyl cyclase), $G_{\alpha i/o}$ (inhibits adenylyl cyclase), $G_{\alpha q/11}$ (activates phospholipase C), $G_{\alpha 12/13}$ (regulates small GTP binding proteins).[88,89] The opioid and cannabinoid receptors belong to the $G_{\alpha i/o}$ family.

Upon ligand (agonist) binding, the activated receptors catalyze the exchange of guanosine-5`- diphosphate (GDP) for guanosine-5`- triphosphate (GTP) on the α-subunit of heterotrimeric G-proteins and these conformational changes result in the dissociation of G_α from the dimeric $G_{\beta\gamma}$ subunits.[90] GPCRs coupled to $G_{\alpha i/o}$ proteins inhibit the activity of adenylate cyclase enzyme that is responsible for adenosine triphosphate (ATP) to 3',5'-cyclic adenosine monophosphate (cAMP) conversion. Cyclic AMP serves as a second messenger

that activates protein kinase A and other downstream effectors.[91] The G_α subunit due to its intrinsic GTPase activity hydrolyses GTP to GDP which leads to the re-association of the heterotrimeric G protein complex, and then the trimer is ready to start a new cycle.[91,88] In order to avoid the continuous agonist stimulation, the GPCR kinases (GRKs) phosphorylate the *C*-terminus of GPCRs leading to the recruitment of β-arrestins, that results in receptor desensitization, inactivation and internalization.[92]

Over the years many GPCR assays and GPCR ligand screening methods were developed and tested. The radioligand binding assay on receptor-containing membranes can be used to characterize the interaction between a GPCR and its ligands (affinity of orthosteric/allosteric ligands, receptor density, association/dissociation rates). G-protein dependent functional assays characterize the biological properties of the test compounds. [^{35}S]GTPγS binding assays directly measure the guanine nucleotide exchange of G proteins, an early event after GPCR activation[93] and can distinguish between full or partial agonists, neutral antagonists, inverse agonists, and allosteric regulators. cAMP measurement assay shows the decrease/increase of cellular cAMP levels upon modulation of adenylate cyclase activity by GPCR agonist/antagonist ligands. The most general G-protein independent functional assays are the agonist induced receptor internalization assay on cultured cells and β-arrestin recruitment assays.[91]

1.4. Synergistic interaction and multitargeting of the opioid and cannabinoid receptors

Both the MOR and the CB receptors are class A GPCRs and they can form functional homo- or heteromeric associates that is a general feature of GPCRs.[94-97] Many studies have described the formation of the MOR-DOR, MOR-NK1 and MOR-CB1 receptor heteromers that have been confirmed experimentally.[98,99] The opioid and cannabinoid receptors are known to closely interact with each other in several levels. This is due to their similar structure, their common signaling pathways (adenylyl cyclase inhibition, mitogen-activated protein (MAP) kinase stimulation, inhibition of voltage gated calcium channels, activation of potassium channels), and their overlapping anatomical distribution and co-localization both in areas of the central nervous system known to participate in antinociception (periaqueductal gray (PAG), raphe nuclei, central-medial thalamic nuclei, dorsal horn of the spinal cord) and in the periphery.[100,101] The interaction of these two receptors has been studied extensively to achieve more effective antinociception.[102-105] The synergy of opioid and cannabinoid receptors in analgesia has been exploited by the co-administration of morphine and non-selective

cannabinoid agonists with promising results.[103,106-109] Beyond the combinatoin therapy, the multitarget drug approach can also address or influence the homo- and heteromeric membrane receptor interactions and the possible physiological effects of these protein-protein interactions.[110,111] Bivalent compounds containing two pharmacophores in a single molecule have been developed to target the MOR and CB receptors or their associates in a simultaneous or parallel way. Dimeric compounds of the MOR agonist α-oxymorphamine and the CB_1 antagonist/inverse agonist rimonabant were found to exhibit antinociception in tail flick test without producing tolerance in 24 h.[112] In another study the MOR agonist fentanyl was coupled to rimonabant, but the resulting compounds became antagonists and did not produce analgesic effect in hot plate test.[113] Previously, a dimeric compound was prepared by coupling an enkephalin-related peptide to rimonabant, but the resulting derivative did not produce analgesic effect in hot plate and tail flick tests.[114] This special case of the multitarget ligand approach can lead to the development of more potent and active compounds because the pharmacokinetics and the pharmacodynamics of the covalently coupled drugs are identical in this form and their stoichiometric presence in tissues can produce synergistic interactions.[115-119]

2. Aims of the study

Mu opioid receptor (MOR) agonists are the most common therapeutics clinically used to alleviate pain. However, their dose-limiting adverse effects including respiratory depression, sedation, constipation, tolerance and dependence associate with MOR agonists, that inspires the development of analgesics with distinct mechanism of action.[119] Combination therapy has also been demonstrated to be effective for improving analgesic effects without the additive elevation of the side-effects.[103,120] The co-administration of MOR and cannabinoid (CB) receptor agonists has been shown to result in enhanced antinociceptive effect with decreased opiate-related side-effects, and the synergism of opioid and cannabinoid ligands has been extensively studied to improve antinociception.[66,100,104-108,121-125]

Based on the reported synergism of MOR and CB agonists, our aim was to develop novel opioid-cannabinoid bivalent agonists with increased analgesic- and decreased side-effects.

The aims of the study presented here were the following:

- To design, synthesize two series of opioid-cannabinoid bivalent ligands and hemopressins.
- To radiolabel the cannabinoid pharmacophore (JWH-018) of the bivalent ligands and the truncated hemopressin heptapeptide (Hp1-7) for direct *in vitro* characterization of their receptor binding on rat and mouse brain membrane homogenates.
- To compare the binding sites of classical cannabinoid ligands and hemopressins in displacement assay using [^{3}H]JWH-018 and [^{3}H]Hp(1-7).
- To examine the synthetized bivalent ligands and hemopressins in receptor-binding studies in order to study the effects of the modifications on the affinity and selectivity.
- To study the agonist/antagonist properties and the MOR, CB1/CB2 mediated G-protein activation of bivalent ligands and hemopressins using ligand-stimulated [^{35}S]GTPγS functional assay.
- To investigate the permeability of selected bivalent derivatives through the blood brain barrier.
- To test the *in vivo* antinociceptive effects of the *in vitro* most effective bivalent ligands.

3. Materials and Methods

3.1. Chemicals

The purity of all reagents and solvents were analytical or the highest commercially available grade. Starting materials, buffer components, GDP, GTPγS were purchased from Sigma-Aldrich Kft. (Budapest, Hungary), fatty acid free bovine serum albumin (BSA) was from Serva (Heidelberg, Germany), DAMGO was obtained from Bachem AG (Bubendorf, Switzerland), Ile^{5,6}-deltorphin-2, JWH-018, hemopressins were prepared in the Laboratory of Chemical Biology (BRC, Hungary), naloxone, oxycodone were kindly provided by Endo Laboratories (Wilmington, DE, USA), WIN-55,212-2 was purchased from Tocris Inc. (Bristol, UK), [^{35}S]GTPγS (s.a. >37 TBq/mmol) was purchased from Hartmann Analytic (Braunschweig, Germany). The radioligands [^{3}H]JWH-018 (s.a. 1.48 TBq/mmol), [^{3}H]WIN-55,212-2 (s.a. 485 GBq/mmol), [^{3}H]DAMGO (s.a. 1.43 TBq/mmol), [^{3}H]Ile^{5,6}-deltorphin-2 (s.a. 725 GBq/mmol), [^{3}H]HS-665 (s.a. 1.13 TBq/mmol) and [^{3}H]Hp(1–7) (s.a. 1.04 TBq/mmol) were prepared in the Laboratory of Chemical Biology (BRC, Hungary). Tritium labeling was carried out in a self-designed vacuum manifold and radioactivity was measured with a Packard Tri-Carb 2100 TR liquid scintillation analyser using Insta Gel scintillation cocktail of PerkinElmer.

3.2. Analytical Methods

Analytical thin layer chromatography (TLC) was performed on 5×10 cm glass plates precoated with silica gel 60 F_{254} (Merck, Darmstadt, Germany), spots were visualized with UV light. Flash chromatography was carried out on silica gel 60 (Sigma Ltd., St. Louis, MO, USA) using the indicated solvents. Analytical HPLC separations were performed with a Merck-Hitachi LaChrom system on a Vydac 218TP54 (250×4.6 mm, 5 μm) column using the indicated gradients of ACN (0.08% (v/v) TFA) (eluent B) in H_2O (0.1%(v/v) TFA) (eluent A) at a flow rate of 1 mL/min, and UV detection at λ= 216 nm was applied. Radio-HPLC was performed on a Jasco HPLC system equipped with a Packard Radiomatic 505 TR Flow Scintillation Analyser. ^{1}H and ^{13}C NMR spectra were recorded on a Bruker Avance 500 MHz or on a Varian Mercury 300 MHz spectrometer and chemical shifts (δ) are reported in ppm after calibration to the solvent signals. The assignments are based on ^{1}H, ^{13}C(DEPT), HSQC, HMBC, GQ-COSY and 2D-TOCSY experiments, and on the reported assignment of JWH-

018. Molecular weight of the compounds was determined by ESI-MS analysis on a Finnigan Mat LCQ spectrometer.

3.3. Details of the preparation and analytical characterization of compounds 1-25

Details of the preparation and analytical characterization of compounds **1-25** are described in the appendix

3.4. General procedure for the synthesis of the peptidic compounds in solution

To an ice-cooled mixture containing the *N*-protected amino acid or peptide (0.28 mmol) in DCM (5 mL), EDC.HCl (1.1 equiv., 0.28 mmol), HOBt (1.1 equiv., 0.28 mmol), NMM (3.3 equiv., 0.85 mmol) and the required protected amino acid (1 equiv., 0.25 mmol) dissolved in DMF (2.5 mL) were added. The reaction mixture was allowed to warm at r.t. and stirred for 16 h and evaporated under reduced pressure. The residue was then dissolved in EtOAc and washed three times with 5% citric acid, $NaHCO_3$ and finally with brine. The organic phase was dried over Na_2SO_4, and the solvent evaporated under reduced pressure to give the desired product. All final Boc-protected peptide intermediates have been purified by flash chromatography on silica gel 60 and then treated with a mixture of TFA/DCM (1:1) for 30 min at r.t. The final products as TFA salts were lyophilised and then characterized as described in the Appendix.

3.5. Preparation of hemopressins on solid support

The solid phase peptide synthesis was carried out manually in a silanized glass reaction vessel. N^{α}-Boc-Leu- or N^{α}-Boc-His(Tos)-PAM resin (0.15 mmol) was swollen for 30 min in DMF. After Boc-deprotection with neat TFA and subsequent washings (three times with DMF and *i*-PrOH), TBTU activated N^{α}-Boc-protected amino acids (0.45 mmol) were added for chain elongation in DMF and the unreacted resin bound peptides were end-capped with an excess of Ac_2O in the presence of DIEA in DMF. Couplings were monitored with the Kaiser-test.[126] After removal of the *N*-terminal protecting group, peptides were cleaved from the resin with HF in the presence of anisole. The crude peptide-resin mixtures were washed with diethylether, then the peptides were dissolved in aqueous TFA and lyophilized. The resulting crude peptides were dissolved in aqueous TFA, and introduced onto an analytical Vydac

218TP54 column and eluted using a linear gradient of 1.5 %/min of acetonitrile in water containing 0.1% TFA, starting from 15% acetonitrile at a flow rate of 1 mL/min, with UV detection at λ= 215 nm. The same elution conditions were used for the purification of the peptides on a Vydac 218TP1010 semipreparative column at a flow rate of 4 mL/min; isolated yields 56% (Hp(1–7)), 74% (ΔPro^1-Hp(1–7)), 38% (Hp(1–9)) and 42% (RVD-Hp(1–9)). Molecular weights of the peptides were confirmed by MALDI-TOF mass spectrometry (Hp(1–7) $[M+H]^+$ m/z 864.42; ΔPro^1-Hp(1–7) $[M+H]^+$ m/z 862.63; Hp(1–9) $[M+H]^+$ m/z 1089.26; RVD-Hp(1–9) $[M+H]^+$ m/z 1424.80).

3.6. Radiolabeling of JWH-018

Tritium labeling was performed with 3.6 mg of naphthalen-1-yl(5-bromo-1-pentyl-1*H*-indol-3-yl)methanone (**25)** (8.5 μmol) dissolved in 0.6 mL of EtOAc in the presence of 3 mg of Pd/C (10% Pd) catalyst and triethylamine (1.5 μL, 10.7 μmol). The reaction mixture was degassed prior to tritium reduction by two freeze-thaw cycles, and then it was stirred under 0.25 bar tritium gas for 4 h at r.t. The unreacted tritium gas was then adsorbed onto pyrophoric uranium and the catalyst was filtered off with a syringe filter. The filtrate was evaporated in vacuo and the labile tritium was removed by repeated evaporations from EtOH solution. Finally 7.03 GBq of [^{3}H]JWH-018 was isolated as a white solid that was purified by HPLC on a Phenomenex Luna C18(2) column (k'= 8.08 (t_R= 19.1 min), linear gradient of 50→95% B in A over 25 min). The specific activity was determined by using an HPLC peak area calibration cuve recorded with **24,** and it was found to be 1.48 TBq/mmol. The tritium labeled JWH-018 was dissolved in EtOH (37 MBq/mL) and stored under liquid nitrogen.

3.7. Radiolabeling of hemopressin(1–7)

The precursor peptide ΔPro^1-Hp(1–7) (2 mg, 2.32 μmol) was dissolved in DMF and 3 mg Pd/$BaSO_4$ catalyst was added to the solution. The reaction mixture was degassed prior to tritium reduction by two freeze–thaw cycles. Then it was stirred under 0.4 bar tritium gas for 1 h at r.t., followed by the filtration of the catalyst through a Whatman GF/C glass fiber filter. The filtrate was evaporated and labile tritium was removed by repeated evaporations from aqueous EtOH solution. Finally 2.85 GBq of crude [^{3}H]Hp(1–7) was obtained that was purified by HPLC. Quantitative analyses of the concentration and radioactivity of [^{3}H]Hp(1–7) were performed by RP-HPLC via UV and radioactivity detection using a calibration curve

made by Hp(1–7), and the specific activity of [^{3}H]Hp(1–7) was found to be 1.04 TBq/mmol (28 Ci/mmol). The radioligand was aliquoted as ethanolic solutions and stored in liquid nitrogen until application.

3.8. Preparation of brain membrane homogenates

Male Wistar rats and guinea pigs were locally bred and handled according to the European Communities Council Directives (86/609/ECC) and to the Hungarian Act for the Protection of Animals in Research (XXVIII.tv. Section 32). Crude membrane fractions were prepared from the brain without cerebellum. Brains were quickly removed from the euthanized animals and directly put in ice-cold 50 mM Tris-HCl (pH 7.4) buffer. The collected tissue was then homogenized in 30 volumes (v/w) of ice-cold buffer with a Braun Teflon-glass homogenizer at the highest rpm. The homogenate was centrifuged at 20 000 × g for 25 min and the resulting pellet was suspended in the same volume of cold buffer followed by incubation at 37°C for 30 min to remove endogenous ligands. After centrifugation the pellets were taken up in five volumes of 50 mM Tris-HCl (pH 7.4) buffer containing 0.32 M sucrose and stored in aliquots at –80°C. Prior to the experiment, aliquots were thawed and centrifuged at 20 000 × g for 25 min and the pellets were resuspended in 50 mM Tris-HCl (pH 7.4), homogenized with a Dounce followed by the determination of the protein content by the method of Bradford. The membrane suspensions were immediately used either in radioligand binding experiments or in [^{35}S]GTPγS functional assays.

3.9. Radioligand binding assays

Binding experiments of [^{3}H]JWH-018 were performed at 30°C for 60 min in 50 mM Tris-HCl binding buffer (pH 7.4) containing 2.5 mM EGTA, 5 mM $MgCl_2$ and 0.5 mg/mL fatty acid free BSA in plastic tubes in a total assay volume of 1 mL that contained 0.3–0.5 mg/mL membrane protein. Binding experiments of [^{3}H]Hp(1-7) were carried out at 37°C in plastic tubes in a final volume of 1 mL 50 mM Tris-HCl (pH 7.4) containing 3 mM $MgCl_2$, 0.2–0.5 mg/mL membrane protein and 1% (w/v) BSA.

Association time course of [^{3}H]JWH-018 binding was obtained by incubating 0.6 nM [^{3}H]JWH-018 with rat brain membrane (0.45 mg/mL protein) at 30°C for various period time (0–90 min) in the absence or presence of 10 μM JWH-018 to assess specific binding. Dissociation time course of [^{3}H]JWH-018 was obtained by incubating 0.6 nM [^{3}H]JWH-018

with rat brain membrane (0.45 mg/mL protein) at 30°C for 60 min, then dissociation was initiated by the addition of 10 μM JWH-018 after different periods of incubation time. The kinetic equilibrium dissociation constant (K_d) for [^{3}H]JWH-018 in rat brain membrane homogenate was calculated as $K_d = k_d/k_a$, where k_d is the dissociation rate constant, k_a is the association rate constant calculated as $k_a = (k_{obs}-k_d)/[[^3H]JWH-018]$, k_{obs} is the observed pseudo-first order rate constant. Saturation binding experiments were performed by measuring the specific binding of [^{3}H]JWH-018 (0.5−35 nM) to rat brain membranes to determine the equilibrium dissociation constant (K_d) and the maximal number of binding sites (B_{max}). The non-specific binding was determined in the presence of 10 μM JWH-018. Competition binding experiments were carried out by incubating brain membranes with opioid and cannabinoid receptor specific tritiated radioligands in the presence of increasing concentrations (10^{-11}–10^{-5} M) of various competing unlabeled ligands. MOR competition experiments were performed at 25°C for 60 min with 2 nM [^{3}H]DAMGO (K_d= 0.5 nM), DOR competition experiments were performed at 35°C for 45 min with 3 nM [^{3}H]Ile^{5,6}-deltorphin-2 (K_d= 2.0 nM) and KOR competition experiments were performed at 25°C for 30 min with 1 nM [^{3}H]HS-665 (K_d= 0.64 nM) in 50 mM Tris-HCl binding buffer (pH 7.4) using rat brain (MOR, DOR) or gunine pig brain membrane homogenate (KOR). Non-specific binding was determined in the presence of 10 μM naloxone (MOR, DOR) or HS-665 (KOR). CB receptor binding experiments were performed at 30°C for 60 min on rat brain membrane homogenates with 0.6 nM [^{3}H]JWH-018 (K_d= 6.5 nM) or with 1.5 nM [^{3}H]WIN-55,212-2 (K_d= 10.1 nM). Non-specific binding was determined in the presence of 10 μM JWH-018 or WIN-55,212-2. The competition experiments were terminated by diluting the suspensions with ice-cold wash buffer (50 mM Tris-HCl, 2.5 mM EGTA, 5 mM $MgCl_2$, 0.5% fatty acid free BSA (pH 7.4) for cannabinoid binding, or 50 mM Tris-HCl (pH 7.4) for opioid binding) followed by rapid filtration through Whatman GF/B or GF/C (MOR, KOR) glass fiber filters (Whatman Ltd, Maidstone, England) presoaked with 0.1% polyethyleneimine (only for CB receptor binding). Filtration was performed with a 24-well Brandel cell harvester (Gaithersburg, MD, USA). Filters were air-dried and immersed into Ultima Gold MV scintillation cocktail and then radioactivity was measured with a TRI-CARB 2100TR liquid scintillation analyser (Packard).

3.10. Ligand stimulated [^{35}S]GTPγS binding assay

Rat brain membranes (30 μg protein/tube) were incubated with 0.05 nM [^{35}S]GTPγS (PerkinElmer) and with 10^{-10}–10^{-5} M unlabeled ligands in the presence of 30 μM GDP, 100

mM NaCl, 3 mM $MgCl_2$ and 1 mM EGTA in 50 mM Tris-HCl buffer (pH 7.4) for 60 min at 30°C. Basal [^{35}S]GTPγS binding was measured in the absence of ligands and set as 100%. Nonspecific binding was determined by the addition of 10 μM unlabeled GTPγS and subtracted from total binding. Incubation, filtration and radioactivity measurement of the samples were carried out as described above.

3.11. Cell culture and permeability assay

Primary rat brain endothelial cells, pericytes and astroglia cells were isolated and cultured according to the method described in our previous studies.[127,128] To induce BBB characteristics the isolated cells were co-cultured with the help of 12-well tissue culture inserts (Transwell, polycarbonate membrane, 3 μm pore size, Corning Costar, USA). After two days of co-culture brain endothelial cells became confluent and 550 nM hydrocortisone (Sigma) was added to the culture medium and one day before the experiment cells were treated with CPT-cAMP (250 mM, Sigma) and RO 201724 (17.5 mM; Sigma) for 24 h to tighten junctions and elevate transendothelial resistance.[129] Permeability tests on the co-cultured BBB model were performed when transendothelial electrical resistance values expressed to the surface area of the inserts reached 123.8 ± 12.9 Ω cm^2, n= 16. The resistance of cell-free inserts was subtracted from the measured data. During the permeability assay the culture medium was changed with the same as used in the growth period, but it also contained 10 % serum. Compounds [^{3}H]**11** and [^{3}H]**19** were applied in the upper compartment in a final concentration of 0.25 and 0.75 μM. Compound permeability was measured from the AB (from blood to brain) direction. After 15, 30 and 60 min samples were collected both from the upper and lower compartments and the transport of [^{3}H]**11** and [^{3}H]**19** was determined by measuring the radioactivity using a TRI-CARB 2100TR liquid scintillation analyser (Packard). Flux of the compounds across coated, cell-free inserts was also measured. Endothelial permeability coefficients (P_e) were calculated from clearance values of [^{3}H]**11** and [^{3}H]**19** as described previously.[129]

3.12. Data analysis

In competition binding studies, the inhibitory constants (K_i) were calculated from the inflexion points of the displacement curves using nonlinear least-square curve fitting option and the Cheng-Prusoff equation as $K_i = EC_{50}/(1 + [ligand]/K_d)$. In [^{35}S]GTPγS binding studies,

data were expressed as the percentage stimulation of the specific [^{35}S]GTPγS binding over the basal activity. Each experiment was performed in triplicate and analyzed with the sigmoid dose-response curve fitting option to obtain potency (ED_{50}) and efficacy (E_{max}).

Statistical comparison of the [^{35}S]GTPγS binding results were performed by analysis of variance (one-way ANOVA) followed by the Bonferroni's multiple comparison test (***, $P< 0.001$; **, $P< 0.01$) . To indicate significant difference in the E_{max} of compound **11** and **19** in the presence of 10 μM naloxone compared to the basal activity unpaired Student's t-test was used. $P< 0.05$ was considered significant. All data and curves were analyzed by the GraphPad Prism 5.0 Software, San Diego, CA, USA.

4. Results

4.1. Synthesis of monomeric and bivalent compounds

In order to develop novel bivalent ligands targeting both the MOR and CB receptors or their heteroreceptor complexes with the capability to produce antinociception, two types of heterodimeric compounds containing an opioid and a cannabinoid pharmacophore were designed. One of the two sets was composed of oxycodone, while the other contained the tetrapeptide Tyr-D-Ala-Gly-Phe as the opioid pharmacophore. The MOR agonist oxycodone[130-132] is widely used in the treatment of severe pain either in monodrug therapy or in combination with other drugs such as cannabinoids.[106,119,133,134] The enkephalin-related tetrapeptide Tyr-D-Ala-Gly-Phe[135-138] was also applied to diversify the ligand set and to investigate the peptidic modification of a CB receptor agonist. Because CB receptor agonists can modulate hyperalgesia of various origin and show effective therapeutic value against inflammatory and neuropathic pain[139] both opioid pharmacophores were combined with the full agonist naphthalen-1-yl(1-pentyl-1*H*-indol-3-yl)methanone (JWH-018 or AM 678). This indole-type cannabimimetic that structurally relates to WIN-55,212-2 binds to both the CB1 and CB2 receptors with low nanomolar affinity, and exhibits in vivo cannabinoid pharmacological effects.[42,49,140]

The bivalent compounds were prepared in a convergent way, and the conjugation of the opioid and cannabinoid pharmacophore units was performed directly or via spacers of different length (1, 2, 3, 6,13 atoms) and polarity.

4.1.1. Oxycodone – JWH-018 bivalent compounds

Oxycodone and JWH-018 were modified at the 6-oxo and at the *N*-pentyl groups, respectively, to obtain the key intermediates. Condensation of oxycodone with 2-(aminooxy)acetic acid in EtOH resulted in the linker conjugated *O*-carboxymethyl ketoxime **1** (Scheme 1) and this way the introduction of a new asymmetric centre was excluded. Furthermore, the ketoximes are stable under physiological conditions, therefore the bivalent ligands are probably stable against hydrolysis. In comparison, when reductive amination was applied to introduce the amino linker group into oxymorphone[112,141,142] carbon 6 became chiral resulting in epimeric products. In the next step the carboxymethyl group of **1** was activated as an *O*-benztriazolyl ester, that was used for the *N*-acylation of the mono-protected

spacers *N*-Boc-ethylenediamine, *N*-Boc-1,6-diaminohexane and *N*-Boc-4,7,10-trioxa-1,13-tridecanediamine. The final acidolytic removal of the Boc protecting group resulted in the amines **5**–**7**.

JWH-018 was functionalized by introducing a terminal carboxyl group to the *N*-pentyl substituent of the indole ring. This modification does not affect the aromatic groups of JWH-018 that are responsible for aromatic interactions with the CB receptors.[52] Furthermore, the introduction of heteroatoms to the alkyl group may be tolerated by CB1 receptors as in the case of the morpholino group of WIN-55,212-2.[143,144] The carboxyl derivative of JWH-018 (**9**) was prepared in a way analogous to that reported by Huffman et al.[52] The *N*-alkylation of indole was achieved with 6-bromohexanoic acid, then **8** was selectively acylated at position 3 with 1-naphthoyl chloride in the presence of Et_2AlCl. Finally, **9** was activated as an *O*-benztriazolyl ester and it was used for the *N*-acylation of the amines **5**–**7** resulting in the heterodimerized compounds **10**–**12**.

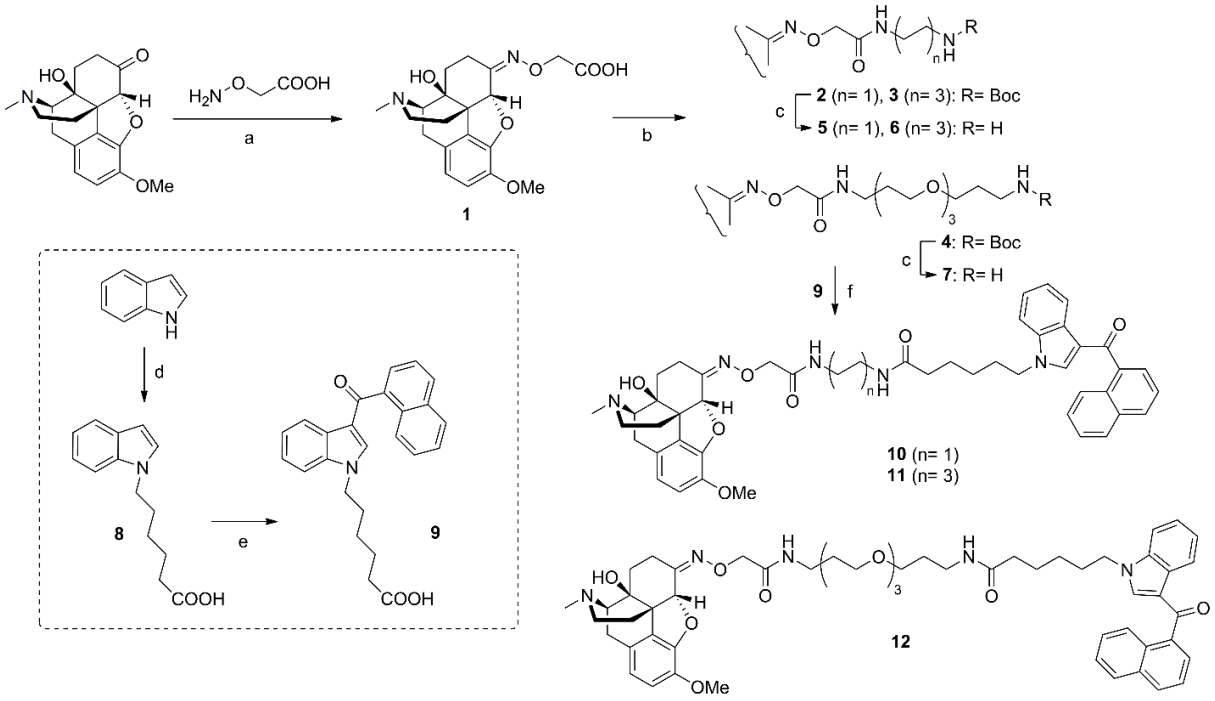

Scheme 1. Preparation of oxycodone – JWH-018 bivalent compounds
Reagents and conditions: a) EtOH, pyridine, 80°C, 75 min, 93%; b) HOBt, DIC, DIEA, DMF, 50°C, 16h, 81% (**2**), 77% (**3**), 66% (**4**); c) TFA/DCM (1:1), 30 min, 95% (**5**), 96% (**6**), 95% (**7**); d) 6-bromohexanoic acid, TEA, ACN, 80°C, 16 h, 77% (**8**); e) 1-naphthoyl chloride, Et_2AlCl, DCM, 0°C, 16 h, 42% (**9**); f) HOBt, DIC, DIEA, DMF, 50°C, 16 h, 79% (**10**), 71% (**11**), 61% (**12**).

4.1.2. Peptide– JWH-018 bivalent compounds

In the case of the peptidic compounds the *C*-terminal carboxyl function of the peptide acids was used for the conjugation. The peptidic compounds **18**–**21** were prepared in a similar convergent way (Scheme 2) and glycine, 3-aminopropanoic acid or 4-aminobutanoic acid were used as spacers between the opioid and cannabinoid pharmacophores. Indole was regioselectively acylated with 1-naphthoyl chloride and the resulting 3-(α-naphthoyl)-indole **13** was *N*-alkylated with *N*-Boc-5-bromopentane-1-amine (**14**). Acidolytic removal of the Boc protecting group of the carbamate **15** resulted in the JWH-018 derivative **16** with a terminal amine in the *N*-pentyl group. The *N*-acetylation of **16** with Ac_2O in the presence of triethylamine in DCM at r.t. resulted in the control compound **17**. The elongation of **16** with the opioid peptide or with a spacer amino acid followed by the opioid peptide were achieved in stepwise Boc/*t*Bu solution phase peptide synthesis using EDC and HOBt as coupling agents. All peptide intermediates were purified by flash chromatography on silica gel and the peptidic compounds **18**–**21** were obtained in 12-25% overall yield.

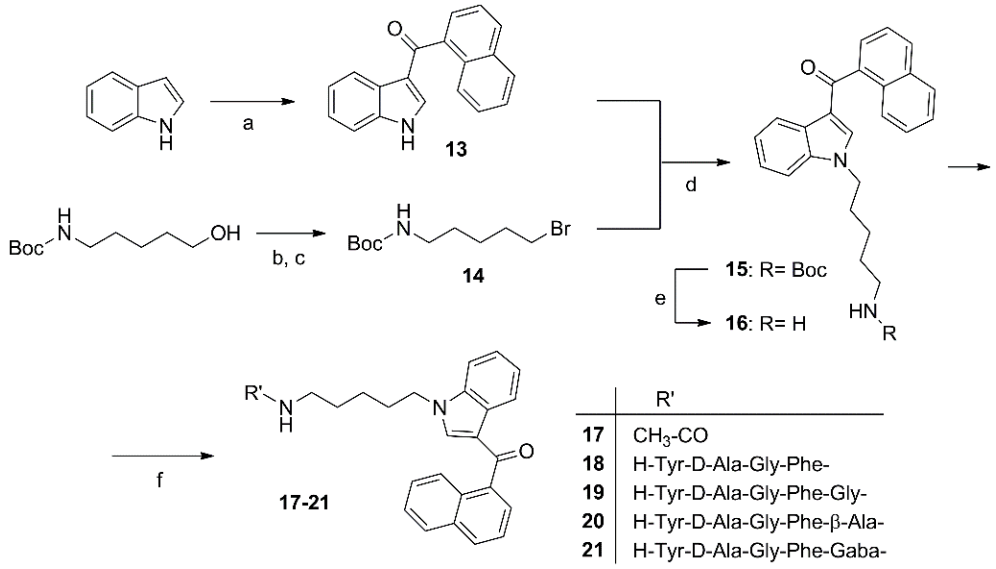

Scheme 2. Preparation of peptide – JWH-018 bivalent compounds
Reagents and conditions: a) 1-Naphthoyl chloride, Et_2AlCl, DCM, 0°C, 16 h, 70% (**13**); b) MsCl, TEA, DCM, –10°C, 5 h; c) LiBr, THF, reflux, 16 h, 72% (**14**); d) NaH, DMF, 80°C, 18 h, 85% (**15**); e) TFA/DCM (1:1), r.t., 30 min, 97% (**16**); f) Ac_2O, TEA, DCM, r.t., 16 h, 91% (**17**), or Boc stepwise peptide synthesis: EDC, HOBt.H_2O, NMM, DMF, DCM, and deprotection with TFA/DCM (1:1), r.t., 30 min; overall yields 21% (**18**), 14% (**19**), 25% (**20**), 12% (**21**).

4.2. Radiolabeling of JWH-018

The *in vitro* characterization of the bivalent compounds in radioligand displacement studies required appropriate opioid and cannabinoid radioligands. The most commonly used CB radioligands in heterologous competition binding experiments are [^{3}H]CP-55,940, [^{3}H]HU-243, [^{3}H]WIN-55,212-2, [^{3}H]SR-141716A (rimonabant), [^{3}H]SR-144528 and [^{3}H]Sch225336.[145] However, the structural diversity of the CB receptor ligands[6] and the presence of allosteric site on the CB receptors[146] prompted us to prepare a novel radioligand relevant for the investigation of the CB receptor binding affinities of the JWH-018 containing bivalent compounds. JWH-018 was identified as a potent synthetic CB receptor agonist among indole-type cannabinoids that structurally relates to WIN-55,212-2 and was found to be more potent than Δ^9-THC.[42,52,151] JWH-018 exhibits typical cannabinoid pharmacology *in vivo* and has high affinity for both CB receptors (K_i(CB1)= 9.00 nM, K_i(CB2)= 2.94 nM).[51,140] JWH-018 was labeled with tritium as outlined in Scheme 3 and the resulting radioligand was validated *in vitro*.

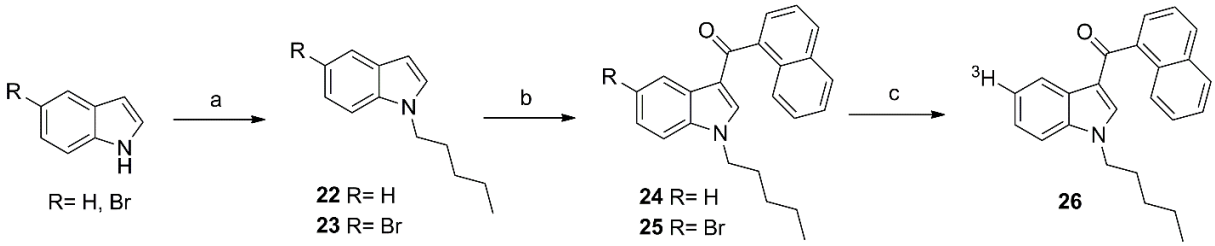

Scheme 3. Tritium labeling and preparation of JWH-018
Reagent and conditions: a) (**22**) 1-iodopentane, TEA, ACN, 80°C, 16 h, 75%, (**23**) 1-iodopentane, NaOH, DMF, r.t., 4 h 66%; b) Et_2AlCl, 1-naphthoyl chloride, DCM, 0°C, 16 h, 72% (**24**), 82% (**25**); c) $^3H_{2(g)}$, Pd/C, EtOAc, TEA, r.t., 4 h.

N-Alkylation of 5-bromoindole with 1-iodopenthane was achieved in the presence of triethylamine followed by acylation with 1-naphthoyl chloride that resulted in the brominated precursor **25**. Then **25** was dehalogenated with tritium gas under heterogeneous catalytic conditions and [^{3}H]JWH-018 (**26**) was obtained with a specific activity of 1.48 TBq/mmol. In a similar way, unlabeled JWH-018 (**24**) was also prepared for the radioligand binding experiments (Scheme 3).

4.3. Characterization of the novel CB receptor radioligand [^{3}H]JWH-018

Before its application in radioligand competition assays, [^{3}H]JWH-018 was characterized in various *in vitro* receptor binding experiments. Association and dissociation binding experiments were performed to characterize the interaction of [^{3}H]JWH-018 with membrane receptors using rat brain membrane homogenates. Association binding experiments were carried out in the presence of 0.6 nM [^{3}H]JWH-018 at 30°C and they revealed specific binding of [^{3}H]JWH-018 to rat brain membranes (Figure 4A). At this temperature the specific binding determined in the presence of 10 μM JWH-018 reached steady-state after 40 min, and it remained stable up to 90 min, the longest incubation time investigated (not shown). The specific binding was found to be 65% of the total binding at 0.6 nM radioligand concentration under equilibrium conditions. Analyzing the association curve provided an observed pseudo-first order rate constant (k_{obs}) of 0.124 ± 0.01 min^{-1}. In the dissociation experiments, rat brain membranes were incubated with 0.6 nM of [^{3}H]JWH-018 at 30°C for 60 min and dissociation of the ligand–receptor complex was initiated by the addition of 10 μM JWH-018 at different incubation periods (Figure 4B). It was found that 60% of the radioligand dissociated from the membranes. Dissociation proceeded with a monophasic kinetics and it resulted in a dissociation rate constant (k_d) of 0.105 ± 0.01 min^{-1}. The equilibrium dissociation constant (K_d) calculated from the kinetic data was 3.4 nM under our experimental conditions. Saturation binding experiments were then performed to determine the K_d and B_{max} values. The radioligand was incubated with rat brain membranes at increasing concentrations (0–35 nM) in the absence or presence of JWH-018. The specific binding of [^{3}H]JWH-018 was found to be saturable and of high affinity in the nanomolar range (Figure 4C).

Accordingly, a single-site binding was calculated from the non-linear fitting of the specific binding data and resulted in an apparent K_d value of 6.5 ± 1.22 nM and a high receptor density (B_{max}) of 1120 ± 89 fmol/mg protein.

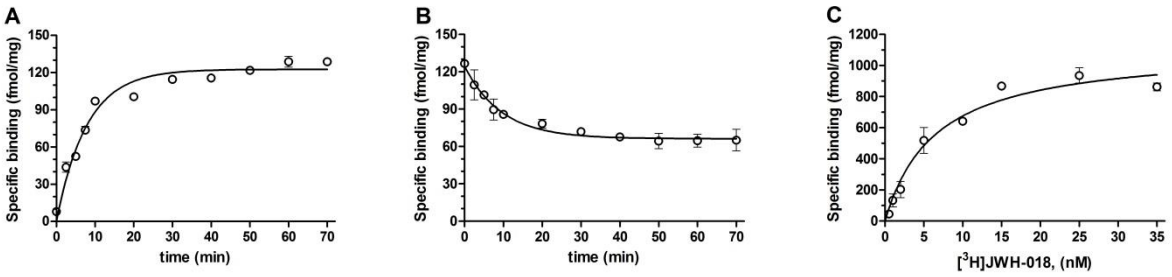

Figure 4. Binding of [^{3}H]JWH-018 to rat whole brain membrane homogenates (0.45 mg/mL protein). (A) Association and (B) dissociation time courses of [^{3}H]JWH-018 at 30°C; (C) saturation isotherm of specific CB receptor binding of [^{3}H]JWH-018 at 30°C for 60 min incubation. Data are means ± SEM (n≥ 3).

Because [^{3}H]JWH-018 labeled membrane receptors of the rat brain membrane homogenate with high densities and it displayed specific binding to a receptor protein, the binding site of [^{3}H]JWH-018 was further investigated in competition experiments using selective and non-selective cannabinoid ligands. The displacement curves are summarized in Figure 5 and the calculated inhibitory constants (K_i) are summarized in the table of Figure 5. In homologous displacement experiments the full agonist JWH-018 exhibited a K_i value of 3.4 ± 0.80 nM. WIN-55,212-2, another full agonist cannabinoid ligand displayed high affinity to the JWH-018 binding sites, while the partial agonist Δ^9-tetrahydrocannabinol (Δ^9-THC) competed for the JWH-018 binding sites with 11-times lower affinity. The CB2 receptor selective, inverse agonist AM 630 was found to be effective in displacing [^{3}H]JWH-018 from CB2 receptors. Further experiments revealed that the CB1 receptor selective antagonist/inverse agonist rimonabant and the structurally very similar CB1 selective antagonist/inverse agonist AM 251 were less effective in displacing [^{3}H]JWH-018 from CB1 receptors on rat brain membrane homogenate. AM 251 displaced 80% of the radioligand from JWH-018 binding sites, while the CB2 selective inverse agonist AM 630 displaced approximately 70% of [^{3}H]JWH-018 from CB2 receptors on rat brain membrane homogenate. Compound **25** was also investigated in heterologous displacement studies, because beside to be a precursor for tritium labeling it is a potentially bioactive JWH-018 derivative substituted at position 5 with bromine. It exhibited good CB receptor affinity in displacing [^{3}H]JWH-018 with a K_i value of 59 ± 3.3 nM. Interestingly, the 5-bromo-substituted intermediate **25** exhibited receptor affinity similar to that of rimonabant, AM 630 and AM 251. Furthermore, the results confirm that JWH-018 is a non-selective full agonist in the low nanomolar range with a CB1/CB2 receptor selectivity ratio of 3 (K_i(AM 251)= 69 ± 9.1 nM) / K_i(AM 630)= 23 ± 19 nM) that is similar to other reported data.[51] In our experimental model, the investigated cannabinoid ligands competed for [^{3}H]JWH-018 binding sites with the following order of

potency: JWH-018 > WIN-55,212-2 > AM 630 > rimonabant > **25** > AM 251 > Δ^9-THC > hemopressin(1-9) (Figure 5A, B).

Then competition binding experiments were performed to compare the ability of the endogenous peptide cannabinoid RVD-hemopressin and its derivatives hemopressins(1–7) and (1-9) to inhibit the binding of [^{3}H]JWH-018 in rat brain membrane homogenate. It was found that neither the *N*- and *C*-terminally truncated hemopressin(1–7),[147] nor the CB_1 negative and CB_2 receptor positive allosteric modulator RVD-hemopressin[40,41] could displace the bound radioligand. Only the nonapeptid CB_1 inverse agonist/antagonist hemopressin(1-9)[27] was able to compete with [^{3}H]JWH-018 with an apparently high inhibitory constant of 2793 ± 4.1 nM, however, hemopressin(1-9) could only partially (c.a. 40%) displace [^{3}H]JWH-018 (Figure 5B). These results indicated that the allosteric binding site of the peptidic ligands is different from that of the non-peptidic cannabinoid agonists/inverse agonists, and that JWH-018 presumably bound to the orthosteric binding site of the CB receptor.

It was also important to investigate whether [^{3}H]JWH-018 interacts with the opioid receptors because this radioligand was prepared to characterize the CB receptor binding of the opioid-cannabinoid bivalent ligands. The effects of the opioid ligands morphine, naloxone and endomorphins-1 and -2 on the specific binding of [^{3}H]JWH-018 were measured in the presence of increasing concentration of the opioids. It was found that none of them decreased the specific binding of [^{3}H]JWH-018 even at a concentration of 10 μM, meaning that [^{3}H]JWH-018 did not bind to the opioid receptors (Figure 5C). Finally, competition binding experiments were carried out to evaluate the ability of JWH-018 to inhibit the specific binding of the μ-, δ- and κ-opioid receptor selective radioligands [^{3}H]DAMGO, [^{3}H]Ile^{5,6}-deltorphin-2 and [^{3}H]HS-665,[148] respectively (Figure 5D). For KOR binding the guinea pig brain was used because it contains KORs in higher density as compared to the rat brain. It was found that JWH-018 did not exhibit any binding affinity to the MOR, DOR and KORs when compared to the homologue displacements with DAMGO, Ile^{5,6}-deltorphin-2 or HS-665, respectively.

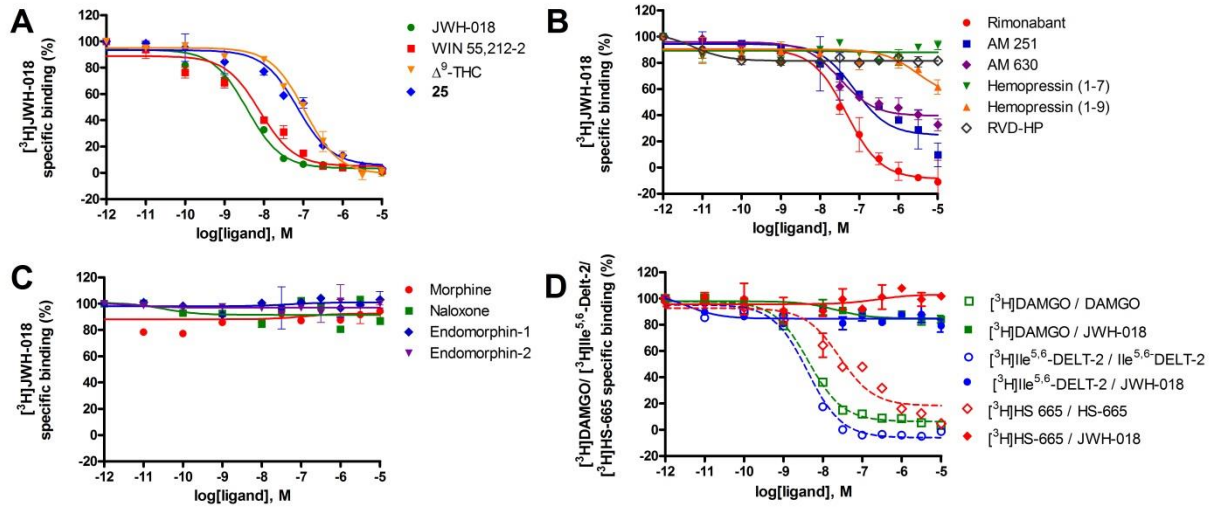

Cannabinoid ligand	K_i (nM)	Cannabinoid ligand	K_i (nM)
JWH-018	3.4 ± 0.8	AM 251	69 ± 9.1
WIN-55,212-2	7.2 ± 2.8	AM 630	27 ± 2.2
Δ^9-THC	82 ± 4.5	Hemopressin (1-7)	>10000
25	59 ± 3.3	Hemopressin (1-9)	2793 ± 41
Rimonabant	43 ± 5.5	RVD-Hemopressin	>10000

Figure 5. Characterization of JWH-018 binding sites in competition binding experiments in rat or guinea pig ([^{3}H]HS665) whole brain membrane homogenates. (A-C) The specific binding of [^{3}H]JWH-018 in the presence of unlabeled cannabinoid or opioid ligands. (D) The specific binding of the MOR, DOR and KOR specific radioligands [^{3}H]DAMGO, [^{3}H]Ile^{5,6}-deltorphin-2 and [^{3}H]HS-665, respectively, in the presence of JWH-018 (filled symbols) or in the presence of the corresponding unlabeled opioid ligand (open symbols). Data are mean percentage of specific binding ± SEM (n≥ 3). Table shows the calculated inhibitory constants against [^{3}H]JWH-018. K_i values were calculated as $K_i = EC_{50}/(1 + [ligand]/K_d)$, where K_d= 6.5 nM was obtained from the saturation experiment; data are means ± SEM, n≥3.

4.4. Radioligand binding studies

In order to assess the effects of the structural changes of the monomeric ligands on the biological activity and to evaluate the heterodimeric compounds for affinity and selectivity, the novel synthetic compounds were subjected to radioligand displacement assays.

Displacements of the MOR selective radioligand [^{3}H]DAMGO, the DOR selective [^{3}H]Ile^{5,6}-deltorphin-2, the KOR selective [^{3}H]HS-665 and the cannabinoid radioligands

[^{3}H]JWH-018 and [^{3}H]WIN-55,212-2 by the linker conjugated oxycodone derivatives (**5**–**7**) and by the related bivalent compounds (**10**–**12**) were investigated in rat or guinea pig brain membrane homogenates (Figure 6, Table 1). It was found that the modification of oxycodone at position 6 with the *O*-carboxymethyl oxime function (**1**) resulted only in a 2.7-fold loss of MOR affinity, a 4-fold increased affinity for the DOR and loss of KOR affinity. The MOR selectivity of oxycodone over DOR was reduced 90% by the introduction of the linker group in **1**. The introduction of a terminal carboxyl function to the pentyl chain of JWH-018 (**9**) decreased the CB receptor affinity down to the 200 nM range. These findings encouraged us to further investigate the bivalent ligands and their synthetic intermediates. The introduction of the spacer molecules to **1** resulted in only minor loss of MOR affinity (K_i= 17-74 nM), that was beneficial to prepare the bivalent compounds with spacers of different physico-chemical properties. The introduction of the ethylenediamine (**5**) and the 1,6-diaminohexane spacers (**6**) resulted in 2-fold and 5-fold loss of MOR affinity, respectively, while the incorporation of the *O*-,*O*'-bis(3-aminopropyl)-diethyleneglycol spacer (**7**) resulted in an 8-fold loss of MOR affinity as compared to the parent compound oxycodone. The dimeric compounds **10**–**12** exhibited good affinity to the MOR that was only 2-4-fold lower than the MOR affinity of the parent oxycodone. The selectivity of the dimeric compounds **10**–**12** for the MOR over DOR was 15-19, while their MOR selectivity over KOR was found to be 9-10. Next, compounds **10**–**12** were further characterized to reveal their CB receptor affinities. In competition binding experiments the capabilities of the bivalent compounds to displace [^{3}H]JWH-018 and [^{3}H]WIN-55,212-2 were investigated, and it was found that they displaced 40–70% of the specific bound radioligands [^{3}H]JWH-018 or [^{3}H]WIN-55,212-2. The dimeric compound **10** exhibited the highest CB receptor affinity against [^{3}H]WIN-55,212-2, however **11** displaced [^{3}H]JWH-018 most efficiently.

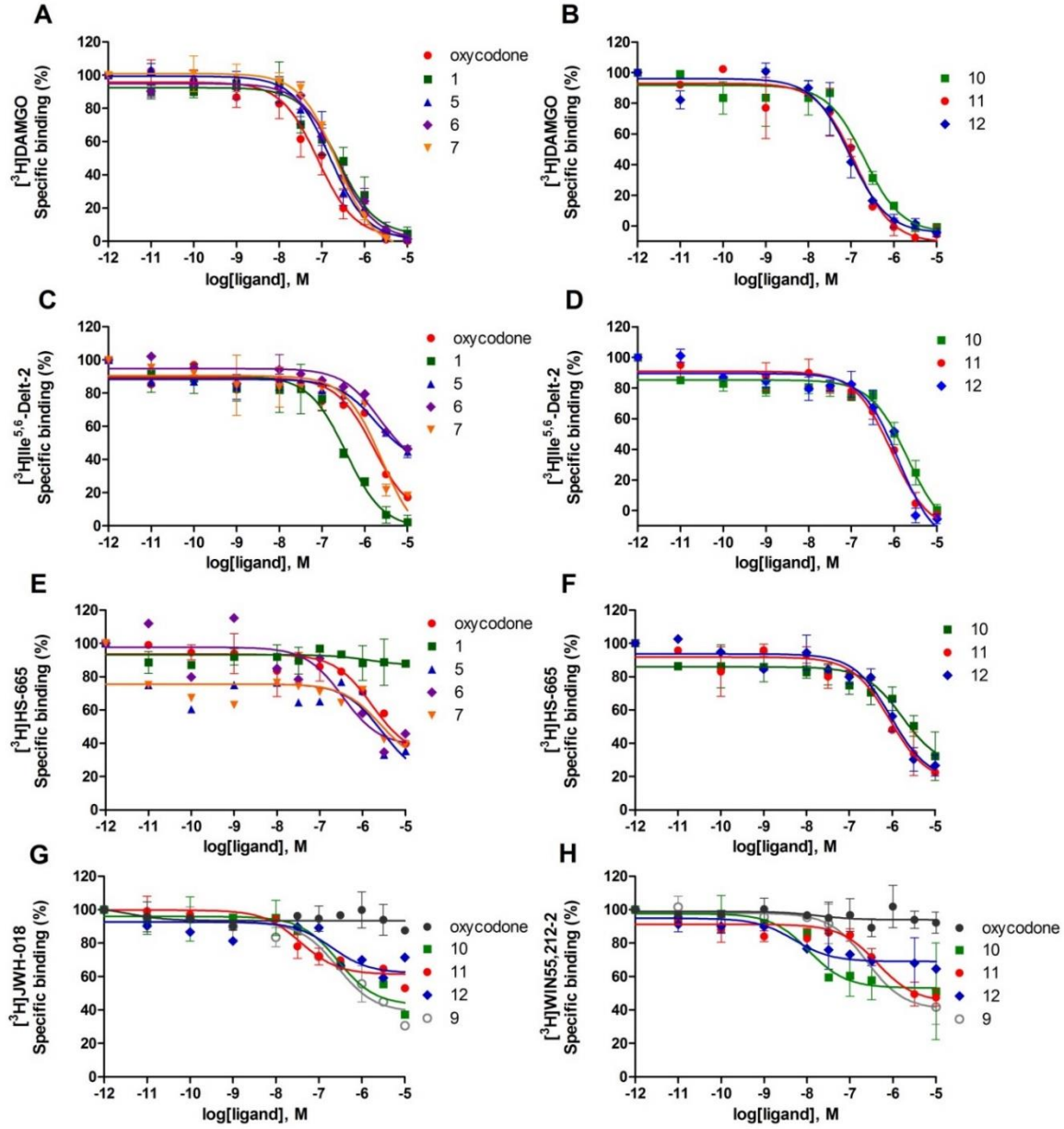

Figure 6. Concentration-dependent effects of the indicated compounds on equilibrium binding of [^{3}H]DAMGO (A-B, MOR), [^{3}H]Ile^{5,6}-deltorphin-2 (C-D, DOR), [^{3}H]HS-665 (E-F, KOR), [^{3}H]JWH-018 and [^{3}H]WIN55,212-2 (G-H, CB receptors) in rat and guinea pig brain membrane homogenates. Figures represent the relative specific binding of the radioligands in the presence of increasing concentrations (10^{-11}–10^{-5} M) of the synthetic compounds. Data are mean values ± SEM ($n \geq 3$). K_i values were calculated according to the Cheng–Prusoff equation ($K_i = EC_{50}/(1 + [ligand]/K_d)$) and are listed in Table 1.

In the next step the peptidic compounds were evaluated for affinity and selectivity by radioligand displacement assays. First, the effect of the structural modification of the monomeric compounds was investigated in displacement studies on rat or guinea pig brain membrane homogenates (Figure 7, Table 2). The opioid pharmacophore Tyr-D-Ala-Gly-Phe-NH_2 exhibited high affinity to the MOR (K_i= 0.8 nM), a 130-times weaker affinity to the

DOR and 210-times weaker affinity to the KOR, and it had no affinity to the CB receptors. The introduction of an amino group into the terminal methyl group of the pentyl chain of JWH-018 resulted in **16** and this modification led to decreased affinity to the [^{3}H]JWH-018 or [^{3}H]WIN-55,212-2 labeled binding sites. The control compound **17** was also prepared and investigated to reveal the effect of the terminal peptide acylamido modification of the JWH-018 pentyl group on the CB receptor binding. The *N*-acetylation of **16** diminished the positively charged functional group and the CB receptor affinity of **17** was found to be higher (K_i= 145 nM) than that of **16**. When **16** was *N*-acylated with the peptide acid Tyr-D-Ala-Gly-Phe-OH or with its *C*-terminally extended derivatives, the resulting bivalent compounds **18**–**21** exhibited minor loss in MOR, DOR and KOR affinity. The binding affinity of **19** and **21** for KOR was 2-3 times higher than that of the Tyr-D-Ala-Gly-Phe-NH_2. In [^{3}H]JWH-018 and [^{3}H]WIN-55,212-2 displacement experiments **19** exhibited the highest affinity to the CB receptors among the peptidic bivalent compounds (K_i= 251 and 317 nM, respectively), and **19** was able to decrease the [^{3}H]JWH-018 and [^{3}H]WIN-55,212-2 specific binding by about 45-50%. In contrast, the CB receptor affinity of **18**, **20** and **21** decreased significantly.

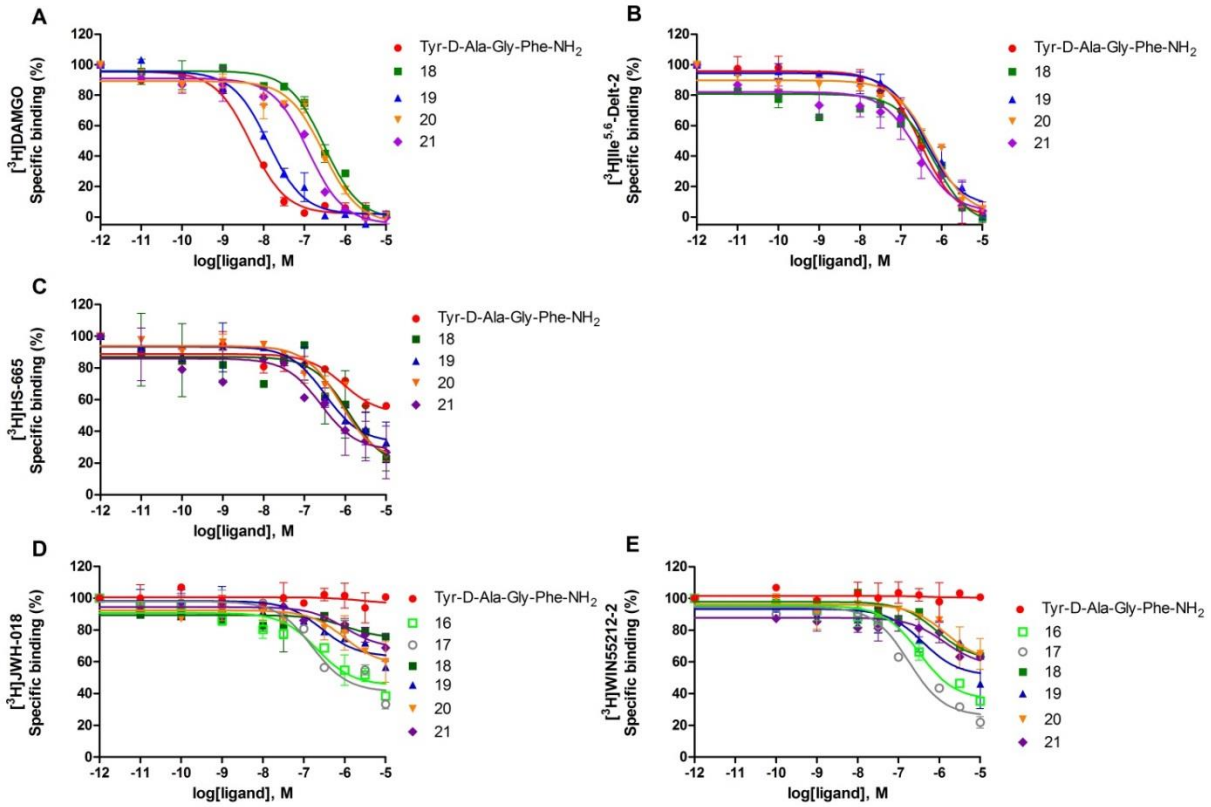

Figure 7. Concentration-dependent effects of the indicated compounds on equilibrium binding of [^{3}H]DAMGO (A, MOR), [^{3}H]Ile^{5,6}-deltorphin-2 (B, DOR), [^{3}H]HS-665 (C, KOR), [^{3}H]JWH-018 and [^{3}H]WIN55,212-2 (D-E, CB receptors) in rat and guinea pig brain membrane homogenates. Figures represent the relative specific binding of the radioligands in the presence of increasing concentrations (10^{-11}–10^{-5} M) of the synthetic compounds. Data are mean values ± SEM (n≥ 3). K_i values were calculated according to the Cheng–Prusoff equation ($K_i = EC_{50}/(1 + [ligand]/K_d)$) and are listed in Table 2.

4.5. [^{35}S]GTPγS functional binding assays

To determine whether the linker modified ligands **1** and **9**, the spacer conjugates **5**–**7** and the bivalent compounds **10**–**12** retain their ability to stimulate the receptor-associated G-proteins, the synthetic compounds were subjected to ligand-stimulated [^{35}S]GTPγS binding assays in rat brain membrane homogenate. It is important to mention that this preparation abundantly contains both MOR and CB receptors, therefore it is an appropriate model to investigate the capability of the MOR agonist oxycodone and its derivatives, and also the cannabinoid agonist JWH-018 and its derivatives. In these experiments the oxycodone derivatives exhibited lower potencies than the parent oxycodone, and significant reduction of the stimulatory effects was also observed (Figure 8, Table 1). Coupling of the spacers to **1** decreased the efficacy and the partial opioid agonist oxycodone became weaker partial

agonists/neutral antagonists. The full agonist JWH-018 efficiently stimulated the G-proteins, demonstrated high potency (EC_{50}= 69 ± 10 nM) and high stimulatory activity (E_{max}= 163 ± 3.1%), while the introduction of the carboxyl function in **9** changed the full agonist to a weak inverse agonist. Accordingly, the bivalent compounds were expected to show altered pharmacology, as compared to oxycodone. The bivalent compounds **10** and **12** did not induce significant changes in basal [^{35}S]GTPγS binding values, however as described earlier these compounds displayed noticeable opioid and cannabinoid receptor affinity. In contrast, **11** exhibited high G-protein stimulatory effect (E_{max}= 147 ± 3.8%, EC_{50}= 215 nM) demonstrating the agonist character of **11**. To explore the activation of MOR and/or CB1/CB2 receptor-mediated signaling induced by **11**, the G-protein activation was investigated with **11** in the absence or presence of 10 μM naloxone, 10 μM rimonabant or 10 μM AM 630. The stimulatory effect of **11** (E_{max}= 147 ± 4.0%, EC_{50}= 224 ± 5.0 nM) was reduced by the opioid antagonist naloxone[147] (10 μM) (E_{max}= 112 ± 2.1%, EC_{50}= 397 ± 34 nM). Because naloxone did not reduce the G-protein stimulatory effect to the basal level, the residual activity suggested that **11** could activate the CB receptors as well. The CB1 antagonist/inverse agonist rimonabant (10 μM) slightly antagonized the G-protein stimulatory effect of **11** (E_{max}= 139 ± 2.4%, EC_{50}= 452 ± 24 nM), while the CB2 antagonist/inverse agonist AM 630 (10 μM) had greater antagonistic effect (E_{max}= 122 ± 2.7%, EC_{50}= 340 ± 7.5 nM) (Figure 9). In order to decrease the stimulatory effect of **11** to the basal level, the co-presence of naloxone, rimonabant and AM 630 was required. Taken together, these interactions indicated a bivalent opioid and CB (mostly CB2) receptor dependent agonist effect of **11**.

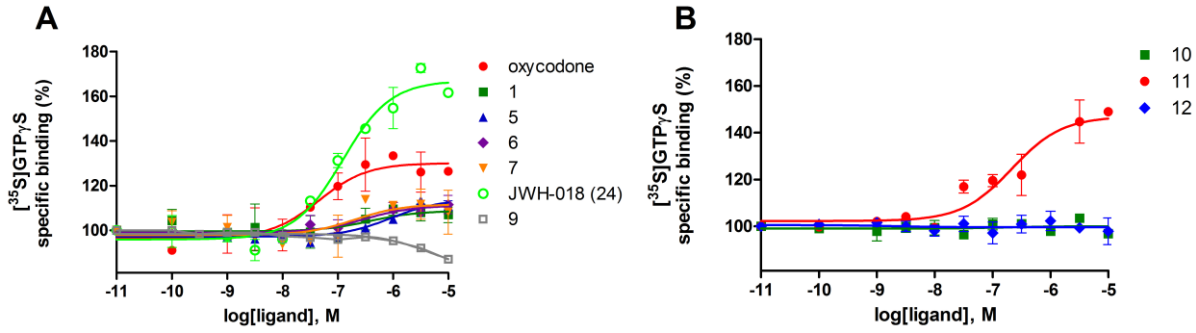

Figure 8. The effect of the synthetic compounds on G-protein activation in [^{35}S]GTPγS binding assays in rat brain membrane homogenates. Figures represent relative specific binding of [^{35}S]GTPγS in the presence of increasing concentrations (10^{-10}–10^{-5} M) of the indicated compounds. Data are mean percentage of specific binding ± SEM (n≥ 3) over the basal activity of 100%. The maximal G-protein stimulation efficacy (E_{max}) and ligand potency (EC_{50}) values are listed in Table 1.

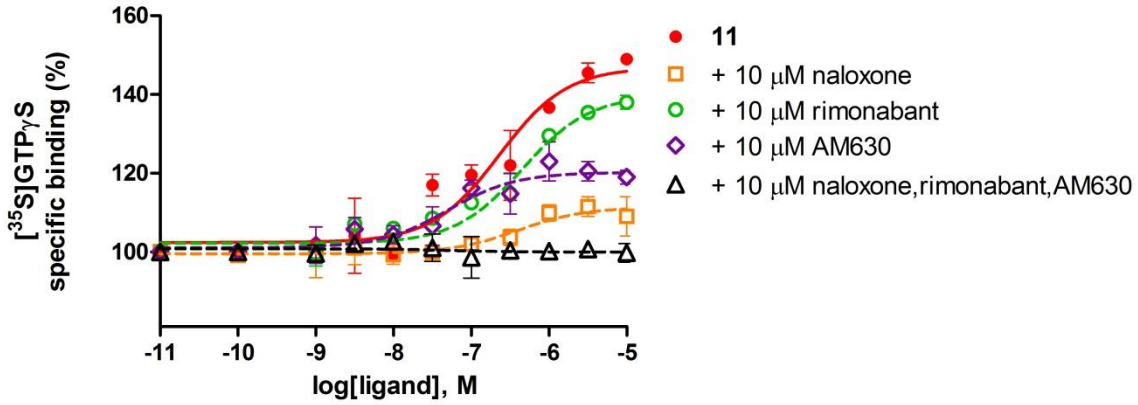

	E_{max} (%)	EC_{50} (nM)
11	147 ± 4.0	224 ± 5.0
11 + 10 μM naloxone	112 ± 2.1$^{***/\#}$	397 ± 34***
11 + 10 μM rimonabant	139 ± 2.4***	452 ± 24***
11 + 10 μM AM 630	122 ± 2.7***	340 ± 7.5**
11 + 10-10 μM (naloxone, rimonabant, AM 630)	100 ± 1.1***	n.r.

Figure 9. Opioid and cannabinoid receptor-mediated effects of **11** on G-protein activation in [^{35}S]GTPγS binding assays in rat brain membrane homogenates. Figure represents relative specific binding of [^{35}S]GTPγS with the increasing concentrations (10^{-10}–10^{-5} M) of **11** in the absence or presence of 10 μM naloxone, 10 μM rimonabant or 10 μM AM 630. Data are mean percentage of specific binding ± SEM (n= 3–5) over the basal activity. The calculated maximal G-protein stimulation efficacy (E_{max}) and ligand potency (EC_{50}) values are listed below the graph. Statistical comparison of E_{max} and EC_{50} were performed by one-way ANOVA followed by the Bonferroni's multiple comparison test (***, P< 0.001; **, P< 0.01). $^{\#}$ indicates significant difference (unpaired Student's t-test, P< 0.05) in the E_{max} of **11** in the presence of 10 μM naloxone compared to the basal activity. n.r. not relevant.

Next, the signaling properties of the peptidic bivalent compounds were evaluated in [^{35}S]GTPγS binding experiments (Figure 10, Table 2). According to the G-protein activation and receptor binding affinity, **16** may act as a neutral antagonist on CB receptors, since it did not stimulate G-proteins but displayed a considerable CB receptor affinity in [^{3}H]JWH-018 displacement assays. The *N*-acetylated compound **17** significantly reduced [^{35}S]GTPγS specific binding by nearly 20% as compared to the basal activity level, indicating an inverse agonistic effect. The weak inverse agonistic effect of **17** might be mediated through CB receptors, since it showed a relatively good affinity to the [^{3}H]JWH-018 binding site. The opioid pharmacophore H-Tyr-D-Ala-Gly-Phe-NH_2 increased the G-protein basal activity with a maximum efficacy of 157% and with a potency in the 200 nM range. The bivalent compounds **18**, **20** and **21** exhibited significantly decreased capability of G-protein activation, but **19** exhibited signaling with a maximum efficacy of 160 ± 1.9% that was similar to that of

the monofunctional opioid and cannabinoid pharmacophores. The binding affinity of **19** to the opioid receptors remained nearly the same as the parent tetrapeptide amide or **24**. The stimulatory effect of **19** (E_{max}= 160 ± 1.9%, EC_{50}= 112 ± 7.5 nM) was reduced by the opioid antagonist naloxone[147] (E_{max}= 121 ± 2.5%, EC_{50}= 1473 ± 118 nM). The antagonistic effect of naloxone was found to be incomplete, and the residual activity of **19** indicated CB receptor activation (Figure 11). In contrast to **11**, the CB2 antagonist/inverse agonist AM 630 exerted weak antagonistic effect to **19** (E_{max}= 148 ± 3.0%, EC_{50}= 671 ± 12 nM), however, the CB1 antagonist/inverse agonist rimonabant could antagonize more efficiently the G-protein activation effect of **19** (E_{max}= 125 ± 1.9%, EC_{50}= 378 ± 20 nM). The stimulatory effect of compound **19** decreased to the basal level in the co-presence of naloxone, rimonabant and AM 630. These interactions suggested a bivalent opioid and CB (mostly CB1) receptor dependent agonist effect of **19**.

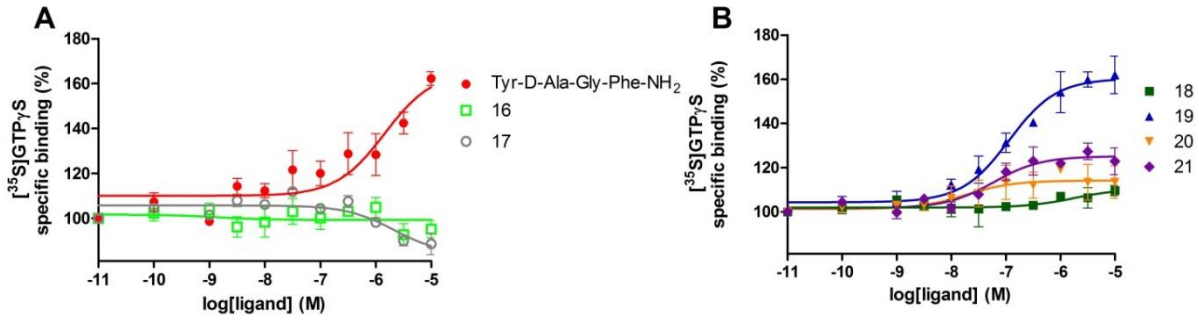

Figure 10 The effect of the synthetic compounds on G-protein activation in [^{35}S]GTPγS binding assays in rat brain membrane homogenates. Figures represent relative specific binding of [^{35}S]GTPγS in the presence of increasing concentrations (10^{-10}–10^{-5} M) of the indicated compounds. Data are mean percentage of specific binding ± SEM (n≥ 3) over the basal activity of 100%. The maximal G-protein stimulation efficacy (E_{max}) and ligand potency (EC_{50}) values are listed in Table 2.

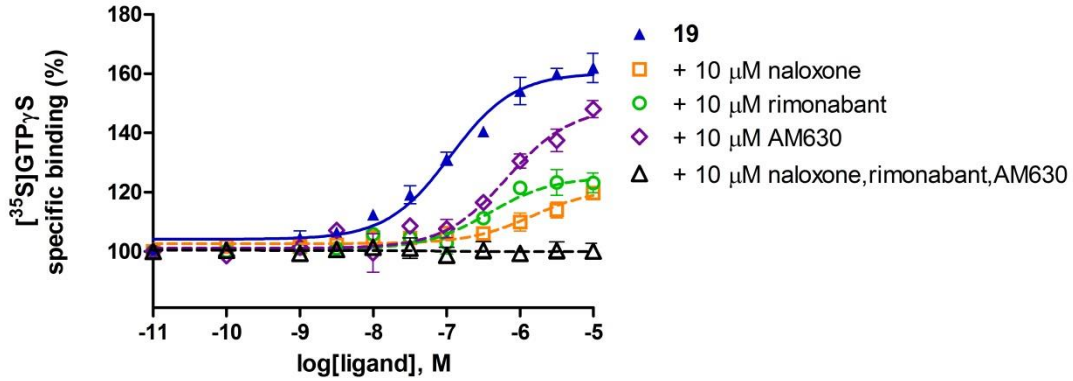

	E_{max} (%)	EC_{50} (nM)
19	160 ± 1.9	112 ± 7.5
19 + 10 μM naloxone	121 ± 2.5$^{***/\#}$	1473 ± 118***
19 + 10 μM rimonabant	125 ± 1.9***	378 ± 20***
19 + 10 μM AM 630	148 ± 3.0***	671 ± 12***
19 + 10 μM (naloxone, rimonabant, AM 630)	100 ± 1.2***	n.r.

Figure 11. Opioid and cannabinoid receptor-mediated effects of **19** on G-protein activation in [^{35}S]GTPγS binding assays in rat brain membrane homogenates. Figure represents relative specific binding of [^{35}S]GTPγS with the increasing concentrations (10^{-10}–10^{-5} M) of **19** in the absence or presence of 10 μM naloxone, 10 μM rimonabant or 10 μM AM 630. Data are mean percentage of specific binding ± SEM (n= 3–5) over the basal activity. The calculated maximal G-protein stimulation efficacy (E_{max}) and ligand potency (EC_{50}) values are listed below the graph. Statistical comparison of E_{max} and EC_{50} were performed by one-way ANOVA followed by the Bonferroni's multiple comparison test (***, $P< 0.001$). $^{\#}$ indicates significant difference (unpaired Student's t-test ($P< 0.05$) in the E_{max} of **19** in the presence of 10 μM naloxone compared to the basal activity. n.r. not relevant.

Because the bivalent compounds **10** and **12** with noticeable MOR and CB receptor affinity did not induce significant changes in basal [^{35}S]GTPγS binding, their antagonist effect was investigated in details. In control experiments the G-protein stimulatory agonist effect of oxycodone was antagonized by the opioid antagonist naloxone, and that of JWH-018 was antagonized by the co-addition of the CB1 selective rimonabant and the CB2 selective AM 630. It was found that the maximum agonist effects of oxycodone, Tyr-D-Ala-Gly-Phe-NH_2, JWH-018, **11** and **19** were reduced to the basal level by compounds **10** and **12** as well (Figure 12). These data demonstrated that compounds **10** and **12** acted as antagonists of the MOR and CB receptors.

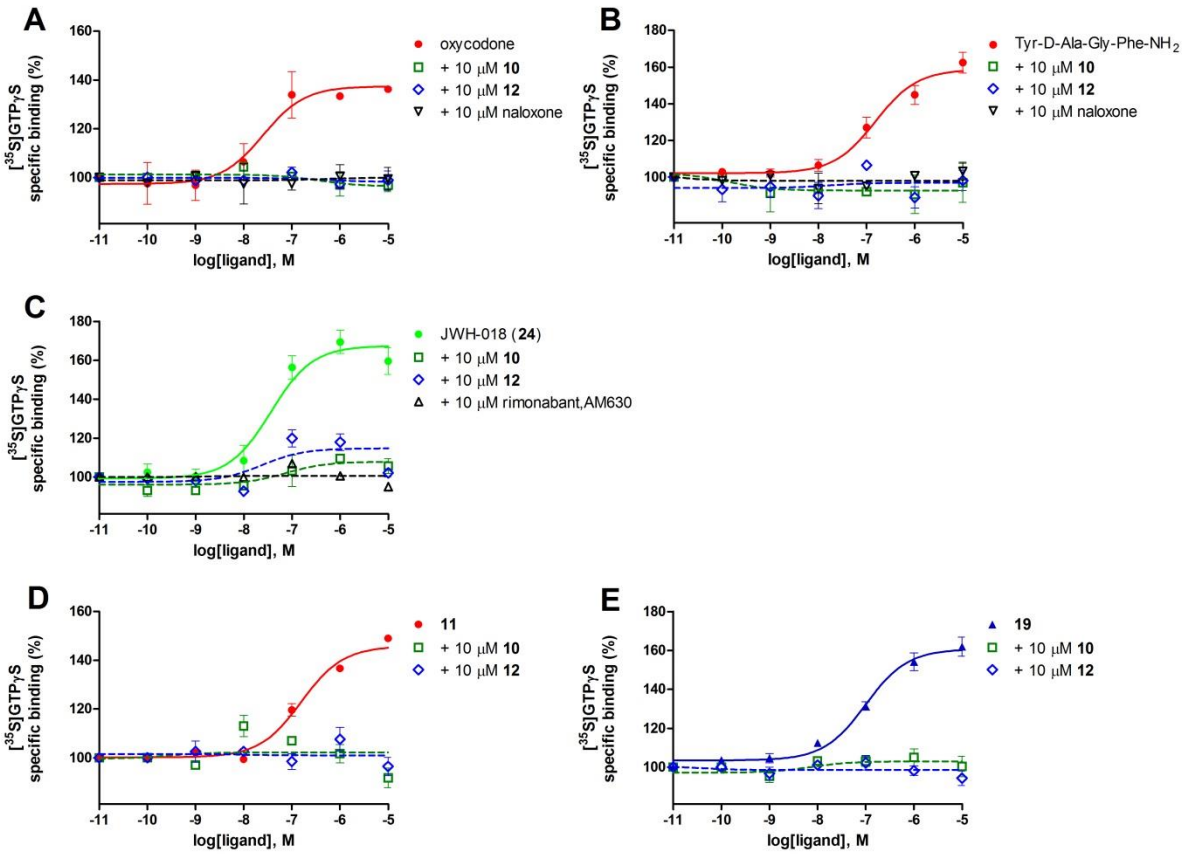

Figure 12. The antagonist effect of **10** and **12** in agonist induced [^{35}S]GTPγS binding assays in rat brain membrane homogenates. Figures represent relative specific binding of [^{35}S]GTPγS with the increasing concentrations (10^{-10}–10^{-5} M) of oxycodone, Tyr-D-Ala-Gly-Phe-NH_2, JWH-018, **11** and **19** in the absence (filled symbols) or in the presence (open symbols) of 10 μM of naloxone, rimonabant, AM630, **10** or **12**. Data are mean percentage of specific binding ± SEM (n≥ 3) over the basal activity of 100%. The calculated parameters are listed in the Appendix Table A1.

Table 1. Inhibitory constant values and signaling properties of oxycodone and JWH-018 derivatives

compound	K_i (nM)							E_{max} (%)	EC_{50} (nM)
	[^{3}H]DAMGO	[^{3}H]Ile^{5,6}-deltorphin-2	[^{3}H]HS-665	$K_{i\delta}/K_{i\mu}$	$K_{i\kappa}/K_{i\mu}$	[^{3}H]JWH-018	[^{3}H]WIN-55,212-2		
oxycodone	8.9± 0.4	487± 36	325 ± 32	55	37	>10000	>10000	135 ± 4.6	51 ± 2.5
JWH-018	>10000	>10000	>10000	-	-	3.4 ± 0.8	2.9 ± 0.4	163 ± 3.1	69 ± 10
1	24 ± 0.2	110 ± 14	>10000	5	-	n.d.	n.d.	109 ± 3.2	225 ± 27
5	17 ± 0.9	533 ± 33	471 ± 44	31	28	n.d.	n.d.	113 ± 2.1	450 ± 11
6	41 ± 3.6	659 ± 14	380 ± 43	16	10	n.d.	n.d.	111 ± 2.5	305 ± 14
7	74 ± 3.0	757 ± 55	503 ± 50	10	7	n.d.	n.d.	112 ± 7.1	200 ± 55
9	n.d.	n.d.	n.d.	-	-	247 ± 48	205 ± 28	81 ± 4.7	4225 ± 148
10	33 ± 4.0	623 ± 43	337 ± 40	19	10	255 ± 47	9.3 ± 1.8	100 ± 1.7	n.r.
11	18 ± 5.0	263 ± 15	172 ± 19	15	10	34 ± 8	12 ± 3.5	147 ± 3.8	215 ± 4.5
12	20 ± 1.0	386 ± 23	186 ± 37	19	9	183 ± 32	78 ± 23	99 ± 1.2	n.r.

K_i values were obtained from the displacement curves shown in Figure 6, n.d. not determined. The E_{max} and EC_{50} values were calculated from the dose-response curves of Figure 8, n.r.: not relevant. Data are means ± SEM, n≥3.

Table 2. Inhibitory constant values and signaling properties of peptidic compounds

compound	K_i (nM)							E_{max} (%)	EC_{50} (nM)
	[^{3}H]DAMGO	[^{3}H]Ile^{5,6}-deltorphin-2	[^{3}H]HS-665	$K_{i\delta}/K_{i\mu}$	$K_{i\kappa}/K_{i\mu}$	[^{3}H]JWH-018	[^{3}H]WIN-55,212-2		
Tyr-D-Ala-Gly-Phe-NH_2	0.8 ± 0.1	107 ± 19	173 ± 15	134	216	>10000	>10000	157 ± 3.9	191± 7
JWH-018	>10000	>10000	>10000	-	-	3.4 ± 0.8	2.9 ± 0.4	163 ± 3.1	69 ± 10
16	n.d.	n.d.	n.d.	-	-	190 ± 17	269 ± 21	102 ± 3.5	n.r.
17	n.d.	n.d.	n.d.	-	-	145 ± 13	149 ± 18	83 ± 5.6	2154 ± 100
18	50 ± 2.7	214 ± 2.0	231 ± 35	4	5	1013 ± 45	823 ± 62	110 ± 3.8	1801 ± 102
19	2.1± 0.3	134 ± 12	63 ± 13	64	30	251 ± 18	317 ± 47	160 ± 1.9	114 ± 10
20	48 ± 5.1	190 ± 33	151 ± 25	4	3	919 ± 48	1216 ± 102	114 ± 1.6	18 ± 6
21	20 ± 3.5	92 ± 25	50 ± 15	5	3	928 ± 45	1042 ± 28	125 ± 1.5	60 ± 10

K_i values were obtained from the displacement curves shown in Figure 7, n.d. not determined. The E_{max} and EC_{50} values were calculated from the dose-response curves of Figure 10, n.r.: not relevant. Data are means ± SEM, n≥3.

4.6. Permeability of compounds 11 and 19 through the brain endothelium

In order to evaluate whether the agonist bivalent compounds **11** and **19** can effectively target central or periferial opioid and CB receptors, the permeability of [^{3}H]**11** and [^{3}H]**19** through brain endothelial cells was measured using a well characterized triple co-culture blood-brain barrier (BBB) model.[127,128] The required tritium labeled bifunctional compounds were prepared from iodinated precursor compounds. Compound **9** was iodinated with iodine monochloride in MeOH then it was reduced with tritium gas. The amine **6** was then *N*-acylated with [^{3}H]**9** under the conditions outlined in Scheme 1 that yielded [^{3}H]**11**. In the case of **19**, bis(pyridine)iodonium(I) tetrafluoroborate[149] was used to prepare the iodo-derivative of **19** that was reduced with tritium gas to obtain [^{3}H]**19**. In the *in vitro* BBB permeability measurement [^{3}H]**11** and [^{3}H]**19** were applied in 0.25 and 0.75 μM concentrations and their fluxes in the blood to brain direction was measured. Similar endothelial permeability coefficients were calculated (2-3 × 10^{-6} cm/s) for both molecules at both donor concentrations (Figure 13). This value is not significantly different from the permeability coefficient of fluorescein, a hydrophilic reference molecule with a limited permeability to the brain.[127,150] The penetration of **11** and **19** was fifteen times higher across empty inserts indicating that the membrane of the inserts was permeable for the molecules. These experiments revealed that the bivalent compounds **11** and **19** exhibited limited penetration, thus *intrathecal* administration was necessary during *in vivo* experiments.

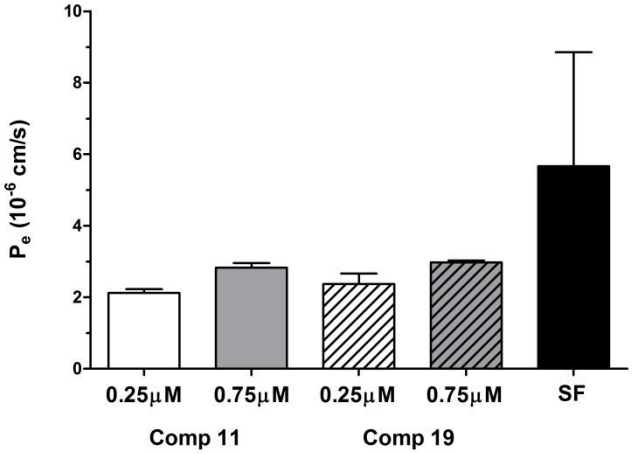

Figure 13. Evaluation of the flux of compounds **11** and **19** across an *in vitro* BBB model consisting of primary rat brain endothelial cells, pericytes and astrocytes. Permeability of sodium fluorescein (SF) is also given as reference. P_e: permeability coefficient, data are mean ± SD, n= 4.

4.7. Preparation and receptor binding properties of [^{3}H]hemopressin(1-7)

Due to these favorable characteristics of hemopressins explained in the introduction and to the fact that the truncated Hp(1–7) peptide was found to be as potent as Hp(1–9) in *in vitro* and *in vivo* studies[27] Hp(1–7) was chosen for radiolabeling without any structural modification.[147] The radioligand [^{3}H]Hp(1-7) was obtained by the catalytic reduction of ΔPro^1-Hp(1-7) with tritium gas, and the specific activity of 1.04 TBq/mmol was sufficient for performing the *in vitro* pharmacological experiments.

Various binding assays were performed to characterize the interaction of [^{3}H]Hp(1-7) with membrane receptors using rat brain membrane homogenate that is known to contain CB1 receptors abundantly. The comparison of radioligand binding experiments carried out in the presence and in the absence of protease inhibitors revealed that [^{3}H]Hp(1-7) was sufficiently stable up to an incubation time of 30 min. Association binding experiments carried out in the presence of 2 nM [^{3}H]Hp(1-7) and a protein concentration of 0.45 mg/mL revealed specific binding of [^{3}H]Hp(1-7) to rat brain membranes at 37°C. At this temperature, specific binding reached steady-state in 5 min (Figure 14A) that remained stable up to 60 min. The specific binding was 50-70% of the total binding at 2 nM radioligand concentration under equilibrium conditions. Table 3 summarizes the calculated equilibrium binding parameters. In the dissociation experiments, rat brain membranes were incubated with 2 nM [^{3}H]Hp(1-7) at 37 ^{o}C for 10 min and dissociation of the ligand–receptor complex was initiated by the addition of 10 μM Hp(1-7) after different incubation periods. Dissociation proceeded with a monophasic kinetics (Figure 14B) providing a dissociation rate constant (k_d) of 0.842 ± 0.150 min^{-1}. It was found that 55 % of the radioligand dissociated from the membranes. The kinetically derived equilibrium dissociation constant (K_d) calculated from the association and dissociation experiments was assessed to be 7.2 ± 1.2 nM under our experimental conditions.

In the next step saturation radioligand binding experiments were carried out on brain homogenates of rat and CB1 knockout mouse in the presence of increasing radioligand concentrations for 30 min. The specific binding of [^{3}H]Hp(1-7) was found to be saturable and of high affinity in both tissue homogenates (Figures 15A, B).

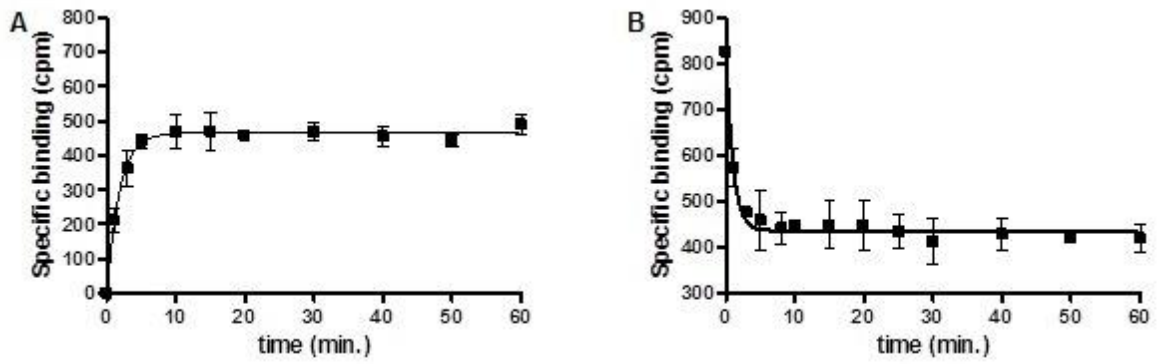

Figure 14. (A) Association time course of [^{3}H]Hp(1-7) binding at 37°C. 2 nM [^{3}H]Hp(1-7) was incubated with rat brain membrane for various time in the absence or presence of 10 μM Hp(1-7) to assess specific binding. (B) Dissociation time course of [^{3}H]Hp(1-7) binding at 37°C. 2 nM [^{3}H]Hp(1-7) was incubated with rat brain membrane for 10 min, then dissociation was initiated by the addition of 10 μM Hp(1-7) after different time periods. Data are means ± S.E.M, n= 3.

Table 3. Kinetic parameters for [^{3}H]Hp(1-7) at rat brain membrane binding sites.

	Kinetic parameters
k_{obs}	1.08 ± 0.12 min^{-1}
k_a	0.119 ± 0.001 $nM^{-1}min^{-1}$
k_d	0.842 ± 0.150 min^{-1}
K_d	7.2 ± 1.4 nM

k_{obs} is the observed pseudo-first order rate constant, k_d is the dissociation rate constant, k_a is the association rate constant calculated as $k_a = (k_{obs}-k_d)/[[^3H]Hp(1-7)]$. The equilibrium dissociation constant K_d was calculated as $K_d = k_d/k_a$. Data were calculated from the average ± S.E.M values of at least 3 independent experiments.

Single-site bindings were calculated for both saturation curves by non-linear fitting of the specific binding data points that resulted in a dissociation equilibrium constants (K_d) of 14.5 ± 3.2 nM and 10.8 ± 1.8 nM in rat and in CB1 knockout mouse brain membrane, respectively. Furthermore, high receptor densities (B_{max}= 830 ± 120 and 990 ± 145 fmol/mg protein in rat and in CB1 knockout mouse brain membrane, respectively) were observed (Table 4). These K_d and B_{max} values suggested that the target receptor for the Hp(1-7) peptide was present in both tissue homogenates and indicated the specific interaction of [^{3}H]Hp(1-7) with a highly abundant receptor protein.

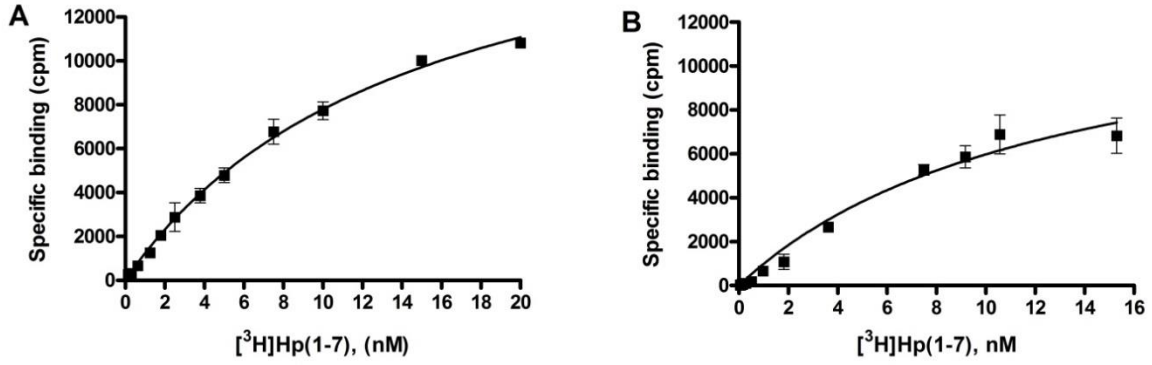

Figure 15. Saturation isotherms of [^{3}H]Hp(1-7). Increasing concentrations of the radioligand were incubated with membrane homogenates of rat brain (A) or CB1 knockout mouse brain (B) in the absence or presence of 10 μM Hp(1-7). Only specific binding data are presented as means ± S.E.M of at least 3 independent experiments.

Table 4. Equilibrium binding data of [^{3}H]Hp(1-7)

Tissue	K_d (nM)	B_{max} (fmol/mg protein)
Rat brain membrane	14.5 ± 3.2	830 ± 120
CB1 knockout mouse brain membrane	10.8 ± 1.8	990 ± 145

Dissociation equilibrium constants (K_d) and receptor densities (B_{max}) were calculated by fitting of the saturation curves measured in brain membrane homogenates of wild-type rat or CB1 knockout mouse in the absence or presence of 10 μM Hp(1-7). Data are means ± S.E.M of at least 3 independent experiments.

The saturation binding experiments indicated that the binding site of [^{3}H]Hp(1-7) might be different from the CB1 receptor, therefore we further characterized the labelled Hp(1-7) in competition receptor binding assays in rat brain membrane homogenates. First, different non-peptidic cannabinoid agonists and inverse agonists were used as competitor ligands. It was found that neither the non-selective cannabinoid full agonist JWH-018, the CB1 receptor inverse agonist AM251 nor the CB1 receptor inverse agonist rimonabant could displace the bound radioligand in rat brain membranes. Only the unlabelled Hp(1-7) was able to compete with its tritium labelled analogue, but with a high apparent inhibitory constant in the 100 nanomolar range (Figure 16A). In contrast, a K_d value of 14.5 ± 3.2 nM was obtained by the analysis of the kinetic curves. Since [^{3}H]HP(1-7) was found to be stable against proteolysis under the binding conditions, these findings suggested that the interaction of [^{3}H]Hp(1-7) with the CB1 receptors in rat brain membrane homogenate was different from that of other non-peptidic cannabinoids.

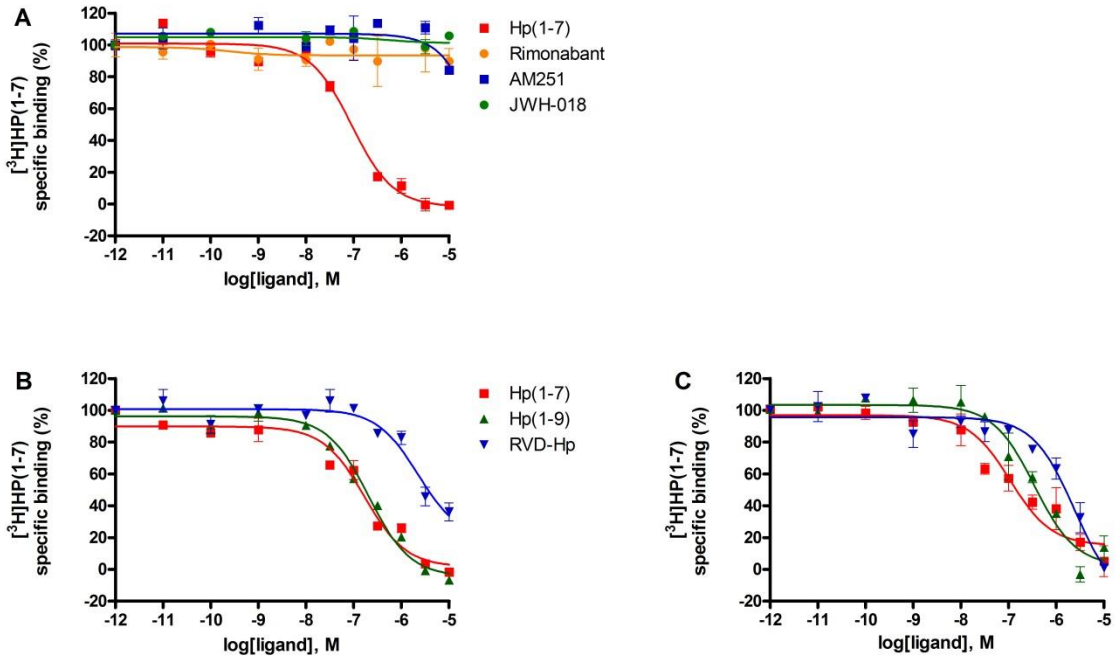

Figure 16. Competitive binding curves of [^{3}H]Hp(1-7) by various orthosteric synthetic cannabinoid ligands and hemopressins. Brain membranes of rat (A, B) or CB1 knockout mouse (C) were incubated with 2 nM [^{3}H]Hp(1-7) in the presence of increasing concentrations (10^{-11}–10^{-5} M) of the indicated compounds. Non-specific binding was measured in the presence of 10 μM Hp(1-7), data are means ± S.E.M., n= 3.

Table 5. Inhibitory constants (K_i) of hemopressins against [^{3}H]Hp(1-7) in brain membrane homogenates.

	K_i (nM)	
Ligand	rat brain membrane	CB1 knockout mouse brain
Hp(1-7)	111 ± 14	94 ± 25
Hp(1-9)	184 ± 28	401 ± 78
RVD-Hp(1-9)	1940 ± 121	3208 ± 396

Hemopressins were co-incubated with [^{3}H]Hp(1-7) in brain homogenate of rat or CB1 knockout mouse. Data are means ± S.E.M of at least 3 independent experiments.

Next, competition experiments were performed to investigate the ability of the hemopressins Hp(1-7), Hp(1-9) and RVD-Hp(1-9) to inhibit the binding of [^{3}H]Hp(1-7) to rat brain membrane homogenate (Figure 16B). These hemopressins could displace [^{3}H]Hp(1-7) from the binding site with different inhibitory constants (Table 5), and the parent Hp(1-7) displayed the highest affinity (K_i= 111 ± 14 nM) to the binding site. The Hp(1-9) peptide provided a slightly higher inhibitory constant (K_i= 184 ± 28 nM), but still within the same range. These data indicated that Hp(1-7) and Hp(1-9) might bind to the same site or conformation of a

receptor protein, however both Hp(1-9) and Hp(1-7) might prefer a receptor conformation or binding site different from those of the non-peptidic cannabinoid agonists. In contrast, the Arg-Val-Asp-extended hemopressin (RVD-Hp(1-9)) displayed the lowest binding affinity (K_i= 1940 ± 121 nM) to the [^{3}H]Hp(1-7) labelled sites. The findings of the saturation and competition binding studies indicated the existence of a non-cannabinoid binding site or a receptor protein. In order to provide further evidences for this presumption, the ability of cannabinoid ligands and hemopressins to compete with [^{3}H]Hp(1-7) in CB1 knockout mouse brain membrane homogenate was investigated (Figure 16C). It was found that Hp(1-7) displayed the lowest inhibitory constant (K_i= 94 ± 25 nM), and this affinity was close to that detected in rat brain membrane homogenate (Table 5). The similar affinity values obtained for Hp(1-7) in the homologue displacement studies both in rat and CB1 knockout mouse brain membrane homogenates strongly suggest that the receptor of the Hp(1-7) peptide has to be present in both tissue samples. Furthermore, the higher difference in inhibitory constants (K_i= 184 ± 28 nM vs. 401 ± 78 nM) for the Hp(1-9) peptide in rat and CB1 knockout mouse brain homogenates may refer to binding to different regions of the same receptor in the two species or binding to the same region of the receptors with sequence heterogeneity in the two mammalian species. Similarly to the findings in whole rat brain membrane homogenate, the RVD-Hp(1-9) peptide showed marginal binding affinity (K_i= 3208 ± 396 nM) to the [^{3}H]Hp(1-7) labelled sites.

4.8. Ligand stimulated [^{35}S]GTPγS binding studies of hemopressins

Since hemopressins were reported to be the agonist ligands of the CB1 receptor, we were curious how Hp(1-7) and Hp(1-9) activate G-proteins. The CB1 receptor full agonist JWH-018 and the inverse agonist rimonabant were applied as positive controls to validate the conditions of the ligand stimulated [^{35}S]GTPγS binding assay in rat brain membranes. JWH-018 stimulated GTP binding with the highest efficacy (E_{max}= 165 ± 25%) and lowest potency (EC_{50}= 9.5 ± 1.2 nM) in good agreement with literature data[151] (Figure 17). Rimonabant also behaved as described in the literature.[152] HP(1-7) displayed low potency (EC_{50} = 21 ± 1.5 nM) and marginal stimulatory activity (E_{max}= 112 ± 8%) as compared to the well-known non-peptidic cannabinoids (Figure 17 and Table 6). Hp(1-9) also showed low potency (EC_{50}= 29 ± 3.5 nM), but did not activate [^{35}S]GTPγS binding (E_{max}= 104 ± 7%). Next, Hp(1-7) and Hp(1-9) were tested in [^{35}S]GTPγS binding assays using membranes prepared from the brain of

CB1 knockout mice. We used the opioid full agonist DAMGO as a positive control to compare [^{35}S]GTPγS activation and to test the proper operation of our experimental setup (Figure 18 and Table 7). The agonist control compound DAMGO exhibited low potency (EC_{50} = 177 ± 21 nM) and significant stimulation (E_{max}= 167 ± 20%) of [^{35}S]GTPγS binding as compared to Hp(1-7) and Hp(1-9).

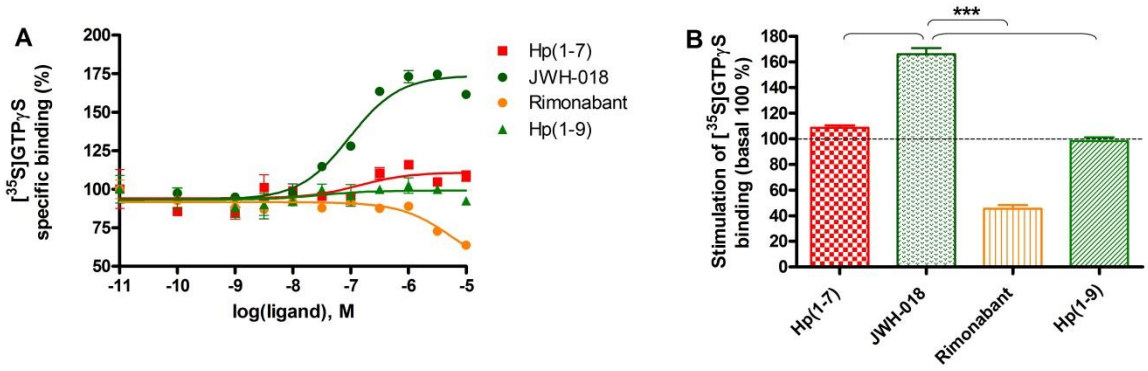

Figure 17. [^{35}S]GTPγS binding stimulated by Hp(1-7), Hp(1-9) and cannabinoid ligands in rat brain membrane homogenate. JWH-018 and rimonabant were used as positive controls. Rat brain membranes were incubated with 0.05 nM [^{35}S]GTPγS in the presence of increasing concentrations (10^{-10}-10^{-5} M) of the indicated compounds. Non-specific binding was measured with 10 μM GTPγS. Data are expressed as means ± S.E.M., n= 3. Statistical comparison of E_{max} and EC_{50} were performed by one-way ANOVA followed by the Bonferroni's multiple comparison test (***, P< 0.001).

Table 6. Summary of the results of [^{35}S]GTPγS functional binding assays in rat brain membrane preparation.

Ligands	EC_{50} (nM)	E_{max} (%)
Hp(1-7)	21 ± 1.5	112 ± 8
Hp(1-9)	29 ± 3.5	104 ±7
JWH-018	9.5 ± 1.2	165 ± 25
rimonabant	539 ± 65	46 ± 7

Nonspecific binding was determined by the addition of 10 μM unlabeled GTPγS. Each data represents the mean ± SEM from 4 independent experiments performed in triplicate.

The Hp(1-7) peptide demonstrated a higher potency (EC_{50}= 655 ± 98 nM), in comparison with the potency obtained in rat brain membrane homogenate. However, Hp(1-7) displayed very similar stimulatory effects in both wild type rat and CB1 knockout mouse brain homogenates (E_{max}= 112 ± 12 and 117 ± 18%). Similarly to the competitive displacement studies this finding suggests that the ligand activates a G-protein or binds to a protein through the same binding site or receptor protein(s) that is/are present in both types of tissues. Consequently, its main target protein cannot be the CB1 receptor because it is not supposed to be present in the brain membrane preparation of CB1 knockout mice. The Hp(1-9) peptide showed higher potency (EC_{50}= 65 ± 12 nM), but a stimulatory effect (E_{max}= 111 ± 17%)

roughly equivalent with that of the Hp(1-7) peptide. This difference in the potency value may reflect different binding mode or interaction of the Hp(1-9) peptide with its binding protein.

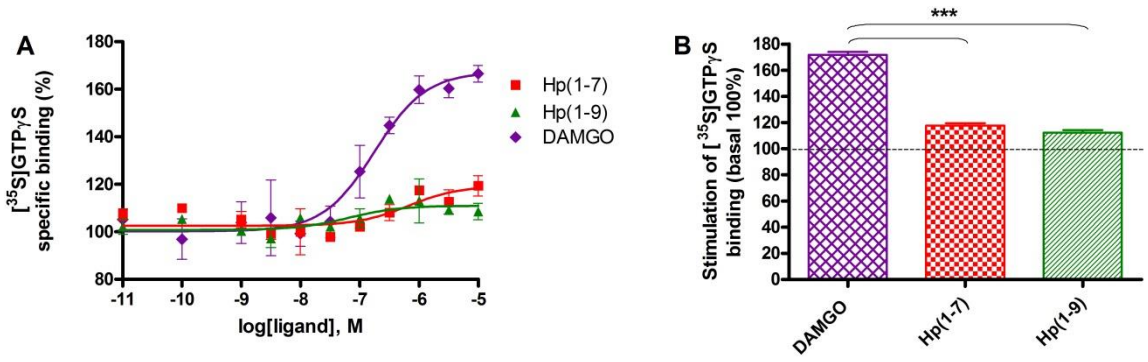

Figure 18. [^{35}S]GTPγS binding stimulated by DAMGO, Hp(1-7) and Hp(1-9) in CB1 knockout mouse brain membrane homogenate. Mouse brain membranes were incubated with 0.05 nM [^{35}S]GTPγS in the presence of increasing concentrations (10^{-10}-10^{-5} M) of the indicated compounds. Non-specific binding was measured in the presence of 10 μM GTPγS. Data are means ± S.E.M., n= 3. Statistical comparison of E_{max} and EC_{50} were performed by one-way ANOVA followed by the Bonferroni's multiple comparison test (***, P< 0.001).

Table 7. Summary of the results of [^{35}S]GTPγS functional binding assay in CB1 knockout mouse brain membrane preparation.

Ligands	EC_{50} (nM)	E_{max} (%)
Hp(1-7)	655 ± 98	117 ± 18
Hp(1-9)	65 ± 12	111 ± 17
DAMGO	177 ± 21	167 ± 20

Nonspecific binding was determined by the addition of 10 μM unlabeled GTPγS. Each data represents the mean ± SEM from 4 independent experiments performed in triplicate.

.

5. Discussion

The involvement of the MOR and CB receptors in pain management is well documented and numerous studies report the synergistic interaction of the opioid and cannabinoid agonists.[153] The association of the opioid and cannabinoid GPCRs to form homo- or heterodimers and multimers[154] initiated the preparation of multitargeting compounds by covalent linking of pharmacophores with the aim of accomplishing simultaneous or parallel receptor-ligand interactions. Such multitargeting ligands are frequently called bivalent ligands suggesting the simultaneous interaction of a small molecule bivalent ligand with two protomers of a GPCR receptor complex. However, the distance of the ligand binding sites on the protomers may require long spacers of 20-50 Å length that can modify the physico-chemical properties of the original monomeric compounds to an extent that can lead to significant decrease in receptor affinity, to increased non-specific interactions or to decreased solubility in body fluids. The development of multitargeting compounds with parallel or independent protomer interactions is a more realistic goal when short spacers can be applied.[155] Unfortunately, in the case of very short spacers the pharmacology of the original compounds can interfere significantly that can result in the loss of the original effects.[113,114]

In our design, 2 to 13 atoms spacers were applied with the aim of achieving the co-presence of MOR and cannabinoid pharmacophores in the extracellular space. This way the differences in pharmacokinetics and pharmacodynamics of the single compounds can be eliminated, and either a single protomer of a receptor multimer or more protomers in a parallel way can be activated by the bivalent compound. In our work JWH-018, a full agonist of CB receptors was conjugated with the opioid agonists oxycodone or with the enkephalin-related tetrapeptide Tyr-D-Ala-Gly-Phe via spacers of different length and hydrophobicity. The structural diversity of the CB receptor ligands[156] and the presence of allosteric sites on the CB receptors prompted us to prepare and validate [^{3}H]JWH-018 as an appropriate radioligand competitor of the bivalent compounds in *in vitro* experiments. In our compound set **11** and **19** bound to both the MOR and CB receptors, and they exhibited agonist-induced GPCR activation with high efficacy, suggesting a possible synergistic interaction of the covalently linked agonists. Compound **11** preferred MOR and CB2, whereas compound **19** preferred MOR and CB1 receptor mediated interactions as revealed by using specific antagonists in [^{35}S]GTPγS studies. At spinal level a synergistic interaction of the opioid and cannabinoid agonists was observed in the case of the bivalent compounds **11** and **19**. Because MOR and

CB receptor agonists can be effectively applied in the treatment of chronic pain including neuropatic pain, these findings can help to develop multitargeting antinociceptive drugs.

In the future, JWH-018 was planned to substitute with a novel class of peptidic compounds that are probably free of cannabinoid side-effects. The recently discovered α-hemoglobin derived hemopressins have been postulated to be negative allosteric modulators and endogenous agonist ligands of the CB1 receptors. These peptides have been demonstrated to possess *in vitro* and *in vivo* pharmacological potencies similar to those of the prototypic endogenous and synthetic cannabinoid ligands, but with less side-effects.[27,30-32] Accordingly, hemopressins appear to be excellent lead compounds for the development of peptidic research tools for the investigation of the endocannabinoid system. Their reported pharmacological characteristics prompted us to prepare a radiolabelled peptide ligand that acts on the CB1 receptor and thus, enables the direct investigation of the endocannabinoid system and the binding properties of new synthetic CB1 receptor ligands.

The Hp(1-9) peptide and its extended or truncated derivatives were demonstrated to be orally active and to exert antinociceptive effects apparently mediated by the CB1 receptors.[32] The physiological activity upon oral administration suggests that these peptides are at least partially resistant to proteolysis, and also that they may be able to cross the blood-brain barrier. Due to these favorable characteristics and to the fact that the truncated Hp(1-7) peptide was also found to be as potent as Hp(1-9) in *in vitro* and *in vivo* studies,[27] Hp(1-7) was chosen for radiolabelling.

The tritium labelled Hp(1-7) was investigated in various radioligand binding assays to characterize the interaction of Hp(1-7) and CB receptors. Data analysis of the receptor binding kinetics of [^{3}H]Hp(1-7) showed that the radioligand reaches equilibrium and steady-state rapidly under the experimental conditions. Saturation binding experiments revealed single site binding and very high receptor densities in both wild type rat brain membrane and CB1 knockout mouse brain membrane homogenates. In displacement studies, [^{3}H]Hp(1-7) was not able to compete with the most commonly used CB1 receptor agonist/inverse agonist cannabinoid ligands. However, we found competition with Hp(1-9) in both types of brain homogenates which suggests that both Hp(1-7) and Hp(1-9) may be able to bind to the same receptor or allosteric site. This result is contradictory because the CB1 knockout mouse brain homogenate is not supposed to contain CB1 receptors.

On the other hand, the presence of allosteric binding site of CB1 receptors for hemopressins has been demonstrated.[36,41] Based on our direct *in vitro* receptor binding results and the large number of literature data, we hypothesize that hemopressins interact with the

CB1 receptor allosteric binding site(s). They more likely up-regulate the endocannabinoid production and the subsequent endocannabinoid release may be responsible for the observed analgesic effects. This assumption seems to be further supported by the study of Toniolo and co-workers[157]. Their results suggested that Hp(1-9) could inhibit monoacylglycerol-lipase activity in dorsal root ganglions which may lead to an increase of 2-arachydonyl-glycerol inducing analgesia. Furthermore, they hypothesized that Hp(1-9) can interact with the peripheral voltage-gated potassium channels and reduce calcium influx in a synergistic manner with the peripheral cannabinoid receptors. The authors also concluded that Hp(1-9) can induce an increase of endocannabinoid level which would, in turn, lead to the activation of descending inhibitory pain pathways inducing analgesia. However, we cannot fully exclude the existance of allosteric binding site for hemopressins, especially based on the findings of Straiker and co-workers.[36] They studied positive and negative allosteric modulators of the endocannabinoid-mediated synaptic transmission in cultured hippocampal neurons. In their study, RVD-Hp(1-9) that did not apparently exhibit binding to the CB1 receptor in our system attenuated depolarization-induced suppression of excitation. Interestingly, Hp(1-9) was ineffective in this model of endocannabinoid signaling.

This peptide family can be applied in bivalent molecules as a CB receptor targeting moiety without cannabinoid side effects.

6. Summary

- ✓ Two series of bivalent compounds containing an opioid (oxycodone or Tyr-D-Ala-Gly-Phe) and a cannabinoid (JWH-018) pharmacophore were designed, synthesized and characterized in *in vitro* radioligand binding assays, functional [^{35}S]GTPγS binding assays and *in vivo* antinociceptive tests.
- ✓ Two novel cannabinoid receptor radioligands, [^{3}H]JWH-018 and [^{3}H]Hp(1-7) were prepared and validated.
- ✓ The [^{3}H]JWH-018 bound to the CB receptor binding site with high affinity (K_d= 6.5 nM) and fast kinetics and labeled high receptor density (B_{max}= 1120 ± 89 fmol/mg protein). In displacement studies [^{3}H]JWH-018 competed with the classical orthosteric CB receptor ligands but not with hemopressins and opioid ligands.
- ✓ The [^{3}H]Hp(1-7) displayed saturable binding in rat brain membrane- and also in a CB1 knockout mouse brain homogenate. The receptor bound [^{3}H]Hp(1-7) couldn't be displaced by JWH-018, rimonabant and AM251.
- ✓ The *C*-6 substitution of oxycodone did not significantly affected the MOR binding and MOR selectivity, but led to loss of KOR affinity. The introduction of spacers with increasing length and polarity slightly reduced the MOR affinity and selectivity.
- ✓ The introduction of a terminal carboxyl, amino and acylamido function to the pentyl chain of JWH-018 resulted in 73-fold, 55-fold and 43-fold loss of CB receptor affinity, respectively.
- ✓ The functional binding assays revealed that the *C*-6 substitution of oxycodone and the conjugation of linkers to this position reduced the G-protein activation efficacy and led to weak partial agonists with lower potency.
- ✓ The modification of the full agonist JWH-018 with a carboxyl, an amino or acylamido group resulted in inverse agonist or antagonist ligands.
- ✓ In competition binding assays the affinity and selectivity of the bivalent compounds **10** and **12** to the MOR decreased slightly and their CB receptor affinity was even lower.
- ✓ The MOR affinity and selectivity of the bivalent compounds **18**, **20**, **21** reduced, the CB receptor affinity of **18**, **20** and **21** decreased significantly.
- ✓ In the functional binding assays the bivalent compounds **10** and **12** were found to be antagonists, whereas **18**, **20**, **21** acted as partial agonists.
- ✓ In competition binding assays the bivalent compounds **11** (K_i (MOR)= 18 nM; K_i (CB)= 34 nM) and **19** (K_i (MOR)= 2.1 nM; K_i (CB) = 251 nM) showed the highest affinity to both MOR and CB receptors.

- ✓ In functional binding assays it was found that the agonist bivalent compound **11** exerted its G-protein activation through the MOR and CB2 receptors, while the agonist bivalent compound **19** exerted its G-protein activation through the MOR and CB1 receptors.
- ✓ Dimerization of MOR and CB agonists resulted in the agonist bivalent compounds **11** and **19** with antiallodynic activity *in vivo*.
- ✓ At spinal level bivalent compound **11** and **19** were equieffective with the parent drugs at 20 μg dose in a chronic osteoarthritis pain model in rats.

7. References

1. Di Marzo, V. Targeting the endocannabinoid system: to enhance or reduce? *Nat. Rev. Drug Discov.* **7**, 438–455 (2008).

2. Pacher, P., Bátkai, S., Kunos, G. The endocannabinoid system as an emerging target of pharmacotherapy. *Pharmacol. Rev.* **58**, 389–462 (2006).

3. Pertwee, R. G. Targeting the endocannabinoid system with cannabinoid receptor agonists: Pharmacological strategies and therapeutic possibilities. *Philos. Trans. R. Soc. B Biol. Sci.* **367**, 3353–3363 (2012).

4. Pacher, P., Kunos, G. Modulating the endocannabinoid system in human health and disease: Successes and failures. *FEBS J.* **280**, 1918–43 (2013).

5. Hofer, S. C., Ralvenius, W. T., Gachet, M. S., Fritschy, J. M., Zeilhofer, H. U., Gertsch, J. Localization and production of peptide endocannabinoids in the rodent CNS and adrenal medulla. *Neuropharmacol.* **98**, 78–89 (2015).

6. Vemuri, V. K., Makriyannis, A. Medicinal chemistry of cannabinoids. *Clin. Pharmacol. Ther.* **97**, 553–8 (2015).

7. Matsuda, L. A., Lolait, S. J., Brownstein, M. J., Young, A. C., Bonner, T. I. Structure of a cannabinoid receptor and functional expression of the cloned cDNA. *Nature* **346**, 561–4 (1990).

8. Gérard, C. M., Mollereau, C., Vassart, G., Parmentier, M. Molecular cloning of a human cannabinoid receptor which is also expressed in testis. *Biochem. J.* **279**, 129–34 (1991).

9. Munro, S., Thomas, K. L., Abu-Shaar, M. Molecular characterization of a peripheral receptor for cannabinoids. *Nature* **365**, 61–5 (1993).

10. Lovinger, D. M. Presynaptic modulation by endocannabinoids. *Handb. Exp. Pharmacol.* **184**, 435–477 (2008).

11. Mackie, K. Distribution of cannabinoid receptors in the central and peripheral nervous system. *Handb. Exp. Pharmacol.* **168**, 299–325 (2005).

12. Pertwee, R. G. Cannabinoid pharmacology: the first 66 years. *Br. J. Pharmacol.* **147**, S163-71 (2006).

13. Klein, T. W. Cannabinoid-based drugs as anti-inflammatory therapeutics. *Nat. Rev. Immunol.* **5**, 400–411 (2005).

14. Van Sickle, M. D., Duncan, M., Kingsley, P.J., Mouihate, A., Urbani, P., Mackie, K., Stella, N., Makriyannis, A., Piomelli, D., Davison, J.S., Marnett, L. J., Di Marzo, V., Pittman, Q. J., Patel, K. D., Sharkey, K. A. Identification and functional characterization of brainstem cannabinoid CB2 receptors. *Science* **310**, 329–32 (2005).

15. Dhopeshwarkar, A., Mackie, K. CB2 cannabinoid receptors as a therapeutic target-what does the future hold? *Mol. Pharmacol.* **86**, 430–437 (2014).

16. Malan, T. P., Ibrahim, M. M., Deng, H., Liu, Q., Mata, H. P., Vanderah, T., Porreca, F., Makriyannis, A. CB2 cannabinoid receptor-mediated peripheral antinociception. *Pain* **93**, 239–45 (2001).

17. Di Marzo, V., Petrosino, S. Endocannabinoids and the regulation of their levels in health and disease. *Curr. Opin. Lipidol.* **18**, 129–40 (2007).

18. Boyd, S. T. The endocannabinoid system. *Pharmacotherapy* **26**, 218S–221S (2006).

19. Di Marzo, V., Fontana, A. Anandamide, an endogenous cannabinomimetic eicosanoid: 'killing two birds with one stone'. *Prostaglandins. Leukot. Essent. Fatty Acids* **53**, 1–11 (1995).

20. Rodríguez de Fonseca, F., Del Arco, I., Bermudez-Silva, F. J., Bilbao, A., Cippitelli, A., Navarro, M. The endocannabinoid system: physiology and pharmacology. *Alcohol Alcohol.* **40**, 2–14 (2004).

21. Alexander, S. P. H., Kendall, D. A. The complications of promiscuity: endocannabinoid action and metabolism. *Br. J. Pharmacol.* **152**, 602–23 (2007).

22. Devane, W. A., Hanus, L., Breuer, A., Pertwee, R. G., Stevenson, L. A., Griffin, G., Gibson, D., Mandelbaum, A., Etinger, A., Mechoulam, R. Isolation and structure of a brain constituent that binds to the cannabinoid receptor. *Science* **258**, 1946–9 (1992).

23. Maccarrone, M., Bab, I., Bíró, T., Cabral, G. A., Dey, S. K., Di Marzo, V., Konje, J. C., Kunos, G., Mechoulam, R., Pacher, P., Sharkey K. A., Zimmer, A. Endocannabinoid signaling at the periphery: 50 years after THC. *Trends Pharmacol. Sci.* **36**, 277–296 (2015).

24. Hashimotodani, Y., Ohno-Shosaku, T., Kano, M. Endocannabinoids and Synaptic Function in the CNS. *Neurosci.* **13**, 127–137 (2007).

25. Katona, I., Freund, T. F. Multiple functions of endocannabinoid signaling in the brain. *Annu. Rev. Neurosci.* **35**, 529–558 (2012).

26. Fonseca, B. M., Costa, M. A., Almada, M., Correia-da-Silva, G., Teixeira, N. A. Endogenous cannabinoids revisited: a biochemistry perspective. *Prostaglandins Other Lipid Mediat.* **102–103**, 13–30 (2013).

27. Heimann, A. S., Gomes, I., Dale, C. S., Pagano, R. L., Gupta, A., de Souza, L. L., Luchessi, A. D., Castro, L. M., Giorgi, R., Rioli, V., Ferro, E. S., Devi, L. A. Hemopressin is an inverse agonist of CB1 cannabinoid receptors. *Proc. Natl. Acad. Sci. U. S. A.* **104**, 20588–20593 (2007).

28. Rioli, V., Gozzo, F. C., Heimann, A. S., Linardi, A., Krieger, J. E., Shida, C. S., Almeida, P. C., Hyslop, S., Eberlin, M. N., Ferro, E. S. Novel natural peptide substrates for endopeptidase 24.15, neurolysin, and angiotensin-converting enzyme. *J. Biol. Chem.* **278**, 8547–8555 (2003).

29. Hama, A., Sagen, J. Activation of spinal and supraspinal cannabinoid-1 receptors leads to antinociception in a rat model of neuropathic spinal cord injury pain. *Brain Res.* **1412**, 44–54 (2011).

30. Dale, C. S., Pagano Rde, L., Rioli, V., Hyslop, S., Giorgi, R., Ferro, E. S.

Antinociceptive action of hemopressin in experimental hyperalgesia. *Peptides* **26**, 431–6 (2005).

31. Gomes, I., Dale, C. S., Casten, K., Geigner, M. A., Gozzo, F. C., Ferro, E. S., Heimann, A. S., Devi, L. A. Hemoglobin-derived peptides as novel type of bioactive signaling molecules. *AAPS J.* **12**, 658–669 (2010).

32. Bomar, M. G., Galande, A. K. Modulation of the cannabinoid receptors by hemopressin peptides. *Life Sci.* **92**, 520–524 (2013).

33. Tanaka, K., Shimizu, T., Yanagita, T., Nemoto, T., Nakamura, K., Taniuchi, K., Dimitriadis, F., Yokotani, K., Saito, M. Brain RVD-haemopressin, a haemoglobin-derived peptide, inhibits bombesin-induced central activation of adrenomedullary outflow in the rat. *Br. J. Pharmacol.* **171**, 202–213 (2014).

34. Han, Z. L., Fang, Q., Wang, Z. L., Li, X. H., Li, N., Chang, X. M., Pan, J. X., Tang, H. Z., Wang, R. Antinociceptive effects of central administration of the endogenous cannabinoid receptor type 1 agonist VDPVNFKLLSH-OH [(m)VD-hemopressin(α)], an N-terminally extended hemopressin peptide. *J. Pharmacol. Exp. Ther.* **348**, 316–23 (2014).

35. Pan, J. X., Wang, Z. L., Li, N., Zhang, N., Wang, P., Tang, H. H., Zhang, T., Yu, H. P., Zhang, R., Zheng, T., Fang, Q., Wang, R. Effects of neuropeptide FF and related peptides on the antinociceptive activities of VD-hemopressin(α) in naive and cannabinoid-tolerant mice. *Eur. J. Pharmacol.* **767**, 119–125 (2015).

36. Straiker, A., Mitjavila, J., Yin, D., Gibson, A., Mackie, K. Aiming for allosterism: Evaluation of allosteric modulators of CB1 in a neuronal model. *Pharmacol. Res.* **99**, 370–376 (2015).

37. Nguyen, T., Li, J. X., Thomas, B. F., Wiley, J. L., Kenakin, T. P., Zhang, Y. Allosteric modulation: An alternate approach targeting the cannabinoid CB1 receptor. *Med. Res. Rev.* **37**, 441–474 (2017).

38. Leone, S., Recinella, L., Chiavaroli, A., Martinotti, S., Ferrante, C., Mollica, A., Macedonio, G., Stefanucci, A., Dvorácskó, Sz., Tömböly, Cs., De Petrocellis, L., Vacca, M., Brunetti, L., Orlando, G. Emotional disorders induced by hemopressin and RVD-hemopressin(α) administration in rats. *Pharmacol. Reports* **69**, 1247–1253 (2017).

39. Ferrante, C., Recinella, L., Leone, S., Chiavaroli, A., Di Nisio, C., Martinotti, S., Mollica, A., Macedonio, G., Stefanucci, A., Dvorácskó, Sz., Tömböly, Cs., De Petrocellis, L., Vacca, M., Brunetti, L., Orlando, G. Anorexigenic effects induced by RVD-hemopressin(α) administration. *Pharmacol. Reports* **69**, 1402–1407 (2017).

40. Petrucci, V., Chicca, A., Glasmacher, S., Paloczi, J., Cao, Z., Pacher, P., Gertsch, J. Pepcan-12 (RVD-hemopressin) is a CB2 receptor positive allosteric modulator constitutively secreted by adrenals and in liver upon tissue damage. *Sci. Rep.* **7**, 9560 (2017).

41. Bauer, M., Chicca, A., Tamborrini, M., Eisen, D., Lerner, R., Lutz, B., Poetz, O., Pluschke, G., Gertsch, J. Identification and quantification of a new family of peptide endocannabinoids (Pepcans) showing negative allosteric modulation at CB1 receptors.

J. Biol. Chem. **287**, 36944–36967 (2012).

42. Wiley, J. L., Marusich, J. A., Huffman, J. W. Moving around the molecule: Relationship between chemical structure and in vivo activity of synthetic cannabinoids. *Life Sci.* **97**, 55–63 (2014).

43. Herkenham, M., Lynn, A. B., Little, M. D., Johnson, M. R., Melvin, L. S., de Costa, B. R., Rice, K. C. Cannabinoid receptor localization in brain. *Proc. Natl. Acad. Sci. U. S. A.* **87**, 1932–1936 (1990).

44. Pertwee, R. G. Cannabis and cannabinoids: Pharmacology and rationale for clinical use. *Complement. Med. Res.* **6**, 12–15 (1999).

45. Devane, W. A., Dysarz, F. A., Johnson, M. R., Melvin, L. S., Howlett, A. C. Determination and characterization of a cannabinoid receptor in rat brain. *Mol. Pharmacol.* **34**, 605–613 (1988).

46. Marini, P., Cascio, M. G., King, A., Pertwee, R. G., Ross, R. A. Characterization of cannabinoid receptor ligands in tissues natively expressing cannabinoid CB2 receptors. *Br. J. Pharmacol.* **169**, 887–899 (2013).

47. Pertwee, R. G. The pharmacology of cannabinoid receptors and their ligands: An overview. *Int. J. Obes.* **30**, S13–S18 (2006).

48. Eissenstat, M. A., Bell, M. R., D'Ambra, T. E., Alexander, E. J., Daum, S. J., Ackerman, J. H., Gruett, M. D., Kumar, V., Estep, K. G., Olefirowicz, E. M., *et al*. Aminoalkylindoles: Structure-activity relationships of novel cannabinoid mimetics. *J. Med. Chem.* **38**, 3094–3105 (1995).

49. Huffman, J. W., Zengin, G., Wu, M. J., Lu, J., Hynd, G., Bushell, K., Thompson, A. L., Bushell, S., Tartal, C., Hurst, D. P., Reggio, P. H., Selley, D. E., Cassidy, M. P., Wiley, J. L., Martin, B. R. Structure-activity relationships for 1-alkyl-3-(1-naphthoyl)indoles at the cannabinoid CB(1) and CB(2) receptors: steric and electronic effects of naphthoyl substituents. New highly selective CB(2) receptor agonists. *Bioorg. Med. Chem.* **13**, 89–112 (2005).

50. Breivogel, C. S., Childers, S. R. Cannabinoid agonist signal transduction in rat brain: comparison of cannabinoid agonists in receptor binding, G-protein activation, and adenylyl cyclase inhibition. *J. Pharmacol. Exp. Ther.* **295**, 328–36 (2000).

51. Aung, M. M., Griffin, G., Huffman, J. W., Wu, M., Keel, C., Yang, B., Showalter, V. M., Abood, M. E., Martin, B. R. Influence of the N-1 alkyl chain length of cannabimimetic indoles upon CB(1) and CB(2) receptor binding. *Drug Alcohol Depend.* **60**, 133–140 (2000).

52. Huffman, J. W., Mabon, R., Wu, M. J., Lu, J., Hart, R., Hurst, D. P., Reggio, P. H., Wiley, J. L., Martin, B. R. 3-Indolyl-1-naphthylmethanes: new cannabimimetic indoles provide evidence for aromatic stacking interactions with the CB(1) cannabinoid receptor. *Bioorg. Med. Chem.* **11**, 539–49 (2003).

53. Holden, J. E., Jeong, Y., Forrest, J. M. The endogenous opioid system and clinical pain management. *AACN Clin. Issues* **16**, 291–301 (2005).

54. Vaccarino, A. L., Olson, G. A., Olson, R. D., Kastin, A. J. Endogenous opiates: 1998.

Peptides **20**, 1527–74 (1999).

55. Horváth, Gy. Endomorphin-1 and endomorphin-2: pharmacology of the selective endogenous mu-opioid receptor agonists. *Pharmacol. Ther.* **88**, 437–63 (2000).

56. Fichna, J., Janecka, A., Piestrzeniewicz, M., Costentin, J., do Rego, J. C. Antidepressant-like effect of endomorphin-1 and endomorphin-2 in mice. *Neuropsychopharmacol.* **32**, 813–21 (2007).

57. Dhawan, B. N., Cesselin, F., Raghubir, R., Reisine, T., Bradley, P. B., Portoghese, P. S., Hamon, M. International Union of Pharmacology. XII. Classification of opioid receptors. *Pharmacol. Rev.* **48**, 567–92 (1996).

58. Harrison, C., Smart, D., Lambert, D. G. Stimulatory effects of opioids. *Br. J. Anaesth.* **81**, 20–8 (1998).

59. Martin, W. R., Eades, C. G., Thompson, J. A., Huppler, R. E., Gilbert, P. E. The effects of morphine- and nalorphine- like drugs in the nondependent and morphine-dependent chronic spinal dog. *J. Pharmacol. Exp. Ther.* **197**, 517–32 (1976).

60. Lord, J. A., Waterfield, A. A., Hughes, J., Kosterlitz, H. W. Endogenous opioid peptides: multiple agonists and receptors. *Nature* **267**, 495–9 (1977).

61. Waksman, G., Hamel, E., Fournié-Zaluski, M. C., Roques, B. P. Autoradiographic comparison of the distribution of the neutral endopeptidase "enkephalinase" and of mu and delta opioid receptors in rat brain. *Proc. Natl. Acad. Sci. U. S. A.* **83**, 1523–7 (1986).

62. Mansour, A., Khachaturian, H., Lewis, M. E., Akil, H., Watson, S. J. Anatomy of CNS opioid receptors. *Trends Neurosci.* **11**, 308–14 (1988).

63. Williams, J. Basic opioid pharmacology. *Rev. Pain* **1**, 2–5 (2008).

64. Bodnar, R. J., Klein, G. E. Endogenous opiates and behavior: 2003. *Peptides* **25**, 2205–2256 (2016).

65. Fischer, B. D., Ward, S. J., Henry, F. E., Dykstra, L. A. Attenuation of morphine antinociceptive tolerance by a CB1 receptor agonist and an NMDA receptor antagonist: Interactive effects. *Neuropharmacol.* **58**, 544–550 (2010).

66. Bushlin, I., Rozenfeld, R., Devi, L. A. Cannabinoid–opioid interactions during neuropathic pain and analgesia. *Curr. Opin. Pharmacol.* **10**, 80–86 (2010).

67. Koneru, A., Satyanarayana, S., Rizman, S. Endogenous opioids : Their physiological role and receptors. *Glob. J. Pharmacol.* **3**, 149–153 (2009).

68. Hughes, J., Smith, T. W., Kosterlitz, H. W., Fothergill, L. A., Morgan, B. A., Morris, H. R. Identification of two related pentapeptides from the brain with potent opiate agonist activity. *Nature* **258**, 577–80 (1975).

69. Li, C. H., Chung, D. Isolation and structure of an untriakontapeptide with opiate activity from camel pituitary glands. *Proc. Natl. Acad. Sci. U. S. A.* **73**, 1145–8 (1976).

70. Chavkin, C., James, I. F., Goldstein, A. Dynorphin is a specific endogenous ligand of the kappa opioid receptor. *Science* **215**, 413–5 (1982).

71. Kakidani, H., Furutani, Y., Takahashi, H., Noda, M., Morimoto, Y., Hirose, T., Asai, M., Inayama, S., Nakanishi, S., Numa, S. Cloning and sequence analysis of cDNA for porcine beta-neo-endorphin/dynorphin precursor. *Nature* **298**, 245–9 (1982).

72. Noda, M., Furutani, Y., Takahashi, H., Toyosato, M., Hirose, T., Inayama, S., Nakanishi, S., Numa, S. Cloning and sequence analysis of cDNA for bovine adrenal preproenkephalin. *Nature* **295**, 202–6 (1982).

73. Mcnally, G. P., Akil, H. Opioid peptides and their receptors: Overview and function in pain modulation. *Neuropsychopharmacol. Fifth Gener. Prog.* 35–46 (2002).

74. Keresztes, A., Tóth, G., Fülöp, F., Szűcs, M. Synthesis, radiolabeling and receptor binding of [^{3}H][(1*S*,2*R*)ACPC^{2}]endomorphin-2. *Peptides* **27**, 3315–3321 (2006).

75. Goldstein, A., Fischli, W., Lowney, L. I., Hunkapiller, M., Hood, L. Porcine pituitary dynorphin: complete amino acid sequence of the biologically active heptadecapeptide. *Proc. Natl. Acad. Sci. U. S. A.* **78**, 7219–23 (1981).

76. McDonald, J., Lambert, D. G. Opioid mechanisms and opioid drugs. *Anaesth. Intensive Care Med.* **17**, 464–468 (2016).

77. Benyhe, S., Zádor, F., Ötvös, F. Biochemistry of opioid (morphine) receptors: Binding, structure and molecular modelling. *Acta Biol. Szeged.* **59**, 17–37 (2015).

78. Brownstein, M. J. A brief history of opiates, opioid peptides, and opioid receptors. *Proc. Natl. Acad. Sci. U. S. A.* **90**, 5391–3 (1993).

79. Vuković, S., Prostran, M., Ivanović, M., Dosen-Mićović, Lj., Todorović, Z., Nesić, Z., Stojanović, R., Divac, N., Miković, Z. Fentanyl analogs: Structure-activity-relationship study. *Curr. Med. Chem.* **16**, 2468–2474 (2009).

80. Handa, B. K., Land, A. C., Lord, J. A., Morgan, B. A., Rance, M. J., Smith, C. F. Analogues of β-LPH61-64 possessing selective agonist activity at mu-opiate receptors. *Eur. J. Pharmacol.* **70**, 531–40 (1981).

81. Fields, H. State-dependent opioid control of pain. *Nat. Rev. Neurosci.* **5**, 565–575 (2004).

82. Matthes, H. W., Maldonado, R., Simonin, F., Valverde, O., Slowe, S., Kitchen, I., Befort, K., Dierich, A., Le Meur, M., Dollé, P., Tzavara, E., Hanoune, J., Roques, B. P., Kieffer, B. L. Loss of morphine-induced analgesia, reward effect and withdrawal symptoms in mice lacking the mu-opioid-receptor gene. *Nature* **383**, 819–23 (1996).

83. Rosenbaum, D. M., Rasmussen, S. G. F., Kobilka, B. K. The structure and function of G-protein-coupled receptors. *Nature* **459**, 356–363 (2009).

84. Hua, T., Vemuri, K., Nikas, S. P., Laprairie, R. B., Wu, Y., Qu, L., Pu, M., Korde, A., Jiang, S., Ho, J. H., Han, G. W., Ding, K., Li, X., Liu, H., Hanson, M. A., Zhao, S., Bohn, L. M., Makriyannis, A., Stevens, R. C., Liu, Z. J. Crystal structures of agonist-bound human cannabinoid receptor CB1. *Nature* **547**, 468–471 (2017).

85. Shao, Z., Yin, J., Chapman, K., Grzemska, M., Clark, L., Wang, J., Rosenbaum, D. M. High-resolution crystal structure of the human CB1 cannabinoid receptor. *Nature* **540**, 602–606 (2016).

86. Manglik, A., Kruse, A. C., Kobilka, T. S., Thian, F. S., Mathiesen, J. M., Sunahara, R. K., Pardo, L., Weis, W. I., Kobilka, B. K., Granier, S. Crystal structure of the μ-opioid receptor bound to a morphinan antagonist. *Nature* **485**, 321–326 (2012).

87. Foord, S. M., Bonner, T. I., Neubig, R. R., Rosser, E. M., Pin, J. P., Davenport, A. P., Spedding, M., Harmar, A. J. International Union of Pharmacology. XLVI. G protein-coupled receptor list. *Pharmacol. Rev.* **57**, 279–88 (2005).

88. Harrison, C., Traynor, J. R. The [^{35}S]GTPγS binding assay: Approaches and applications in pharmacology. *Life Sci.* **74**, 489–508 (2003).

89. Dhanasekaran, N., Dermott, J. M. Signaling by the G12 class of G proteins. *Cell. Signal.* **8**, 235–245 (1996).

90. Bourne, H. R., Sanders, D. A., McCormick, F. The GTPase superfamily: Conserved structure and molecular mechanism. *Nature* **349**, 117–27 (1991).

91. Zhang, R., Xie, X. Tools for GPCR drug discovery. *Acta Pharmacol. Sin.* **33**, 372–84 (2012).

92. Ritter, S. L., Hall, R. A. Fine-tuning of GPCR activity by receptor-interacting proteins. *Nat. Rev. Mol. Cell Biol.* **10**, 819–830 (2009).

93. Milligan, G. G protein-coupled receptor dimerization: Function and ligand pharmacology. *Mol. Pharmacol.* **66**, 1–7 (2004).

94. Hazum, E., Chang, K. J., Cuatrecasas, P. Opiate (enkephalin) receptors of neuroblastoma cells: occurrence in clusters on the cell surface. *Science* **206**, 1077–9 (1979).

95. Casadó, V., Cortés, A., Mallol, J., Pérez-Capote, K., Ferré, S., Lluis, C., Franco, R., Canela, E. I. GPCR homomers and heteromers: A better choice as targets for drug development than GPCR monomers? *Pharmacol. Ther.* **124**, 248–57 (2009).

96. Hiller, C., Kühhorn, J., Gmeiner, P. Class A G-protein-coupled receptor (GPCR) dimers and bivalent ligands. *J. Med. Chem.* **56**, 6542–59 (2013).

97. Ferré, S., Casadó, V., Devi, L. A., Filizola, M., Jockers, R., Lohse, M. J., Milligan, G., Pin, J. P., Guitart, X. G protein-coupled receptor oligomerization revisited: functional and pharmacological perspectives. *Pharmacol. Rev.* **66**, 413–34 (2014).

98. Rodriguez, J. J., Mackie, K., Pickel, V. M. Ultrastructural localization of the CB1 cannabinoid receptor in mu-opioid receptor patches of the rat Caudate putamen nucleus. *J. Neurosci.* **21**, 823–33 (2001).

99. Hojo, M., Sudo, Y., Ando, Y., Minami, K., Takada, M., Matsubara, T., Kanaide, M., Taniyama, K., Sumikawa, K., Uezono, Y. Mu-opioid receptor forms a functional heterodimer with cannabinoid CB1 receptor: Electrophysiological and FRET assay analysis. *J. Pharmacol. Sci.* **108**, 308–19 (2008).

100. Parolaro, D., Rubino, T., Viganò, D., Massi, P., Guidali, C., Realini, N. Cellular mechanisms underlying the interaction between cannabinoid and opioid system. *Curr. Drug Targets* **11**, 393–405 (2010).

101. Viganò, D., Rubino, T., Parolaro, D. Molecular and cellular basis of cannabinoid and opioid interactions. *Pharmacol. Biochem. Behav.* **81**, 360–368 (2005).

102. Bushlin, I., Gupta, A., Stockton, S. D., Miller, L. K., Devi, L. A. Dimerization with cannabinoid receptors allosterically modulates delta opioid receptor activity during neuropathic pain. *PLoS One* **7**, e49789 (2012).

103. Cichewicz, D. L. Synergistic interactions between cannabinoid and opioid analgesics. *Life Sci.* **74**, 1317–1324 (2004).

104. Desroches, J., Beaulieu, P. Opioids and cannabinoids interactions: involvement in pain management. *Curr. Drug Targets* **11**, 462–73 (2010).

105. Desroches, J., Bouchard, J. F., Gendron, L., Beaulieu, P. Involvement of cannabinoid receptors in peripheral and spinal morphine analgesia. *Neurosci.* **261**, 23–42 (2014).

106. Gerak, L. R., France, C. P. Combined treatment with morphine and Δ^9-tetrahydrocannabinol in rhesus monkeys: Antinociceptive tolerance and withdrawal. *J. Pharmacol. Exp. Ther.* **357**, 357–366 (2016).

107. Kazantzis, N. P., Casey, S. L., Seow, P. W., Mitchell, V. A., Vaughan, C. W. Opioid and cannabinoid synergy in a mouse neuropathic pain model. *Br. J. Pharmacol.* **173**, 2521–2531 (2016).

108. Maguire, D. R., Yang, W., France, C. P. Interactions between mu-opioid receptor agonists and cannabinoid receptor agonists in rhesus monkeys: Antinociception, drug discrimination, and drug self-administration. *J. Pharmacol. Exp. Ther.* **345**, 354–362 (2013).

109. Fujita, W., Gomes, I., Devi, L. A. Revolution in GPCR signalling: Opioid receptor heteromers as novel therapeutic targets: IUPHAR Review 10. *Br. J. Pharmacol.* **171**, 4155–4176 (2014).

110. Gomes, I., Ayoub, M. A., Fujita, W., Jaeger, W. C., Pfleger, K. D., Devi, L. A. G protein–coupled receptor heteromers. *Annu. Rev. Pharmacol. Toxicol.* **56**, 403–425 (2016).

111. Christopoulos, A., Changeux, J. P., Catterall, W. A., Fabbro, D., Burris, T. P., Cidlowski, J. A., Olsen, R. W., Peters, J. A., Neubig, R. R., Pin, J. P., Sexton, P. M., Kenakin, T. P., Ehlert, F. J., Spedding, M., Langmead, C. J. International Union of Basic and Clinical Pharmacology. XC. multisite pharmacology: Recommendations for the nomenclature of receptor allosterism and allosteric ligands. *Pharmacol. Rev.* **66**, 918–47 (2014).

112. Le Naour, M., Akgün, E., Yekkirala, A., Lunzer, M. M., Powers, M. D., Kalyuzhny, A. E., Portoghese, P. S. Bivalent ligands that target mu opioid (MOP) and cannabinoid1 (CB1) receptors are potent analgesics devoid of tolerance. *J. Med. Chem.* **56**, 5505–5513 (2013).

113. Fernandez-Fernandez, C., Callado, L. F., Girón, R., Sánchez, E., Erdozain, A. M., López-Moreno, J. A., Morales, P., Rodríguez de Fonseca, F., Fernández-Ruiz, J., Goya, P., Meana, J. J., Martín, M. I., Jagerovic, N. Combining rimonabant and fentanyl in a single entity: Preparation and pharmacological results. *Drug Des. Devel. Ther.* **8**, 263–277 (2014).

114. Mollica, A., Pelliccia, S., Famiglini, V., Stefanucci, A., Macedonio, G., Chiavaroli, A., Orlando, G., Brunetti, L., Ferrante, C., Pieretti, S., Novellino, E., Benyhe, S., Zádor, F., Erdei, A., Szűcs, E., Samavati, R., Dvorácskó, Sz., Tömboly, Cs., *et al.* Exploring the first rimonabant analog-opioid peptide hybrid compound, as bivalent ligand for CB1 and opioid receptors. *J.Enzyme Inhib. Med. Chem.* **32**, 444–451 (2017).

115. Bolognesi, M. L., Cavalli, A. Multitarget drug discovery and polypharmacology. *Chem. Med. Chem.* 1190–1192 (2016).

116. Dvorácskó, Sz., Stefanucci, A., Novellino, E., Mollica, A. The design of multitarget ligands for chronic and neuropathic pain. *Future Med. Chem.* **7,** 2469–2483 (2015).

117. Berque-Bestel, I., Lezoualc'h, F., Jockers, R. Bivalent ligands as specific pharmacological tools for G protein-coupled receptor dimers. *Curr. Drug Discov. Technol.* **5**, 312–318 (2008).

118. Tourwé D. Multitarget Peptides. *www.pharmoutsourcing.com/Featured-Articles/160866-Multitarget-Peptides/* (2014).

119. Wolkerstorfer, A., Handler, N., Buschmann, H. New approaches to treating pain. *Bioorg. Med. Chem. Lett.* **26**, 1103–1119 (2016).

120. Horváth, Gy., Kékesi, G. Interaction of endogenous ligands mediating antinociception. *Brain Res. Rev.* **52**, 69–92 (2006).

121. Welch, S. P., Stevens, D. L. Antinociceptive activity of intrathecally administered cannabinoids alone, and in combination with morphine, in mice. *J. Pharmacol. Exp. Ther.* **262**, 10–18 (1992).

122. Finn, D. P., Beckett, S. R., Roe, C. H., Madjd, A., Fone, K. C., Kendall, D. A., Marsden, C. A., Chapman, V. Effects of coadministration of cannabinoids and morphine on nociceptive behaviour, brain monoamines and HPA axis activity in a rat model of persistent pain. *Eur. J. Neurosci.* **19**, 678–86 (2004).

123. Li, J. X., McMahon, L. R., Gerak, L. R., Becker, G. L., France, C. P. Interactions between Δ^9-tetrahydrocannabinol and mu opioid receptor agonists in rhesus monkeys: Discrimination and antinociception. *Psychopharmacology (Berl).* **199**, 199–208 (2008).

124. Manzanares, J., Corchero, J., Romero, J., Fernández-Ruiz, J. J., Ramos, J. A., Fuentes, J. A. Pharmacological and biochemical interactions between opioids and cannabinoids. *Trends Pharmacol. Sci.* **20**, 287–94 (1999).

125. Maguire, D. R., France, C. P. Antinociceptive effects of mixtures of mu opioid receptor agonists and cannabinoid receptor agonists in rats: Impact of drug and fixed-dose ratio. *Eur. J. Pharmacol.* **819**, 217–224 (2018).

126. Kaiser, E., Colescott, R. L., Bossinger, C. D., Cook, P. I. Color test for detection of free terminal amino groups in the solid-phase synthesis of peptides. *Anal. Biochem.* **34**, 595–598. (1970).

127. Nakagawa, S., Deli, M. A., Kawaguchi, H., Shimizudani, T., Shimono, T., Kittel, A., Tanaka, K., Niwa, M. A new blood–brain barrier model using primary rat brain endothelial cells, pericytes and astrocytes. *Neurochem. Int.* **54**, 253–263 (2009).

128. Walter, F. R., Veszelka, Sz., Pásztói, M., Péterfi, Z. A., Tóth, A., Rákhely, G., Cervenak, L., Ábrahám, C. S., Deli, M. A. Tesmilifene modifies brain endothelial functions and opens the blood-brain/blood-glioma barrier. *J. Neurochem.* **134**, 1040–54 (2015).

129. Deli, M. A., Ábrahám, C. S., Kataoka, Y., Niwa, M. Permeability studies on in vitro blood–brain barrier models: Physiology, pathology, and pharmacology. *Cell. Mol. Neurobiol.* **25**, 59–127 (2005).

130. Monory, K. Greiner, E., Sartania, N., Sallai, L., Pouille, Y., Schmidhammer, H., Hanoune, J., Borsodi, A. Opioid binding profiles of new hydrazone, oxime, carbazone and semicarbazone derivatives of 14-alkoxymorphinans. *Life Sci.* **64**, 2011–2020 (1999).

131. Beardsley, P. M., Aceto, M. D., Cook, C. D., Bowman, E. R., Newman, J. L., Harris, L. S. Discriminative stimulus, reinforcing, physical dependence, and antinociceptive effects of oxycodone in mice, rats, and rhesus monkeys. *Exp. Clin. Psychopharmacol.* **12**, 163–72 (2004).

132. Narita, M., Nakamura, A., Ozaki, M., Imai, S., Miyoshi, K., Suzuki, M., Suzuki, T. Comparative pharmacological profiles of morphine and oxycodone under a neuropathic pain-like state in mice: evidence for less sensitivity to morphine. *Neuropsychopharmacology.* **33**, 1097–1112 (2008).

133. Maguire, D. R., France, C. P. Impact of efficacy at the mu-opioid receptor on antinociceptive effects of combinations of mu-opioid receptor agonists and cannabinoid receptor agonists. *J. Pharmacol. Exp. Ther.* **351**, 383–389 (2014).

134. Maguire, D. R., France, C. P. Interactions between cannabinoid receptor agonists and mu opioid receptor agonists in rhesus monkeys discriminating fentanyl. *Eur. J. Pharmacol.* **784**, 199–206 (2016).

135. McGregor, W. H., Stein, L., Belluzzi, J. D. Potent analgesic activity of the enkephalin-like tetrapeptide H-Tyr-D-Ala-Gly-Phe-NH_2. *Life Sci.* **23**, 1371–6 (1978).

136. Coy, D. H., Kastin, A. J., Walker, M. J., McGivern, R. F., Sandman, C. A. Increased analgesic activities of a fluorinated and a dimeric analogue of [D-Ala^2]-methionine enkephalinamide. *Biochem. Biophys. Res. Commun.* **83**, 977–83 (1978).

137. Lipkowski, A.W., Konecka, A. M., Sroczyńska, I. Double-enkephalins synthesis, activity on guinea-pig ileum, and analgesic effect. *Peptides* **3**, 697–700 (1982).

138. Akil, H. Endogenous opioids: Biology and function. *Annu. Rev. Neurosci.* **7,** 223–255 (1984).

139. Manzanares, J., Julian, M., Carrascosa, A. Role of the cannabinoid system in pain control and therapeutic implications for the management of acute and chronic pain episodes. *Curr. Neuropharmacol.* **4**, 239–257 (2006).

140. Wiley, J. L., Compton, D. R., Dai, D., Lainton, J. A., Phillips, M., Huffman, J. W., Martin, B. R. Structure-activity relationships of indole- and pyrrole-derived cannabinoids. *J. Pharmacol. Exp. Ther.* **285**, 995–1004 (1998).

141. Daniels, D. J., Lenard, N. R., Etienne, C. L., Law, P. Y., Roerig, S. C., Portoghese, P.

S. Opioid-induced tolerance and dependence in mice is modulated by the distance between pharmacophores in a bivalent ligand series. *Proc. Natl. Acad. Sci. U. S. A.* **102**, 19208–19213 (2005).

142. Akgun, E. Javed, M. I., Lunzer, M. M., Smeester, B. A., Beitz, A. J., Portoghese, P. S. Ligands that interact with putative MOR-mGluR5 heteromer in mice with inflammatory pain produce potent antinociception. *Proc. Natl. Acad. Sci. U.S.A.* **110**, 11595–11599 (2013).

143. D'Ambra, T. E., Estep, K. G., Bell, M. R., Eissenstat, M. A., Josef, K. A., Ward, S. J., Haycock, D. A., Baizman, E. R., Casiano, F. M., Beglin, N. C. *et al.* Conformationally restrained analogues of pravadoline: nanomolar potent, enantioselective, (aminoalkyl)indole agonists of the cannabinoid receptor. *J. Med. Chem.* **35**, 124–135 (1992).

144. Compton, D. R., Gold, L. H., Ward, S. J., Balster, R. L., Martin, B. R. Aminoalkylindole analogs: cannabimimetic activity of a class of compounds structurally distinct from Δ^9-tetrahydrocannabinol. *J. Pharmacol. Exp. Ther.* **263**, 1118–1126 (1992).

145. Stern, E., Lambert, D. M. Medicinal chemistry endeavors around the phytocannabinoids. *Chem. Biodivers.* **4**, 1707–28 (2007).

146. Price, M. R., Baillie, G. L., Thomas, A., Stevenson, L. A., Easson, M., Goodwin, R., McLean, A., McIntosh, L., Goodwin, G., Walker, G., Westwood, P., Marrs, J., Thomson, F., Cowley, P., Christopoulos, A., Pertwee, R. G., Ross, R. A. Allosteric modulation of the cannabinoid CB1 receptor. *Mol. Pharmacol.* **68**, 1484–1495 (2005).

147. Dvorácskó, Sz., Tömböly, Cs., Berkecz, R., Keresztes, A. Investigation of receptor binding and functional characteristics of hemopressin(1-7). *Neuropeptides* **58**, 15–22 (2016).

148. Guerrieri, E., Mallareddy, J. R., Tóth, G., Schmidhammer, H., Spetea, M. Synthesis and pharmacological evaluation of [^{3}H]HS665, a novel, highly selective radioligand for the kappa opioid receptor. *ACS Chem. Neurosci.* **6**, 456–463 (2015).

149. Espuña, G., Andreu, D., Barluenga, J., Pérez, X., Planas, A., Arsequell, G., Valencia, G. Iodination of proteins by IPy2BF4, a new tool in protein chemistry. *Biochemistry* **45**, 5957–63 (2006).

150. Hellinger, É., Veszelka, Sz., Tóth, A. E., Walter, F., Kittel, A., Bakk, M. L., Tihanyi, K., Háda, V., Nakagawa, S., Duy, T. D., Niwa, M., Deli, M. A., Vastag, M. Comparison of brain capillary endothelial cell-based and epithelial (MDCK-MDR1, Caco-2, and VB-Caco-2) cell-based surrogate blood–brain barrier penetration models. *Eur. J. Pharm. Biopharm.* **82**, 340–351 (2012).

151. Atwood, B. K., Huffman, J. W., Straiker, A., MacKie, K. JWH018, a common constituent of 'Spice' herbal blends, is a potent and efficacious cannabinoid CB1 receptor agonist. *Br. J. Pharmacol.* **160**, 585–593 (2010).

152. Zádor, F., Kocsis, D., Borsodi, A., Benyhe, S. Micromolar concentrations of rimonabant directly inhibits delta opioid receptor specific ligand binding and agonist-induced G-protein activity. *Neurochem. Int.* **67**, 14–22 (2014).

153. Nielsen, S., Sabioni, P., Trigo, J. M., Ware, M. A., Betz-Stablein, B. D., Murnion, B., Lintzeris, N., Khor, K. E., Farrell, M., Smith, A., Le Foll, B. Opioid-sparing effect of cannabinoids: A systematic review and meta-analysis. *Neuropsychopharmacol.* **42**, 1752–1765 (2017).

154. Vischer, H. F., Castro, M., Pin, J. P. G protein-coupled receptor multimers: A question still open despite the use of novel approaches. *Mol. Pharmacol.* **88**, 561–571 (2015).

155. Peters, J. U. Polypharmacology - Foe or friend? *J. Med. Chem.* **56**, 8955–8971 (2013).

156. Thakur, G. A., Nikas, S. P., Li, C., Makriyannis, A. Structural requirements for cannabinoid receptor probes. *Handb. Exp. Pharmacol.* **168**, 209–246 (2005).

157. Toniolo, E. F., Maique, E. T., Ferreira, W. A. Jr., Heimann, A. S., Ferro, E. S., Ramos-Ortolaza, D. L., Miller, L., Devi, L. A., Dale, C. S. Hemopressin, an inverse agonist of cannabinoid receptors, inhibits neuropathic pain in rats. *Peptides* **56**, 125–131 (2014).

158. Mollica, A., Pinnen, F., Feliciani, F., Stefanucci, A., Lucente, G., Davis, P., Porreca, F., Ma, S.W., Lai, J., Hruby, V. J. New potent biphalin analogues containing p-fluoro-L-phenylalanine at the 4,4′ positions and non-hydrazine linkers. *Amino Acids* **40**, 1503–1511 (2011).

159. Li, C. H., Chung, D. Isolation and structure of an untriakontapeptide with opiate activity from camel pituitary glands. *Proc Natl Acad Sci.***73**, 1145-1148 (1976).

160. Hughes, J., Smith, T.W., Kosterlitz, H.W., Fothergill, L.A., Morgan, G.A., Morris H.R. Identification of two related pentapeptides from the brain with potent opiate agonist activity. *Nature* **258**, 577-580 (1975).

161. Noda, M., Furutani, Y., Takahashi, H., Toyosato, M., Hirose, T., Inayama, S., Nakanishi, S., Numa, S. Cloning and sequence analysis of cDNA for bovine adrenal preproenkephalin. *Nature* **295**, 202-206 (1982).

162. Goldstein, A., Fischli, W., Lowney, L. I., Hunkapiller, M. & Hood, L. Porcine pituitary dynorphin: complete amino acid sequence of the biologically active heptadecapeptide. *Proc Natl Acad Sci U S A* **78**, 7219–23 (1981).

163. Chavkin, C., James, I.F., Goldstein, A. Dynorphin is a specific endogenous ligand of the kappa opioid receptor. *Science* **215**, 413-415 (1982).

164. Kakidani, H., Furutani, Y., Takahashi, H., Noda, M., Morimoto, Y., Hirose, T., Asai, M., Inayama, S., Nakanishi, S., Numa, S. Cloning and sequence analysis of cDNA for porcine beta-neo-endorphin/dynorphin precursor. *Nature* **298**, 245-249 (1982).

165. Zadina, J.E., Hackler, L., Ge, L.J., Kastin, A.J. A potent and selective endogenous agonist for the mu-opiate receptor. *Nature* **386**, 499-502 (1997)

166. Hackler, L., Zadina, J.E., Ge, L.J., Kastin, A.J Isolation of relatively large amount of endomorphin-1 and endomorphin-2 from human brain cortex. *Peptides* **18**, 1635-1639 . (1997)

Appendix

Oxycodone *O*-carboxymethyloxime (1). Oxycodone (1 g, 3.17 mmol) was dissolved in 250 mL of EtOH then 365 mg of 2-(aminooxy)acetic acid hemihydrochloride (3.32 mmol) and 400 μL of pyridine were added. The solution was stirred at 80°C for 75 min then the precipitate was filtered and dried under vacuum. The crude product was purified by HPLC on a Vydac 218TP1010 column (250 × 10 mm, 10 μm) using a linear gradient of 10→50% B in A over 25 min at a flow rate of 4 mL/min (λ= 216 nm) to give 1.14 g (93%) of pure **1** as a white solid. R_f 0.26 ($CHCl_3$–MeOH–$NH_{3(aq)}$ 9:1:0.1); HPLC k'= 2.46 (t_R= 10.2 min, Alltech Altima HP C18 column (250 × 4.6 mm, 5 μm), linear gradient of 10→60% B in A over 30 min (eluent A: 0.1% (v/v) TFA in H_2O, eluent B: 0.08% (v/v) TFA in ACN), flow rate: 1 mL/min, λ= 216 nm); ^{1}H NMR (500 MHz, MeOD) δ 6.88 (d, 1H, *J*= 8.2 Hz, 2-H), 6.79 (d, 1H, *J*= 8.2 Hz, 1-H), 5.03 (s, 1H, 5-H), 4.54 and 4.53 (2×s, 2×1H, C$\underline{H}_2$-COOH), 3.85 (s, 3H, OCH_3), 3.59 (d, 1H, *J*= 6.4 Hz, 9-H), 3.47 (d, 1H, *J*= 19.9 Hz, 10-H), 3.19 (dd, 1H, *J*= 13.0, 4.6 Hz, 16-H), 3.11 (dd, 1H, *J*= 19.9, 6.4 Hz, 10-H'), 2.93 (s, 3H, NCH_3), 2.87 (dd, 1H, *J*= 13.0, 3.9 Hz, 16-H'), 2.72 (ddd, 1H, *J*= 17.3, 7.0, 2.2 Hz, 15-H), 2.62 (m, 2H, 7-H, 15-H'), 1.75 (m, 1H, 7-H'), 1.71 (dd, 1H, *J*= 7.0, 2.6 Hz, 8-H), 1.46 (ddd, 1H, *J*= 14.1, 11.5, 7.0 Hz, 8-H'); ^{13}C NMR (126 MHz, MeOD) δ 175.6 (COOH), 156.7 (C-6), 146.7 (C-4), 144.8 (C-3), 130.1 (C-12), 124.2 (C-11), 121.1 (C-1), 117.7 (C-2), 87.5 (C-5), 72.9 (O-$\underline{C}H_2$-COOH), 71.2 (C-14), 68.3 (C-9), 57.7 (OCH_3), 48.3 (C-16), 47.2 (C-13), 41.7 (NCH_3), 30.0 (C-7), 28.9 (C-8), 24.7 (C-10), 18.6 (C-15); ESI-MS calcd for $C_{20}H_{24}N_2O_6$ 388.16, found 388.59 $[M+H]^+$.

Oxycodone *O*-(*N*-(2-(*N*-Boc-amino)ethyl)carboxamidomethyl)oxime (2). Oxime **1** (20 mg, 51.5 μmol) and HOBt·H_2O (7.9 mg, 51.5 μmol) were dissolved in 1.5 mL of DMF and DIC (8 μL, 51.5 μmol) was added. It was stirred for 5 min, then tert-butyl 2-aminoethylcarbamate hydrochloride (20 mg, 102 μmol) and DIEA (18 μL, 102 μmol) were added to the solution. The mixture was stirred at 50°C for 16 h then it was evaporated in vacuo. The crude product was purified by column chromatography on silica gel 60 with $CHCl_3$–MeOH (8:2) to give 22.2 mg (81%) of **2** as yellowish oil. R_f 0.45 ($CHCl_3$–MeOH 9:1); HPLC k'= 4.23 (t_R= 14.7 min, linear gradient of 10→70% B in A over 30 min); ^{1}H NMR (500 MHz, $CDCl_3$) δ 6.75 (d, 1H, *J*= 8.0 Hz, 2-H), 6.65 (d, 1H, *J*= 8.0 Hz, 1-H), 6.58 (brs, CONH), 5.88 (brs, CONH), 4.98 (s, 1H, 5-H), 4.58 and 4.55 (2×d, 2×1H, *J*= 15.0 Hz, O-CH_2-CO), 3.87 (s, 3H, OCH_3), 3.84 and 3.81 (2×t, 2×2H, *J*= 6.7, 1"-H, 2"-H), 3.72 (m, 1H, 9-H), 3.30 (m, 1H, 16-H), 3.19 (d, 1H, *J*= 19.9 Hz, 10-H), 3.08 (d, 1H, *J*= 18.5 Hz, 10-H'), 2.94 (brs, 1H, 15-H), 2.90 (s, 3H, NCH_3), 2.76 (m, 2H, 7-H, 16-H'), 2.00 (m, 1H, 15-H'), 1.85 (m,

1H, 8-H), 1.76 (m, 1H, 7-H'), 1.47 (m, 1H, 8-H'), 1.41 (s, 9H, $C(CH_3)_3$); ESI-MS calcd for $C_{27}H_{38}N_4O_7$ 530.27, found 531.30 $[M+H]^+$.

Oxycodone *O*-(*N*-(6-(*N*-Boc-amino)hexyl)carboxamidomethyl)oxime (3). Prepared as described for **2** but tert-butyl 6-aminohexylcarbamate (22 mg, 102 μmol) was used. The crude product was purified by column chromatography on silica gel 60 with $CHCl_3$–MeOH (8:2) to give 23.1 mg (77%) of **3** as pale yellow oil. R_f 0.44 ($CHCl_3$–MeOH 9:1); HPLC k'= 5.13 (t_R= 17.2 min, linear gradient of 10→70% B in A over 30 min); ^{1}H NMR (500 MHz, $CDCl_3$) δ 6.73 (d, 1H, *J*= 8.1 Hz, 2-H), 6.64 (d, 1H, *J*= 8.1 Hz, 1-H), 6.19 (t, 1H, *J*= 4.7 Hz, CONH), 5.76 (brs, CONH), 4.94 (s, 1H, 5-H), 4.58 and 4.54 (2×d, 2×1H, *J*= 15.9 Hz, O-CH_2-CO), 3.86 (s, 3H, OCH_3), 3.80 (m, 1H, 9-H), 3.32 (m, 2H, 1"-H), 3.28 (d, 1H, *J*= 19.7 Hz, 10-H), 3.20 (brs, 1H, 16-H), 3.09 (t, 2H, *J*= 6.2 Hz, 6"-H), 3.08 (d, 1H. *J*= 19.3 Hz, 10-H'), 2.91 (s, 3H, NCH_3), 2.81 (m, 3H, 7-H, 15-H, 16-H'), 2.71 (brs, 1H, 15-H'), 1.85 (brs, 1H, 8-H), 1.77 (d, 1H, *J*= 9.7 Hz, 7-H'), (1.47 and 1.31) (m, 8H, 2"-H, 3"-H, 4"-H, 5"-H), 1.43 (s, 10H, 8-H', $C(CH_3)_3$); ESI-MS calcd for $C_{31}H_{46}N_4O_7$ 586.34, found 587.40 $[M+H]^+$.

Oxycodone *O*-(*N*-(13-(*N*-Boc-amino)-4,7,10-trioxatridecyl)carboxamidomethyl)oxime (4). Prepared as described for **2** but *N*-Boc-4,7,10-trioxa-1,13-tridecanediamine (33 mg, 102 μmol) was used. The crude product was purified by column chromatography on silica gel 60 with $CHCl_3$–MeOH (8:2) to give 23.6 mg (66%) of **4** as yellowish oil. R_f 0.52 ($CHCl_3$–MeOH 9:1); HPLC k'= 5.01 (t_R= 16.8 min, linear gradient of 10→70% B in A over 30 min); ^{1}H NMR (500 MHz, $CDCl_3$) δ 6.82 (d, 1H, *J*= 8.2 Hz, 2-H), 6.73 (d, 1H, *J*= 8.2 Hz, 1-H), 6.43 (t, 1H, *J*= 4.8 Hz, CONH), 5.00 (brs, 1H, CONH), 4.94 (s, 1H, 5-H), 4.58 and 4.53 (2×d, 2×1H, *J*= 15.8 Hz, O-CH_2-CO), 3.86 (s, 3H, OCH_3), 3.83 (t, 2H, *J*= 6.7 Hz, 13"-H), 3.80 (m, 1H, 9-H), (3.61, 3.57, 3.52) (3×m, 12H, 3"-H, 5"-H, 6"-H, 8"-H, 9"-H, 11"-H), 3.43 (q, 1H, *J*= 5.9 Hz, 1"-H), 3.37 (m, 2H, 1"-H', 10-H), 3.21 (m, 1H, 16-H), 3.19 (d, 1H, *J*= 18.7 Hz, 10-H'), 2.95 (s, 3H, NCH_3), 2.80 (d, 1H, *J*= 5.7 Hz, 16-H'), 2.68 (m, 1H, 15-H), 2.56 (m, 2H, 7-H, 15-H'), 1.80 (m, 1H, 8-H), 1.76 (m, 4H, 2"-H, 12"-H), 1.62 (m, 1H, 7-H'), 1.43 (s, 9H, $C(CH_3)_3$), 1.38 (m, 1H, 8-H'); ESI-MS calcd for $C_{35}H_{54}N_4O_{10}$ 690.38, found 691.15 $[M+H]^+$.

Oxycodone *O*-(*N*-(2-aminoethyl)carboxamidomethyl)oxime (5). The *N*-protected oxime **2** (22 mg, 41.5 μmol) was dissolved in 2 mL of DCM containing 50% (v/v) TFA and it was stirred for 30 min at rt. The solution was evaporated in vacuo that yielded the TFA salt of **5**. 21 mg (95%); R_f 0.27 ($CHCl_3$–MeOH 9:1); HPLC k'= 1.65 (t_R= 7.4 min, linear gradient of 10→70% B in A over 25 min); ESI-MS calcd for $C_{22}H_{30}N_4O_5$ 430.22, found 431.30 $[M+H]^+$.

Oxycodone *O*-(*N*-(6-aminohexyl)carboxamidomethyl)oxime (6). Prepared as described for **5**. Yield 22 mg (96%); R_f 0.26 ($CHCl_3$–MeOH 9:1); HPLC k'= 2.28 (t_R= 9.2 min, linear

gradient of 10→70% B in A over 25 min); ESI-MS calcd for $C_{26}H_{38}N_4O_5$ 486.28, found 487.11 $[M+H]^+$.

Oxycodone *O*-(*N*-(13-amino-4,7,10-trioxatridecyl)carboxamidomethyl)oxime (7). Prepared as described for **5**. Yield 22.5 mg (95%); R_f 0.33 ($CHCl_3$–MeOH 9:1); HPLC k'= 2.54 (t_R= 9.9 min, linear gradient of 10→60% B in A over 25 min); ESI-MS calcd for $C_{30}H_{46}N_4O_8$ 590.33, found 591.09 $[M+H]^+$.

6-(1*H*-indol-1-yl)hexanoic acid (8). To a stirred solution of indole (1.17 g, 10 mmol) in ACN (10 mL) were added triethylamine (1.39 mL, 10 mmol) and 6-bromohexanoic acid (1.94 g, 10 mmol), then the solution was stirred at 80°C overnight. The solvent was evaporated in vacuo and the residue was extracted with water and $CHCl_3$ (3×20 mL). The combined organic phase was washed with brine, and dried over Na_2SO_4. After evaporation the crude product was purified by column chromatography on silica gel 60 with EtOAc−*n*-hexane 2:1 to give 1.76 g (77%) of pure **8** as yellow oil. R_f 0.38 (EtOAc–*n*-hexane 2:1); HPLC k'= 4.36 (t_R= 15.0 min, linear gradient of 5→60% B in A over 25 min); ^{1}H NMR (500 MHz, $CDCl_3$) δ 7.63 (d, 1H, *J*= 7.9 Hz, 4-H), 7.33 (d, 1H, *J*= 8.2 Hz, 7-H), 7.20 (t, 1H, *J*= 7.6 Hz, 5-H), 7.10 (t, 1H, *J*= 7.6 Hz, 6-H), 7.09 (d, 1H, *J*= 3.2 Hz, 2-H), 6.48 (d, 1H, *J*= 3.1 Hz, 3-H), 4.13 (t, 2H, *J*= 7.1 Hz, 1'-H), 2.33 (t, 2H, *J*= 7.4 Hz, 5'-H), 1.87 (quin, 2H, *J*= 7.3 Hz, 2'-H), 1.67 (quin, 2H, *J*= 7.5 Hz, 4'-H), 1.38 (quin, 2H, *J*= 7.7 Hz, 3'-H); ^{13}C NMR (126 MHz, $CDCl_3$) δ 178.2 (COOH), 136.0 (C-7a), 128.7 (C-3a), 127.9 (C-2), 121.5 (C-6), 121.1 (C-4), 119.4 (C-5), 109.4 (C-7), 101.1 (C-3), 46.3 (C-1'), 33.8 (C-5'), 30.1 (C-2'), 26.6 (C-3'), 24.4 (C-4'); ESI-MS calcd for $C_{14}H_{17}NO_2$ 231.13, found 231.93 $[M+H]^+$.

6-(3-(1-Naphthoyl)-1*H*-indol-1-yl)hexanoic acid (9). To a stirred solution of **8** (1.5 g, 6.49 mmol) in 5 mL of dry DCM 6.5 mL of 1M Et_2AlCl in hexane (6.49 mmol) was added dropwise. It was stirred at 0°C for 1 h then 1.2 g of 1-naphthoyl chloride (6.49 mmol) dissolved in 3 mL of DCM was added dropwise. The reaction mixture was stirred at 0°C overnight then it was carefully poured into a mixture of ice and 0.1 M HCl and it was extracted with DCM. The combined organic phase was washed with brine and dried over Na_2SO_4. The organic phase was evaporated and the crude product was purified by column chromatography on silica gel 60 with (EtOAc−*n*-hexane 1:1) to give 1.05 g (42%) of pure **9** as yellow oil that became crystalline in a day. R_f 0.26 (EtOAc–*n*-hexane 2:1); HPLC k'= 5.07 (t_R= 17.0 min, linear gradient of 20→100% B in A over 25 min); ^{1}H NMR (500 MHz, $CDCl_3$) δ 8.50 (m, 1H, 4-H), 8.19 (d, 1H, *J*= 8.3 Hz, 15'-H), 7.98 (d, 1H, *J*= 8.2 Hz, 11'-H), 7.92 (d, 1H, *J*= 8.1 Hz, 12'-H), 7.67 (d, 1H, *J*= 7.0 Hz, 9'-H), [7.54 (t, 1H, *J*= 8.2 Hz) and 7.52 (t, 1H, *J*= 8.2 Hz)] (10'-H and 13'-H), 7.47 (t, 1H, *J*= 7.1 Hz, 14'-H), 7.41-7.34 (overlapping m, 4H,

2-H, 5-H, 6-H, 7-H), 4.08 (t, 2H, *J*= 7.3 Hz, 1'-H), 2.26 (t, 2H, *J*= 7.4 Hz, 5'-H), 1.83 (quin, 2H, *J*= 7.4 Hz, 2'-H), 1.62 (quin, 2H, *J*= 7.6 Hz, 4'-H), 1.31 (m, 2H, 3'-H); ^{13}C NMR (126 MHz, $CDCl_3$) δ 192.5 (3-CO), 181.6 (COOH), 138.9 (C-8'), 137.6 (C-2), 136.9 (C-7a), 133.8 (C-11a'), 130.6 (C-15a'), 130.4 (C-11'), 128.4 (C-12'), 127.0 (C-14'), 126.8 (C-3a), 126.5 (C-13'), 126.0 (C-9'), 125.7 (C-15'), 124.7 (C-10'), 123.3 (C-6), 122.7 (C-5), 122.2 (C-4), 117.4 (C-3), 110.1 (C-7), 46.4 (C-1'), 37.3 (C-5'), 29.9 (C-2'), 26.3 (C-3'), 25.3 (C-4'); ESI-MS calcd for $C_{25}H_{23}NO_3$ 385.17, found 386.03 $[M+H]^+$.

Bivalent compound 10. The carboxylic acid **9** (7.4 mg, 19 μmol) and HOBt.H_2O (2.9 mg, 19 μmol) were dissolved in 1.5 mL of DMF and DIC (2.9 μL, 19 μmol) was added. It was stirred for 5 min, then **5** (20.7 mg, 38 μmol) and DIEA (6.6 μL, 38 μmol) were added and the solution was stirred overnight at 50°C. Then it was evaporated in vacuo and the crude product was purified by semipreparative HPLC on a Vydac 218TP1010 column that yielded 12.1 mg of **10** (79%) as yellow oil. R_f 0.63 ($CHCl_3$–MeOH 9:1); HPLC k'= 2.94 (t_R= 13.9 min, linear gradient of 30→60% B in A over 25 min); ^{1}H NMR (500 MHz, $CDCl_3$) δ ^{1}H NMR ($CDCl_3$) δ 8.40 (d, 1H, *J*= 6.8 Hz, 4'-H), 8.15 (d, 1H, *J*= 8.4 Hz, 15'-H), 7.96 (d, 1H, *J*= 8.1 Hz, 11'-H), 7.90 (d, 1H, *J*= 8.1 Hz, 12'-H), 7.65 (d, 1H, *J*= 6.8 Hz, 9'-H), 7.52 (t, 1H, *J*= 7.6 Hz, 10'-H), 7.50 (t, 1H, *J*= 7.5 Hz, 13'-H), 7.45 (t, 1H, *J*= 7.6 Hz, 14'-H), 7.41 (s, 1H, 2'-H), 7.39 (s, 1H, 7'-H), 7.32 (m, 2H, 5'-H, 6'-H), 6.81 (d, 1H, *J*= 8.2 Hz, 2-H), 6.74 (brs, CONH), 6.72 (d, 1H, *J*= 8.2 Hz, 1-H), 6.43 (brs, CONH), 4.99 (s, 1H, 5-H), 4.57 and 4.47 (2×d, 2×1H, *J*= 16.1 Hz, O-CH_2-CO), 4.08 (t, 2H, *J*= 6.9 Hz, 16'-H), 3.85 (s, 3H, OCH_3), 3.73 (brs, 1H, 9-H), 3.26 (2×brs, 5H, 1"-H, 2"-H, 16-H), 3.21 (d, 1H, *J*= 19.0 Hz, 10-H), 3.00 (d, 1H, *J*= 19.0 Hz, 10-H'), 2.84 (s, 4H, NCH_3, 15-H), 2.73 (brs, 2H, 7-H, 16-H'), 2.40 (d, 1H, *J*= 8.2 Hz, 15-H'), 2.09 (t, 2H, *J*= 5.7 Hz, 20'-H), 1.81 (quin, 2H, *J*= 7.1 Hz, 17'-H), 1.76 (m, 1H, 8-H), 1.65 (d, 1H, *J*= 8.0 Hz, 7-H'), 1.56 (quin, 2H, 6.9 Hz, 19'-H), 1.35 (m, 1H, 8-H'), 1.27 (m, 2H, 18'-H); ^{13}C NMR (126 MHz, $CDCl_3$) δ 192.3 (Ar-CO), 174.3 (20'-CONH), 170.9 (O-CH_2-<u>C</u>ONH), 156.7 (C-6), 145.9 (C-4), 143.8 (C-3), 139.0 (C-8'), 138.2 (C-2'), 137.2 (C-7a'), 133.9 (C-11a'), 130.9 (C-15a'), 130.2 (C-11'), 128.6 (C-12), 128.4 (C-12'), 127.1 (C-3a'), 126.9 (C-14'), 126.5 (C-13'), 126.1 (C-9'), 126.0 (C-15'), 124.8 (C-10'), 123.8 (C-6'), 123.0 (C-5'), 122.9 (C-4'), 121.6 (C-11), 120.0 (C-1), 117.6 (C-3'), 115.8 (C-2), 110.3 (C-7'), 86.9 (C-5), 73.2 (O-<u>C</u>H_2-CO), 70.4 (C-14), 65.7 (C-9), 56.8 (OCH_3), 47.3 (C-16), 47.1 (C-16'), 46.2 (C-13), 42.1 (NCH_3), 39.8 and 39.6 (C-1", C-2"), 36.1 (C-20'), 29.6 (C-17'), 29.3 (C-7), 28.6 (C-8), 26.4 (C-18'), 25.1 (C-19'), 24.1 (C-10), 17.3 (C-15); MALDI-MS calcd for $C_{47}H_{51}N_5O_7$ 797.38, found 798.34 $[M+H]^+$.

Bivalent compound 11. Prepared as described for **10**, but **6** (23 mg, 38 μmol) was used. Yield 11.6 mg of **11** (71%) as brown oil. R_f 0.60 ($CHCl_3$–MeOH 9:1); HPLC k'= 6.55 (t_R= 19.7 min, linear gradient of 10→100% B in A over 25 min); ^{1}H NMR (500 MHz, $CDCl_3$) δ 8.41 (d, 1H, *J*= 7.5 Hz, 4'-H), 8.14 (d, 1H, *J*= 8.3 Hz, 15'-H), 7.96 (d, 1H, *J*= 8.2 Hz, 11'-H), 7.90 (d, 1H, *J*= 8.1 Hz, 12'-H), 7.63 (d, 1H, *J*= 6.6 Hz, 9'-H), 7.52 (t, 1H, *J*= 7.9 Hz, 10'-H), 7.50 (t, 1H, *J*= 8.2 Hz, 13'-H), 7.44 (t, 1H, *J*= 7.6 Hz, 14'-H), 7.38 (overlapping d, 1H, 7'-H), 7.37 (s, 1H, 2'-H), 7.33 (m, 2H, 5'-H, 6'-H), 6.81 (d, 1H, *J*= 8.2 Hz, 2-H), 6.72 (d, 1H, *J*= 8.3 Hz, 1-H), 6.26 (brs, 1H, 1"-NH), 6.06 (brs, 6"-NH), 5.00 (s, 1H, 5-H), 4.58 and 4.50 (2×d, 2×1H, *J*= 15.9 Hz, O-CH_2-CO), 4.07 (t, 2H, *J*= 6.8 Hz, 16'-H), 3.85 (s, 3H, OCH_3), 3.78 (brs, 1H, 9-H), 3.30 (q, 1H, *J*= 6.3 Hz, 1"-H), 3.24 (brs, 1H, 16-H), 3.23 (d, 1H, *J*= 19.4 Hz, 10-H), 3.14 (m, 2H, 1"-H', 6"-H), 3.03 (d, 1H, *J*= 19.3 Hz, 10-H'), 2.91 (d, 1H, *J*= 18.7 Hz, 6"-H'), 2.84 (s, 3H, NCH_3), 2.73 (brs, 2H, 7-H, 16-H'), 2.69 (m, 1H, 15-H), 2.60 (m, 1H, 15-H'), 2.11 (t, 2H, *J*= 6.4 Hz, 20'-H), 1.80 (quin, 3H, *J*= 7.0 Hz, 17'-H, 8-H), 1.68 (d, 1H, *J*= 8.5 Hz, 7-H'), 1.57 (quin, 2H, 6.3 Hz, 19'-H), [1.42 (m, 4H) and 1.26 (brs, 4H)] (2"-H, 3"-H, 4"-H, 5"-H), 1.34 (m, 1H, 8-H'), 1.26 (brs, 2H, 18'-H); ^{13}C NMR (126 MHz, $CDCl_3$) δ 192.4 (Ar-CO), 173.8 (20'-CONH), 170.0 (O-CH_2-CONH), 156.8 (C-6), 145.6 (C-4), 143.9 (C-3), 139.0 (C-8'), 138.3 (C-2'), 137.2 (C-7a'), 133.9 (C-11a'), 130.8 (C-15a'), 130.2 (C-11'), 128.4 (C-12'), 128.3 (C-12), 127.1 (C-3a'), 126.9 (C-14'), 126.5 (C-13'), 126.1 (C-9'), 126.0 (C-15'), 124.8 (C-10'), 123.9 (C-6'), 123.1 (C-5'), 123.0 (C-4'), 121.3 (C-11), 120.0 (C-1), 117.6 (C-3'), 116.0 (C-2), 110.2 (C-7'), 86.4 (C-5), 73.3 (O-CH_2-CO), 70.4 (C-14), 66.0 (C-9), 56.9 (OCH_3), 47.6 (C-16), 47.1 (C-16'), 46.0 (C-13), 42.0 (NCH_3), 39.4 (C-6"), 38.7 (C-1"), 36.2 (C-20'), 29.5 (C-17'), (29.2, 28.3, 26.1, 26.0) (C-2", C-3", C-4", C-5"), 29.0 (C-7), 28.4 (C-8), 26.4 (C-18'), 25.3 (C-19'), 24.0 (C-10), 17.9 (C-15); MALDI-MS calcd for $C_{51}H_{59}N_5O_7$ 853.44, found 854.49 $[M+H]^+$.

Bivalent compound 12. Prepared as described for **10**, but **7** (26.8 mg, 38 μmol) was used. Yield 11.1 mg of **12** (61%) as yellow oil. R_f 0.70 ($CHCl_3$–MeOH 9:1); HPLC k'= 3.03 (t_R= 15.3 min, linear gradient of 30→60% B in A over 25 min); ^{1}H NMR (500 MHz, $CDCl_3$) δ 8.42 (d, 1H, *J*= 6.8 Hz, 4'-H), 8.16 (d, 1H, *J*= 8.3 Hz, 15'-H), 7.97 (d, 1H, *J*= 8.1 Hz, 11'-H), 7.90 (d, 1H, *J*= 8.1 Hz, 12'-H), 7.65 (d, 1H, *J*= 6.6 Hz, 9'-H), 7.53 (t, 1H, *J*= 7.6 Hz, 10'-H), 7.51 (t, 1H, *J*= 7.5 Hz, 13'-H), 7.45 (t, 1H, *J*= 7.3 Hz, 14'-H), 7.40 and 7.39 (2×s, 2×1H, 2'-H, 7'-H), 7.34 (m, 2H, 5'-H, 6'-H), 6.80 (d, 1H, *J*= 8.2 Hz, 2-H), 6.71 (d, 1H, *J*= 8.3 Hz, 1-H), 6.68 (brs, CONH), 6.55 (brs, CONH), 5.01 (s, 1H, 5-H), 4.59 and 4.50 (2×d, 2×1H, *J*= 15.9 Hz, O-CH_2-CO), 4.09 (t, 2H, *J*= 6.9 Hz, 16'-H), 3.87 (s, 3H, OCH_3), 3.77 (brs, 1H, 9-H), 3.58-3.41 (m, 12H, 3"-H, 5"-H, 6"-H, 8"-H, 9"-H, 11"-H), 3.26 (brs, 1H, 16-H), 3.27 (brs,

4H, 1”-H, 13”-H), 3.22 (d, 1H, *J*= 19.1 Hz, 10-H), 3.03 (d, 1H, *J*= 18.6 Hz, 10-H’), 2.86 (s, 3H, NCH_3), 2.74 (brs, 2H, 7-H, 16-H’), 2.70 (brs, 1H, 15-H), 2.60 (d, 1H, *J*= 12.0 Hz, 15-H’), 2.12 (t, 2H, *J*= 6.5 Hz, 20’-H), 1.81 (m, 3H, 8-H, 17’-H), 1.70 (m, 5H, 7-H’, 2”-H, 12”-H), 1.59 (quin, 2H, 6.7 Hz, 19’-H), 1.37 (brs, 1H, 8-H’), 1.27 (m, 2H, 18’-H); ^{13}C NMR (126 MHz, $CDCl_3$) δ 192.3 (Ar-CO), 173.7 (20’-CONH), 169.9 (O-CH_2-CONH), 156.7 (C-6), 145.7 (C-4), 143.9 (C-3), 139.0 (C-8’), 138.2 (C-2’), 137.2 (C-7a’), 133.9 (C-11a’), 130.9 (C-15a’), 130.2 (C-11’), 128.4 (2C, C-12, C-12’), 127.1 (C-3a’), 126.9 (C-14’), 126.5 (C-13’), 126.1 (C-9’), 126.0 (C-15’), 124.8 (C-10’), 123.8 (C-6’), 123.05 (C-5’), 122.97 (C-4’), 121.3 (C-11), 119.9 (C-1), 117.6 (C-3’), 116.0 (C-2), 110.2 (C-7’), 86.5 (C-5), 73.3 (O-CH_2-CO), (70.3, 70.1, 70.0, 69.9, 69.4) (7C, C-14, C-3”, C-5”, C-6”, C-8”, C-9”, C-11”), 66.0 (C-9), 57.0 (OCH_3), 47.6 (C-16), 47.1 (C-16’), 46.2 (C-13), 42.0 (NCH_3), 38.1 and 37.1 (C-1”, C-13”), 36.1 (C-20’), 30.6 (C-8), 29.6 (C-17’), 29.2 (C-7), 28.9 (C-2”, C-12”), 26.4 (C-18’), 25.2 (C-19’), 24.1 (C-10), 17.8 (C-15); MALDI-MS calcd for $C_{55}H_{67}N_5O_{10}$ 957.49, found 958.23 $[M+H]^+$.

(1*H*-Indol-3-yl)(naphthalen-1-yl)methanone (13). Indole (250 mg, 2.13 mmol) was dissolved in 5 mL of DCM and 1.74 mL of Et_2AlCl (25% (w/w) in toluene (3.2 mmol) was added at 0^{o}C. The mixture was stirred at 0^{o}C for 30 min and 1-naphthoyl chloride (609 mg, 3.2 mmol dissolved in 8 mL of DCM) was added dropwise to the solution at 0^{o}C, and it was stirred overnight. Then the reaction mixture was quenched with 100 mM $NaHCO_3$. The precipitate was filtered and the filtrate was evaporated in vacuo. The crude product was purified by column chromatography on silica gel 60 (*n*-hexane–EtOAc 2:1) to give **13** (406 mg, 70%) as yellow solid. R_f 0.44 (*n*-hexane–EtOAc 2:1); ^{1}H NMR (300 MHz, $CDCl_3$) δ 10.76 (brs, 1H, N*H* indole), 8.41 (d, 1H, 4-H), 8.10 (d, 1H, *J*= 8.1 Hz, 15’-H), 7.88 (d, 1H, *J*= 8.1 Hz, 11’-H), 7.82 (d, 1H, *J*= 7.8 Hz, 12’-H), 7.59 (d, 1H, *J*= 6.1 Hz, 9’-H), 7.47-7.35 (m, 5H, 10’-H, 13’-H, 14’-H, 2-H, 5-H), 7.27-7.23 (m, 2H, 6-H, 7-H); ^{13}C NMR (300 MHz, $CDCl_3$) δ 192.5 (CO), 139.1 (C-8’), 135.8 (C-7a), 133.6 (C-11a’), 130.7 (C-15a’), 129.8 (C-11’), 128.1 (C-12’), 126.6 (C-14’), 126.2 (C-3a), 126.1 (C-13’), 125.8 (C-9’), 125.7 (C-15’), 124.4 (C-10’), 123.5 (C-6), 122.5 (C-5), 122.3 (C-4), 122.2 (C-3), 117.4 (C-2), 111.8 (C-7); ESI-MS calcd for $C_{19}H_{13}NO$ 271.10, found 272.24 $[M+H]^+$.

tert-Butyl 5-bromopentylcarbamate (14). To a stirred solution of tert-butyl 5-hydroxypentyl-carbamate (500 mg, 2.46 mmol) and TEA (498 mg, 4.92 mmol) in 5 mL DCM at –10^{o}C was added MsCl (338 mg, 2.95 mmol) dropwise and the solution was stirred at the same temperature for 5 h. The reaction was then quenched with water. The organic layer was washed with water, brine, dried over $MgSO_4$, filtered and evaporated under reduced pressure

to give the desired product as yellow oil (552 mg, 80%, R_f 0.5 (EtOAc)) The mesylate was used in the next step without any further purification. Under N_2 atmosphere 5-(tert-butoxycarbonylamino)pentyl methanesulfonate (350 mg, 1.2 mmol) was dissolved in 5 mL THF followed by the addition of LiBr (313 mg, 3.6 mmol) to the solution. The reaction mixture was stirred for 16 h under reflux, then THF was removed under vacuum. The mixture was diluted with 10 mL water and it was extracted with DCM (3 × 10 mL). The combined organic phase was washed with water (3 × 10 mL) and brine (3 × 10 mL), dried over $MgSO_4$ and evaporated in vacuo. The product was purified by column chromatography on silica gel 60 (*n*-hexane–EtOAc 9:1) to give white crystalline product (230 mg, 72%). R_f 0.6 (*n*-hexane–EtOAc 4:1); ^{1}H NMR (300 MHz, $CDCl_3$) δ 4.53 (brs, 1H, NH), 3.40 (t, 2H, *J*= 8.4 Hz, 5-H), 3.10 (q, 2H, *J*= 7.8 Hz, 1-H), 1.86 (quin, 2H, *J*= 7.3 Hz, 4-H), 1.52-1.48 (m, 4H, 2-H, 3-H), 1.43 (s, 9H, CH_3); ESI-MS calcd for $C_{10}H_{20}BrNO_2$ 265.07, found 266.12 $[M+H]^+$.

tert-Butyl (5-(3-(1-naphthoyl)-1*H*-indol-1-yl)pentyl)carbamate (15). To a stirred solution of NaH (60% dispersion in mineral oil, 15.4 mg, 0.44 mmol) in 5 mL of DMF at 0°C was added **13** (100 mg, 0.368 mmol) in 10 mL DMF dropwise and the mixture was stirred at 80°C for 1h. The reaction mixture was cooled to 0°C and a solution of **14** (108 mg, 0.41 mmol) in 5 mL DMF was added dropwise and stirred at 0°C for 30 min, and then stirred for 18 h at r.t. Then it was evaporated and the oily residue was dissolved in EtOAc (50 mL). The organic layer was washed with water (3 × 50 mL) and brine (3 × 50 mL), dried over Na_2SO_4 and evaporated in vacuo. The crude residue was purified by column chromatography on silica gel 60 (ethyl acetate /hexane 1:2) to yield **15** (142 mg, 85%) as orange-red oil. R_f 0.59 (*n*-hexane–EtOAc 2:1); ^{1}H NMR (300 MHz, $CDCl_3$) δ 8.47 (m, 1H, 4-H), 8.17 (d, 1H, *J*= 8.3 Hz, 15'-H), 7.95 (d, 1H, *J*= 8.2 Hz, 11'-H), 7.89 (d, 1H, *J*= 8.1 Hz, 12'-H), 7.63 (d, 1H, *J*= 6.9 Hz, 9'-H), 7.55 (t, 1H, *J*= 7.5 Hz, 10'-H), 7.42 (t, 1H, *J*= 7.1 Hz, 14'-H), 7.33 (t, 1H, *J*= 7.1 Hz, 13'-H), 7.31-7.23 (overlapping m, 4H, 2-H, 5-H, 6-H, 7-H), 4.09 (t, 2H, *J*= 7.3 Hz, 1'-H), 3.04 (t, 2H, *J*= 7.4 Hz, 5'-H), 1.88 (quin, 2H, *J*= 7.3 Hz, 2'-H), 1.57 (quin, 2H, *J*= 7.4 Hz, 4'-H), 1.47 (m, 2H, 3'-H), 1.40 (s, 9H, CH_3); ESI-MS calcd for $C_{33}H_{40}N_2O_3$ 512.30, found 513.25 $[M+H]^+$.

(1-(5-Aminopentyl)-1*H*-indol-3-yl)(naphthalen-1-yl)methanone (16). The Boc-protected amine **15** (137 mg, 0.3 mmol) was dissolved in 2 mL DCM containing 50% (v/v) TFA and it was stirred for 30 min at rt. The solution was evaporated and the product was washed with DCM and evaporated in vacuo to give **16** (135 mg, 97%); R_f 0.56 (MeOH–AcOH 95:5); HPLC k'= 3.64 (t_R= 13.0 min, linear gradient of 20→100% B in A over 25 min); ESI-MS calcd for $C_{28}H_{32}N_2O$ 412.25, found 413.34 $[M+H]^+$.

***N*-(5-(3-(1-Naphthoyl)-1*H*-indol-1-yl)pentyl)acetamide (17).** The amine **16** (17mg, 36 μmol) dissolved in 1 mL of DCM followed by the addition of 0.3 mL TEA and 0.3 mL acetic anhydride. The mixture was then stirred overnight at rt, then it was evaporated in vacuo. The crude **17** was purified by column chromatography on silica gel 60 (EtOAc–DCM 9:1) to give **17** (13 mg, 91%); R_f 0.54 (*n*-hexane–EtOAc 2:1); HPLC k'=4.70 (t_R= 16.0min, linear gradient of 20→100% B in A over 25 min); ^{1}H NMR (300 MHz, $CDCl_3$) δ 8.47 (m, 1H, 4-H), 8.17 (d, 1H, *J*= 8.4 Hz, 15'-H), 7.95 (d, 1H, *J*= 8.2 Hz, 11'-H), 7.88 (d, 1H, *J*= 6.9 Hz, 12'-H), 7.63 (d, 1H, *J*= 6.9 Hz, 9'-H), 7.54-7.42 (m, 3H, 10'-H, 13'-H, 14'-H), 7.37-7.32 (overlapping m, 4H, 2-H, 5-H, 6-H, 7-H), 4.04 (t, 2H, *J*= 8.4 Hz, 1'-H), 3.12 (q, 2H, *J*= 7.3 Hz, 5'-H), 1.88 (s, 3H, CH_3), 1.79 (quin, 2H, *J*= 7.3 Hz, 2'-H), 1.42 (quin, 2H, *J*= 7.3 Hz, 4'-H), 1.25 (quin, 2H, *J*= 7.4 Hz, 3'-H); ^{13}C NMR (300 MHz, $CDCl_3$) δ 192.1 (3-CO), 170.1 (CONH), 138.9 (C-8'), 137.9 (C-2), 137.0 (C-7a), 133.7 (C-11a'), 130.7 (C-15a'), 130.0 (C-11'), 128.2 (C-12'), 127.0 (C-14'), 126.8 (C-3a), 126.3 (C-13'), 125.9 (C-9'), 125.8 (C-15'), 124.6 (C-10'), 123.7 (C-6), 122.9 (2C, C-4, C-5), 117.6 (C-3), 110.0 (C-7), 47.0 (C-1'), 39.2 (C-5'), (29.4 and 29.1) (C-2', C-4'), 24.0 (C-3'), 23.3 (CH_3); ESI-MS calcd for $C_{30}H_{34}N_2O_2$ 454.26, found 455.85 $[M+H]^+$.

Tyr-D-Ala-Gly-Phe-NH_2. It was prepared as described.[158]

Bivalent compound 18. Overall isolated yield 21%; R_f 0.71 (ACN–MeOH–H_2O 4:1:1); HPLC k'= 4.43 (t_R= 15.2 min, linear gradient of 20→100% B in A over 25 min); ^{1}H NMR (300 MHz, (DMSO-d_6) δ 9.34 (s, 1H, Tyr OH), 8.57 (d, 1H, *J*= 6.9 Hz, D-Ala NH), 8.28 (d, 1H, *J*= 7.2 Hz, 15'-H), 8.20 (t, 1H, Gly NH), 8.08-7.94 (m, 8H, Phe ArH, Tyr NH, Phe NH, 5'-NH), 7.74 (s, 1H, 2-H), 7.66-7.44 (m, 5H, 9'-H, 10'-H, 11'-H, 12'-H, 13'-H), 7.33 (quin, 1H, 14'-H), 7.21-7.09 (m, 4H, 4-H, 5-H, 6-H, 7-H), 7.01 (d, 2H, *J*= 8.7 Hz, Tyr ArH), 6.68 (d, 2H, *J*= 8.7 Hz, Tyr ArH), 4.41 (q, 1H, Phe H^{α}), 4.28 (quin, 1H, D-Ala H^{α}), 4.15 (t, 2H, 1'-H), 3.95 (q, 1H, Tyr H^{α}), 3.63 (d, 2H, Gly H^{α}), 2.97-2.67 (m, 6H, Phe H^{β}, Tyr H^{β}, 5'-H), 1.65 (quin, 2H, 2'-H), 1.25 (quin, 2H, 4'-H) 1.10-1.02 (m, 4H, 3'-H, D-Ala H^{β}); ESI-MS calcd for $C_{47}H_{50}N_6O_6$ 794.94, found 795.63 $[M+H]^+$.

Bivalent compound 19. Overall isolated yield 14%; R_f 0.73 (ACN–MeOH–H_2O 4:1:1); HPLC k'= 4.24 (t_R= 14.7 min, linear gradient of 20→100% B in A over 25 min); ^{1}H NMR (300 MHz, (DMSO-d_6) δ 9.30 (s, 1H, Tyr OH), 8.49 (d, 1H, *J*= 6.9 Hz, D-Ala NH), 8.27 (m, 2H, Gly NH, 15'-H), 8.18 (t, 1H, Gly NH), 8.07-7.96 (m, 6H, 9'-H, 10'-H, 11'-H, 12'-H, 13'-H, Tyr NH, Phe NH), 7.87 (brs, 1H, Tyr NH), 7.75 (s, 1H, 2-H), 7.65-7.48 (m, 6H, 14'-H, 4-H, 5-H, 6-H, 7-H, 5'-NH), 7.19-7.13 (m, 5H, Phe ArH), 6.98 (d, 2H, *J*= 8.7 Hz, Tyr ArH),

6.66 (d, 2H, *J*= 8.7 Hz, Tyr ArH), 4.47 (q, 1H, Phe H^{α}), 4.30 (quin, 1H, D-Ala H^{α}), 4.16 (t, 2H, 1'-H), 3.91 (q, 1H, Tyr H^{α}), 3.56 (d, 2H, Gly H^{α}), 2.96-2.70 (m, 6H, 5'-H, Tyr H^{β}, Phe H^{β}), 1.68 (quin, 2H, 2'-H), 1.36 (quin, 2H, 4'-H), 1.18 (quin, 2H, 3'-H), 1.01 (d, 3H, D-Ala H^{β}); ESI-MS calcd for $C_{49}H_{53}N_7O_7$ 851.99, found 852.63 $[M+H]^+$.

Bivalent compound 20. Overall isolated yield 25%; R_f 0.68 (ACN–MeOH–H_2O 4:1:1); HPLC k'= 4.23 (t_R= 14.6 min, linear gradient of 20→100% B in A over 25 min); ^{1}H NMR (300 MHz, (DMSO-d_6) δ 9.33 (s, 1H, OH Tyr), 8.55 (d, 1H, D-Ala NH), 8.28 (d, 1H, 15'-H), 8.20 (t, 1H, Gly NH), 8.09-7.97 (m, 9H, Phe ArH, Phe NH, β-Ala NH, Tyr NH, 5'-NH), 7.77-7.49 (m, 7H, 2-H, 9'-H, 10'-H, 11'-H, 12'-H, 13'-H, 14'-H), 7.34-7.17 (m, 4H, 4-H, 5-H, 6-H, 7-H), 7.01 (d, 2H, Tyr ArH), 6.68 (d, 2H, Tyr ArH), 4.39 (q, 1H, Phe H^{α}), 4.29 (quin, 1H, D-Ala H^{α}), 4.16 (t, 2H, 1'-H), 3.95 (q, 1H, Tyr H^{α}), 3.58 (d, 2H, Gly H^{α}), 2.93-2.71 (m, 6H, 5'-H, Tyr H^{β}, Phe H^{β}), 2.13 (t, 2H, βAla H^{α}), 1.67 (quin, 2H, 2'-H), 1.33 (quin, 2H, 4'-H), 1.21-1.15 (m, 4H, β-Ala H^{β}, 3'-H), 1.05 (d, 3H, D-Ala H^{β}); ESI-MS calcd for $C_{50}H_{55}N_7O_7$ 866.01, found 867.14 $[M+H]^+$.

Bivalent compound 21. Overall isolated yield 12%; R_f 0.67 (ACN–MeOH–H_2O 4:1:1); HPLC k'= 4.27 (t_R= 14.8 min, linear gradient of 20→100% B in A over 25 min); ^{1}H NMR (300 MHz, (DMSO-d_6) δ 9.32 (s, 1H, Tyr OH), 8.54 (d, 1H, D-Ala NH), 8.29 (d, 1H, 15'-H), 8.20 (t, 1H, Gly NH), 8.06-8.00 (m, 8H, Phe ArH, Phe NH, Tyr NH, 5'-NH), 7.75 (s, 1H, 2-H), 7.63-7.52 (m, 6H, 12'-H, 9'-H, 10'-H, 11'-H, 14'-H, 13'-H), 7.30-7.11 (m, 4H, 4-H, 5-H, 6-H, 7-H), 6.96 (d, 2H, Tyr ArH), 6.69 (d, 2H, Tyr ArH), 4.40 (q, 1H, Phe H^{α}), 4.29 (quin, 1H, D-Ala H^{α}), 4.18 (t, 2H, 1'-H), 3.96 (q, 1H, Tyr H^{α}), 3.64 (d, 2H, Gly H^{α}), 2.94-2.70 (m, 7H, Tyr H^{β}, Phe H^{β}, Gaba NH, 5'-H), 1.93 (t, 2H, Gaba H^{α}), 1.69 (quin, 2H, *J*= 7.3 Hz, 2'-H), 1.49 (quin, 2H, Gaba H^{β}), 1.33 (quin, 2H, 4'-H), 1.21 (m, 4H, 3'-H, Gaba H^{γ}), 1.06 (d, 3H, D-Ala H^{β}); ESI-MS calcd for $C_{51}H_{57}N_7O_7$ 880.04, found 881.23 $[M+H]^+$.

1-Pentyl-1*H*-indole (22). To a stirred solution of indole (1.17 g, 10 mmol) in ACN (10 mL) were added TEA (1.01 g, 10 mmol) and 1-iodopentane (1.98 g, 10 mmol), then the solution was stirred at 80°C overnight. The solvent was evaporated in vacuo and the residue was extracted with water and $CHCl_3$ (3×20 mL). The combined organic phase was washed with brine, and dried over Na_2SO_4. After evaporation the crude product was purified by column chromatography (*n*-hexane−EtOAc 95:5) to give 1.40 g (75%) of pure **22** as an oil. R_f 0.70 (*n*-hexane−EtOAc 95:5); HPLC k'= 3.73 (t_R= 13.2 min, linear gradient of 50→100% B in A over 25 min); ^{1}H NMR (500 MHz, $CDCl_3$) δ 7.63 (d, 1H, *J*= 7.9 Hz, 4-H), 7.35 (d, 1H, *J*= 8.1 Hz, 7-H), 7.20 (t, 1H, *J*= 7.6 Hz, 5-H), 7.10 (d, 1H, *J*= 3.1 Hz, 2-H), 7.09 (t, 1H, *J*= 8.0 Hz, 6-

H), 6.49 (d, 1H, *J*= 3.1 Hz, 3-H), 4.12 (t, 2H, *J*= 7.2 Hz, 1'-H), 1.85 (quin, 2H, *J*= 7.2 Hz, 2'-H), 1.33 (m, 4H, 3'-H, 4'-H), 0.89 (t, 3H, *J*= 7.0 Hz, CH_3); ^{13}C NMR (126 MHz, $CDCl_3$) δ 136.1 (C-7a), 128.7 (C-3a), 127.9 (C-2), 121.4 (C-6), 121.1 (C-4), 119.3 (C-5), 109.5 (C-7), 100.9 (C-3), 46.6 (C-1'), 30.1 (C-2'), 29.3 (C-3'), 22.5 (C-4'), 14.1 (CH_3); ESI-MS calcd for $C_{13}H_{17}N$ 187.14, found 188.02 $[M+H]^+$.

5-Bromo-1-pentyl-1*H*-indole (23). 1.96 g of 5-bromo-1*H*-indole (10 mmol) was dissolved in 20 mL of DMF containing 1.6 g of powdered NaOH, then 1-iodopentane (1.98 g, 10 mmol) was added dropwise. After 4 h stirring at ambient temperature the mixture was filtered and the filtrate was evaporated in vacuo. The resulting oil was dissolved in $CHCl_3$ and extracted with water. The organic phase was washed with brine and dried over Na_2SO_4. The crude product was purified by column chromatography (*n*-hexane–EtOAc 95:5) to give 1.75 g (66%) of pure **23** as an oil. R_f 0.62 (*n*-hexane–EtOAc 95:5); HPLC k'= 4.79 (t_R= 16.2 min, linear gradient of 50→100% B in A over 25 min); ^{1}H NMR ($CDCl_3$) ^{1}H NMR (500 MHz, $CDCl_3$) δ 7.74 (d, 1H, *J*= 1.6 Hz, 4-H), 7.27 (dd, 1H, *J*= 8.8 Hz, 1.6 Hz, 7-H), 7.21 (d, 1H, *J*= 8.8 Hz, 6-H), 7.09 (d, 1H, *J*= 3.0 Hz, 2-H), 6.42 (d, 1H, *J*= 2.9 Hz, 3-H), 4.08 (t, 2H, *J*= 7.2 Hz, 1'-H), 1.82 (quin, 2H, *J*= 7.3 Hz, 2'-H), 1.31 (m, 4H, 3'-H, 4'-H), 0.88 (t, 3H, *J*= 7.1 Hz, CH_3); ^{13}C NMR (126 MHz, $CDCl_3$) δ 134.8 (C-7a), 130.3 (C-3a), 129.1 (C-2), 124.3 (C-6), 123.5 (C-4), 112.6 (C-5), 111.0 (C-7), 100.6 (C-3), 46.7 (C-1'), 30.1 (C-2'), 29.2 (C-3'), 22.4 (C-4'), 14.1 (CH_3); ESI-MS calcd for $C_{13}H_{16}BrN$ 265.05, found 266.18 $[M+H]^+$.

Naphthalen-1-yl(1-pentyl-1*H*-indol-3-yl)methanone (24). To a stirred solution of **22** (281 mg, 1.5 mmol) in 10 mL of dry DCM at 0^{o}C was added dropwise 1.5 mL of 1M Et_2AlCl in hexane (1.5 mmol). The solution was stirred at 0 ^{o}C for 1 h followed by the dropwise addition of 286 mg of 1-naphthoyl chloride (1.5 mmol) in 3 mL DCM. The reaction mixture was stirred at 0 ^{o}C overnight then the solution was poured carefully into a mixture of ice and 0.1 M HCl and it was extracted with DCM. The combined organic phase was evaporated and the residue was dissolved in diethyl ether that was washed with 15% K_2CO_3. The organic phase was evaporated and the crude product was purified by column chromatography (*n*-hexane−EtOAc 4:1) to give 368 mg (72%) of pure **24** as an oil. R_f 0.44 (*n*-hexane−EtOAc 4:1); HPLC k'= 4.29 (t_R= 14.8 min, linear gradient of 50→100% B in A over 25 min); ^{1}H NMR (500 MHz, $CDCl_3$) δ 8.48 (m, 1H, 4-H), 8.19 (d, 1H, *J*= 8.4 Hz, 15'-H), 7.97 (d, 1H, *J*= 8.2 Hz, 11'-H), 7.91 (d, 1H, *J*= 8.1 Hz, 12'-H), 7.66 (d, 1H, *J*= 6.9 Hz, 9'-H), [7.53 (t, 1H, *J*= 7.5 Hz) and 7.52 (t, 1H, *J*= 7.1 Hz)] (10'-H and 13'-H), 7.47 (t, 1H, *J*= 7.6 Hz, 14'-H), 7.41-7.35 (overlapping m, 4H, 2-H, 5-H, 6-H, 7-H), 4.07 (t, 2H, *J*= 7.3 Hz, 1'-H), 1.81 (quin, 2H, *J*= 7.4 Hz, 2'-H), 1.28 (m, 4H, 3'-H, 4'-H), 0.85 (t, 3H, *J*= 7.0 Hz, CH_3); ^{13}C NMR (126

MHz, $CDCl_3$) δ 192.2 (CO), 139.3 (C-8'), 138.1 (C-2), 137.2 (C-7a), 133.9 (C-11a'), 131.0 (C-15a'), 130.1 (C-11'), 128.3 (C-12'), 127.2 (C-3a), 126.9 (C-14'), 126.4 (C-13'), 126.2 (C-9'), 126.0 (C-15'), 124.7 (C-10'), 123.7 (C-6), 123.1 (C-5), 123.0 (C-4), 117.7 (C-3), 110.1 (C-7), 47.3 (C-1'), 29.6 (C-2'), 29.1 (C-3'), 22.3 (C-4'), 14.0 (CH_3); ESI-MS calcd for $C_{24}H_{23}NO$ 341.18, found 341.95 $[M+H]^+$.

Naphthalen-1-yl(5-bromo-1-pentyl-1*H*-indol-3-yl)methanone (25). Prepared as described for **24**, but starting from **23** (400 mg, 1.5 mmol). The crude product was purified by column chromatography (*n*-hexane–EtOAc 4:1) to give 517 mg (82%) of pure **25** as an oil. R_f 0.40 (*n*-hexane–EtOAc 4:1); HPLC k'= 5.49 (t_R= 18.2 min, linear gradient of 50→100% B in A over 25 min); ^1H NMR (500 MHz, $CDCl_3$) δ 8.71 (d, 1H, *J*= 1.6 Hz, 4-H), 8.17 (d, 1H, *J*= 8.3 Hz, 15'-H), 7.98 (d, 1H, *J*= 8.2 Hz, 11'-H), 7.92 (d, 1H, *J*= 8.0 Hz, 12'-H), 7.65 (dd, 1H, *J*= 6.9 Hz, 0.7 Hz, 9'-H), [7.53 (t, 1H, *J*= 7.6 Hz) and 7.52 (t, 1H, *J*= 6.7 Hz)] (10'-H and 13'-H), 7.48 (dt, 1H, *J*= 7.7 Hz, 1.2 Hz, 14'-H), 7.45 (dd, 1H, J= 8.7 Hz, 1.8 Hz, 6-H), 7.32 (s, 1H, 2-H), 7.26 (d, 1H, *J*= 8.4 Hz, 7-H), 4.04 (t, 2H, *J*= 7.2 Hz, 1'-H), 1.79 (quin, 2H, *J*= 7.4 Hz, 2'-H), 1.26 (m, 4H, 3'-H, 4'-H), 0.85 (t, 3H, *J*= 7.1 Hz, CH_3); ^{13}C NMR (126 MHz, $CDCl_3$) δ 191.9 (CO), 138.8 (C-8'), 138.5 (C-2), 135.9 (C-7a), 133.9 (C-11a), 130.9 (C-15a), 130.4 (C-11'), 128.7 (C-3a), 128.4 (C-12'), 127.0 (C-14'), 126.8 (C-13'), 126.5 (C-9'), 126.0 (2C, C-15', C-6), 125.8 (C-4), 124.7 (C-10'), 117.2 (C-3), 116.8 (C-5), 111.5 (C-7), 47.5 (C-1'), 29.6 (C-2'), 29.0 (C-3'), 22.3 (C-4'), 14.0 (CH_3); ESI-MS calcd for $C_{24}H_{22}BrNO$ 419.09, found 420.14 $[M+H]^+$.

Tritium labeling of 11. 2 mL 1.15 mg/mL MeOH solution of **9** (6 μmol) was mixed with 250 μL 3 % (v/v) ICl in MeOH (14.2 μmol) and the solution was stirred at ambient temperature for 60 min. Then 50 mg/mL $Na_2S_2O_5$ in water was added until decolorization, and the iodo derivative of **9** was purified by semipreparative HPLC on a Phenomenex Luna C18(2) stationary phase. The resulting 1.6 mg (55%) of iodo-**9** was dissolved in 400 μL DMF and 3 mg of Pd/$BaSO_4$ (10% Pd) catalyst and triethylamine (1.4 μL, 10 μmol) were added and tritium labeling was performed as described for [^{3}H]JWH-018 to give 64 MBq of [^{3}H]**9** with a specific activity of 64 GBq/mmol. Finally, 37 MBq of [^{3}H]**9** and HOBt.H_2O (0.3 mg, 1.9 μmol) were dissolved in 150 μL of DMF and DIC (0.3 μL, 1.9 μmol) was added. It was stirred for 5 min, then **6** (2.1 mg, 2.9 μmol) and DIEA (1.4 μL, 8 μmol) were added and the solution was stirred overnight at rt. It was then evaporated in vacuo and the crude product was purified by HPLC on a Phenomenex Luna C18(2) column that yielded 5.5 MBq [^{3}H]**11**

(15%). S.a. 64 GBq/mmol; HPLC k'= 5.48 (t_R= 13.6 min, linear gradient of 20→100% B in A over 25 min).

Tritium labeling of 19. To a solution of **19** (970 μL 1 mg/mL MeOH, 1 μmol) 1.8 mg of IPy_2BF_4 (Bis(pyridine)iodonium tetrafluoroborate) (4.8 μmol) and 4.4 μL of HBF_4 in Et_2O were added and the reaction mixture was stirred for 1h at rt under nitrogen. The reaction was quenched with a solution of $Na_2S_2O_5$ in water and the iodo derivative of **19** was purified by HPLC on a Phenomenex Luna C18(2) stationary phase yielding 0.8 mg (60%) of diiodo-**19**. It was dissolved in 400 μL DMF and 2.5 mg of $Pd/BaSO_4$ (10% Pd) catalyst and triethylamine (0.8 μL, 5.6 μmol) were added and tritium labeling was performed as described for [^{3}H]JWH-018 to give 80 MBq of [^{3}H]**19** with a specific activity of 185 GBq/mmol. HPLC k'= 6.78 (t_R= 16.3 min, linear gradient of 5→95% B in A over 25 min).

Table A1. Calculated parameters of the antagonist effect of **10** and **12** in agonist induced [^{35}S]GTPγS binding assays in rat brain membrane homogenates.

	E_{max} (%)	EC_{50} (nM)
oxycodone	137±5.3	25±3.1
+ 10 μM **10**	101±1.0***	n.r.
+ 10 μM **12**	100±0.9***	n.r.
+ 10 μM naloxone	99±1.7***	n.r.
Tyr-D-Ala-Gly-Phe-NH_2	159±3.5	154±14
+ 10 μM **10**	102±3.5***	n.r.
+ 10 μM **12**	97±4.1***	n.r.
+ 10 μM naloxone	98±2.4***	n.r.
JWH-018 (**24**)	167±4.1	36±1.8
+ 10 μM **10**	107±3.8***	n.r.
+ 10 μM **12**	110±4.0***	n.r.
+ 10 μM (rimonabant and AM630)	100±3.3***	n.r.
11	146±2.1	198±9.3
+ 10 μM **10**	102±3.2***	n.r.
+ 10 μM **12**	101±2.8***	n.r.
19	161±2.4	110±9.7
+ 10 μM **10**	103±2.3***	n.r.
+ 10 μM **12**	99±1.5***	n.r.

Calculated maximal G-protein stimulation efficacy (E_{max}) and ligand potency (EC_{50}) values of the agonists oxycodone, Tyr-D-Ala-Gly-Phe-NH_2, JWH-018, **11** and **19** in the absence or presence of 10 μM naloxone, 10 μM rimonabant, 10 μM AM 630, 10 μM **10** or 10 μM **12**. Statistical comparison of the E_{max} and EC_{50} values were performed by one-way ANOVA followed by the Bonferroni's multiple comparison test (***, $P< 0.001$). n.r. not relevant.